ANALYSIS OF HEART RATE VARIABILITY AND SKIN CONDUCTANCE USING SIGNAL PROCESSING METHODS

Thesis Submitted for the Award of the Degree of

DOCTOR OF PHILOSOPHY

in

Electrical Engineering

By

ANKITA SONI

Registration Number: 11814246

Supervised By

Dr. KIRTI RAWAL (20248)

School of Electronics and Electrical Engineering (Professor)

Lovely Professional University

LOVELY PROFESSIONAL UNIVERSITY, PUNJAB

2024

DECLARATION

I, hereby declare that the presented work in the thesis entitled "**Analysis of Heart Rate Variability and Skin Conductance using Signal Processing Methods**" in fulfillment of the degree of **Doctor of Philosophy (Ph. D.)** is an outcome of research work carried out by me under the supervision Dr. Kirti Rawal, working as Professor in the School of Electronics and Electrical Engineering of Lovely Professional University, Punjab, India. In keeping with the general practice of reporting scientific observations, due acknowledgments have been made whenever the work described here has been based on the findings of another investigator. This work has not been submitted in part or full to any other University or Institute for the award of any degree.

(Signature of Scholar)

Name of the scholar: Ankita Soni

Registration No.: 11814246

Department/School: School of Electronics and Electrical Engineering

Lovely Professional University,

Punjab, India

CERTIFICATE

This is to certify that the work reported in the Ph. D. thesis entitled "**Analysis of Heart Rate Variability and Skin Conductance using Signal Processing Methods**" submitted in fulfillment of the requirement for the reward of degree of **Doctor of Philosophy (Ph.D.)** in the School of Electronics and Electrical Engineering, is a research work carried out by Ankita Soni, 11814246, is bonafide record of his/her original work carried out under my supervision and that no part of thesis has been submitted for any other degree, diploma or equivalent course.

(Signature of Supervisor)

Name of supervisor: Dr. Kirti Rawal

Designation: Professor

Department/School: School of Electronics and Electrical Engineering

University: Lovely Professional University

Abstract

The Autonomic Nervous System (ANS) is responsible for regulating the fluctuations in Heart Rate Variability (HRV) and Skin Conductance Response (SCR) during different physical activities. HRV is measured by analyzing the beat-to-beat RR interval of the ECG signal, while SCR is measured by assessing the skin's electrical conductivity.

Both HRV and SCR reflect the complex interactions between the ANS and cardiovascular function. Changes in body position can lead to variations in autonomic tone, making postural changes important factors affecting HRV and SCR.

This study investigates the impact of postural changes on the autonomic nervous system and explores the relationship between HRV and SCR. The study involved collecting HRV and SCR data from subjects in both supine and standing positions to better understand the connection between postural changes, HRV, and SCR. These postures were chosen for their significant impact on autonomic balance. The data set includes HRV and SCR measurements from 70 subjects. The BIOPAC®MP36 instrument was used to record HRV, while a NEULOG Galvanic Skin Response Sensor was used for SCR recordings..

The recorded HRV data underwent several analyses using linear, nonlinear, and multiresolution approaches. In addition, the relationship between HRV and SCR was examined.

The time domain methods used in this thesis are SDNN, RMSSD, NN50, and pNN50, while applied frequency domain methods are Low frequency (LF), High frequency (HF), and LF/HF ratio.

As HRV is a nonlinear signal, to capture its nonlinear dynamics, complexity, irregularity, and pattern, the explored nonlinear method is sample entropy analysis. To subdue the limitation of standard sample entropy, a new method has been developed named Composite distance sample entropy (CDSE) and applied to the synthetic dataset as well as the recorded dataset in this research work.

Multiresolution research of HRV was carried out to further enhance the analysis employing a range of traditional wavelet transformations (db2 to db6). With more understanding of HRV dynamics, it is discovered that each HRV signal has unique properties. Consequently, a particular signal-matching wavelet is needed. Thus, A matched wavelet using the stochastic

fractal search algorithm- MWSFSA has been developed and applied to the dataset of 70 subjects.

The study evaluated the performance of various linear, nonlinear, and multi-resolution methods in detecting HRV variance between different postures. It was found that the LF/HF ratio, a frequency domain parameter, is a more accurate indicator of HRV variation in different postures compared to time domain variables such as SDNN, RMSSD, NN50, and pNN50. This suggests that frequency domain measures offer a more comprehensive understanding of the autonomic response to postural changes. Specifically, the LF/HF ratio accurately detected postural variation between supine and standing postures at 85.71%, while NN50 and pNN50 were accurate at 81.42%, and SDNN and RMSSD at 76.87% and 78.57%, respectively.

Further, the study investigated the incorporation of sample entropy to capture complicated patterns and trends because HRV signals are nonlinear. A remarkable 88.57% accuracy in identifying the proper trend of HRV change between postures was found by sample entropy analysis. The ability of nonlinear analysis approaches to reveal minor autonomic changes that linear methods could miss is highlighted by this.

Based on these discoveries, a novel method called "Composite distance sample entropy" that is based on sample entropy was created. This novel strategy outperformed conventional approaches, achieving a significant accuracy rate of 94.28% in detecting HRV variations. The addition of sample entropy demonstrated both its strength as a tool for HRV analysis and its capacity to identify underlying autonomic responses that would have been missed by conventional approaches.

Using traditional Daubechies wavelets (db2 to db6), multiresolution investigations into HRV were conducted to broaden the analysis. This method sought to identify various accuracy levels across various wavelet scales. Results showed distinct accuracies for each wavelet scale, with accuracy rates of 92.85%, 94.28%, 91.42%, 94.28, and 91.48% for db2, db3, db4, db5, and db6, respectively. This investigation showed how well-suited wavelet techniques can capture the finer details of HRV change between postures. The study's outcome was the creation of a matched wavelet model named 'MWSFSA' with a remarkable accuracy rate of 97.14% utilizing the stochastic fractal search algorithm. The ability to improve HRV analysis accuracy, particularly when addressing the complicated dynamics impacted by postural alterations, is demonstrated by the matched wavelet technique.

The decreased HRV variables - SDNN, RMSSD, NN50, pNN50, HF, SE, and CDSE - in standing posture, along with increased values of LF, LF/HF ratio, the mean value of SCR, and HR, indicate an increase in sympathetic activation and a decrease in parasympathetic activity. This suggests a "fight-or-flight" reaction, preparing the body to respond to perceived stress or threat, controlled by the sympathetic nervous system (SNS). The overall rise in physiological arousal is reflected in the elevation of SCR and HR. Skin conductance, influenced by sympathetic innervation, serves as a gauge of sweat gland activity. A higher SCR indicates greater sympathetic outflow and reaction from the sweat glands. The increased HR denotes a faster heart rate, also influenced by sympathetic activity. These changes are commonly observed in situations of heightened arousal, vigilance, or stress. The rise in HR during the standing position reflects the body's attempt to adapt and compensate for the change in posture.

In conclusion, this thorough investigation illuminates the complex interaction between postural changes and HRV, extending its relationship to SCR and providing important new knowledge about autonomic reactions. Understanding HRV dynamics during postural changes is improved by the superiority of frequency domain measures, the potential of nonlinear analysis utilizing "CDSE," and the high precision of matched wavelet techniques "MWSFSA." The results of this study have implications for clinical applications as well as physiological research, and they may help in the identification and treatment of autonomic dysfunction. This study advances the understanding of HRV and SCR responses to postural changes and sets the way for more accurate evaluations of autonomic function and cardiovascular health.

Acknowledgment

First of all, I am grateful to my supervisor, Dr. Kirti Rawal, for her supervision, guidance, and direction during the course of this research as well as for providing me with exceptional experiences. I consider myself incredibly lucky to have an opportunity to collaborate with her. The guidance provided proved to be extremely beneficial.

I would like to thank my loving husband Dr. Tushar Tyagi, for his unending care and support, as he constantly pushed me to never give up. I'd like to dedicate this work to my beloved daughter Shambhavi.

I would like to show my gratitude to Dr. Gaurav Sethi, HOS, School of Electronics and Electrical Engineering, for his valuable suggestions, support, and conducive environment to carry out this research work.

I would like to thank the subjects who have participated in this study. I would like to show my gratitude to all the staff members of the Biomedical Signal Processing and Telemedicine Laboratory, NIT Jalandhar, Punjab, India, for allowing me to do the recording procedure.

I would like to show my gratitude to Mr. Navdeep Dhaliwal, Dr. Amit Dutt, Dr. Alok Jain, and Dr. Amardeep Kang for their support during my research work.

I am also grateful to my friends and fellow researchers, particularly Akshay, Amishi, Ankush, Dr. Pavanpreet Kaur, and Dr. Rekha for their constructive suggestions.

I am also very grateful to my parents, and all my family members for the moral support and care that they have shown towards me during the period of this work. Finally, I thank God for sailing me through all the rough and tough times during this research work.

Date Ankita Soni

TABLE OF CONTENTS

LIST OF FIGURES

LIST OF TABLES

LIST OF ABBREVIATIONS

Abbreviations	Description
AE	Approximation Entropy
ANS	Autonomic Nervous System
CDSE	Composite Distance Sample Entropy
DB	Daubechies wavelet
ECG	Electrocardiogram
EDA	Electrodermal Activity
GSR	Galvanic Skin Response
HF	High Frequency
HR	Heart Rate
HRV	Heart Rate Variability
LF	Low Frequency
MWSFSA	Matched wavelet using stochastic Fractal search algorithm.
NN interval	Normal to Normal interval
NN50	The percentage of successive NN intervals that have a difference of more than 50 ms.
PNN50	The successive NN intervals have a difference of more than 50 ms.
PNS	Parasympathetic Nervous System
RMSSD	The successive difference between adjacent Normal to Normal interval's root mean square.
SC	Skin Conductance
SCR	Skin Conductance Response
SDNN	Normal to Normal (NN) interval's standard deviation
SE	Sample Entropy
SFSA	Stochastic Fractal search algorithm
SNS	Sympathetic Nervous System

CHAPTER 1

INTRODUCTION

This thesis explores the variation of heart rate variability (HRV) and skin conductance response during different body postural activities. The study investigates the variation of HRV in various body postures using different analysis methods, including linear, nonlinear, and multiresolution methods. Additionally, the skin conductance response is analyzed in two different postures, and the relationship between skin conductance response and heart rate is discussed. The chapter covers the research topic, the cardiovascular system, the corresponding physiological background, HRV analysis methods, findings related to the different applied methods, and the structure of the thesis. The literature survey section includes an extensive study of various signal processing techniques to uncover the variation of HRV between different body postures and its relationship with skin conductance response.

1.1 Overview

Nowadays heart rate variability and skin conductance response are common clinical and research tools utilized for identifying different physiological, emotional, and psychological disorders. The autonomic nervous system's activity can be examined by adopting both physiological markers, namely HRV [1] and SCR [2]. HRV and SCR are useful measures for assessing the central and peripheral dynamics of the sympathetic nervous system as well as for tracking the effects of various chronic illnesses and challenging life situations such as stress, excessive workload, etc. While HRV reflects changes arising from both sympathetic and parasympathetic systems, SCR reflects changes caused by sympathetic vagal activity [3]. Therefore, a variety of physical and psychological activities, including altered body postures, exercise, interactions in public, depression, anger, running, cycling, etc., can influence the ANS's response and be identified by HRV and SCR measurement.

The research focused on investigating how different body postures impact heart rate variability and the responses of the body's electrical conductivity. When a person changes from sitting or lying down to standing, the sympathetic nervous system is activated, causing an increase in heart rate and a drop in heart rate variability, followed by a quick return to baseline values. This reaction, known as the "orthostatic challenge," can be used to test the body's ability to maintain blood pressure and blood flow to the brain during postural changes, as well as the efficiency of the autonomic nervous system [4]. Poor autonomic nervous system functioning may lead to a longer return to baseline levels or a greater decline in heart rate variability [5]. Changes in body posture during exercise or physical activity might also impact heart rate variability. For example, changes in body position during yoga, Pilates, or other exercises could result in variations in heart rate and heart rate variability [6]. In summary, the impact of altered body position on heart rate variability is a typical physiological reaction that can provide important information about the operation of the autonomic nervous system.

Thus, it is important to investigate the variation in HRV and skin conductance response for postural changing events i.e., from supine to standing posture. A healthy heart has high variability, which indicates that there is a long interval between each heartbeat [7]. This enables the heart to stay steady and adaptable while responding swiftly to changes in the body's needs. Conversely, a decreased HRV is linked to a higher risk of several illnesses, including obesity, diabetes, and cardiovascular disease. Reduced HRV is an indication of stress, anxiety, or sadness as well as a damaged autonomic nervous system [8]. Numerous methods, such as electrocardiography (ECG), photoplethysmography (PPG), and pulse oximetry, can be used to measure HRV. These techniques offer insightful information about the autonomic nervous system's operation and can be used to gauge a person's general health and well-being [9].

Physical exertion enhanced the subject's physical load and sweat rate. The skin conductance response, which is represented by electrodermal activity (EDA), and sweat production are significantly positively correlated. A range of stimuli, such as emotional imagery, noises, or other sensory signals, can be used to quantify SCR [10-11].

Over the years, a significant amount of research work has been done in which HRV and SCR have been analyzed, but still, both physiological signals have not been examined

for the postural changing activity together. Furthermore, it is difficult to detect the HRV variations accurately and robustly between various postures using the traditional methods of HRV analysis.

As a result, the main driving force behind this work is to evaluate HRV changes by developing HRV analysis methods that can (i) accurately detect HRV differences between various postures and (ii) are useful in finding the relationship between the SCR and HRV regarding this postural changing activity. This research work can be summarized as presented below:

(1) By identifying the changes in skin conductance and HRV when young adults are in a supine posture.

(2) By identifying the changes in HRV and skin conductance when young adults are in a standing posture.

(3) By identifying the variations in the response of skin conductance and HRV from posture changes from supine to standing.

(4) By identifying the effect of postural change on the relationship between HRV, Heart rate, and SCR.

(5) By identifying the correlation between HRV and SCR.

1.2 Anatomical Framework

Heart rate variability (HRV) measurements are a trustworthy indicator that affects the heart's regular rhythm. Increased variability in the heart's inter-beat interval may be beneficial physiologically, according to a steadily increasing amount of research. Heart failure, diabetes, hypertension, and coronary artery disease are just a few pathological illnesses that frequently reflect low HRV [12]. levels. The sympathetic nervous system, which controls autonomic activities such as digestion, breathing, and heart rate, is one of its essential components. This system is activated during emotional experiences, and Skin Conductance Response (SCR) is a useful method for evaluating its activity. SCR is a useful instrument for assessing sympathetic nervous system function since it acts as an indicator of emotional arousal and stress [13].

1.2.1 Human Heart

The human heart is a vital organ that circulates blood throughout the body. It is located slightly to the left side of the chest and is about the size of a fist. The heart consists of four chambers: the right atrium, left atrium, right ventricle, and left ventricle. The right atrium receives oxygen-poor blood from the body and pumps it into the right ventricle. The right ventricle then pumps the blood to the lungs, where it picks up oxygen and releases carbon dioxide [14]. The oxygen-rich blood is then pumped into the left ventricle and returned to the heart through the left atrium. The left ventricle pumps the oxygen-rich blood through the aorta, a large artery, to the rest of the body. The flow of blood from the ventricle to the pulmonary artery is controlled by pulmonary valves, while the flow of oxygen-rich blood from the left atrium to the left ventricle is regulated by the mitral valve. This oxygen-rich blood is then distributed to the body [15] [16] [17]. The various part of the human heart is shown in Figure 1.1.

1.2.2 Cardiac Electrical Conduction

A unique network of cells called the heart's electrical conduction system starts and controls heartbeats. Figure 1.2 represents the electrical activity of the human heart. The functioning of this system is mentioned as follows [15][19]:

(i) The right atrium houses the SA node, which serves as the natural pacemaker of the heart by generating electrical impulses that drive the atria to contract, and where the heartbeat is first initiated.

(ii) The atria constrict and force blood into the ventricles as a result of the electrical impulses that travel throughout them from the SA node.

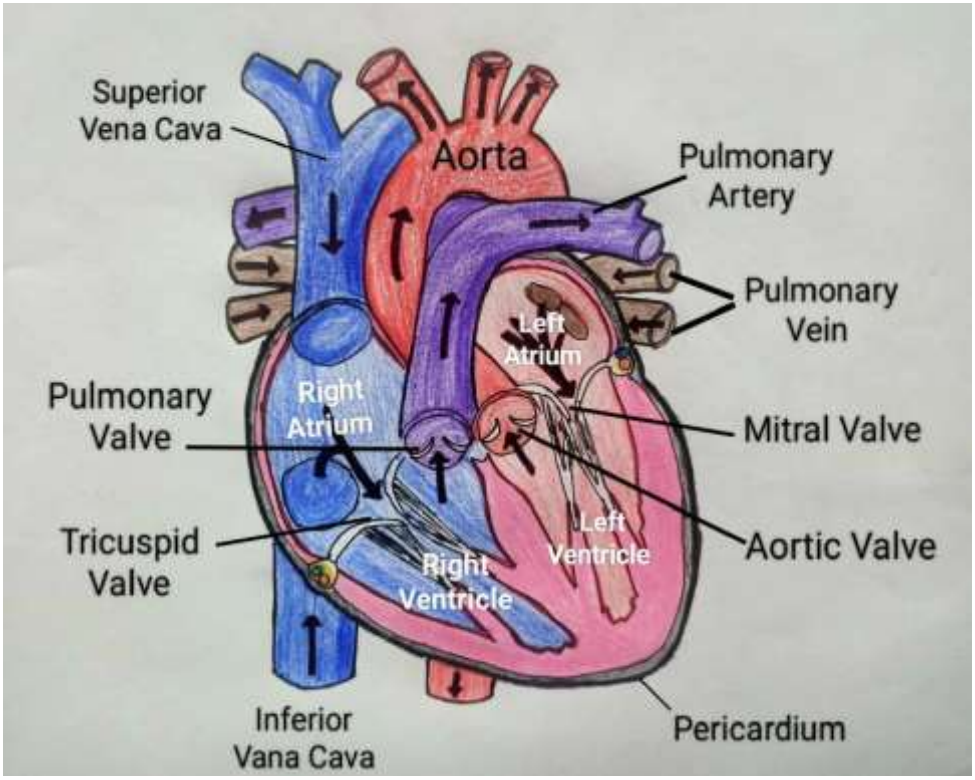

Figure 1.1 Cross Section of Human Heart [18]

(iii) The AV node delays the electrical impulses for a short period so that the atria can fully contract before the ventricles are triggered.

(iv) The bundle of His, a specific channel that carries the electrical impulses from the AV node to the ventricles, is where the electrical impulses move after the delay.

(v) To send the electrical impulses to the Purkinje fibers distributed throughout the ventricles.

(vi) The ventricles contract and pump blood out of the heart as a result of the electrical impulses being distributed throughout them by the Purkinje fibers.

The Electrocardiogram (ECG) signal is produced as a result of all these cardiac actions [20].

1.2.3 Electrocardiogram and wave intervals

A non-invasive diagnostic procedure that monitors the electrical activity of the heart is called an electrocardiogram (ECG or EKG).

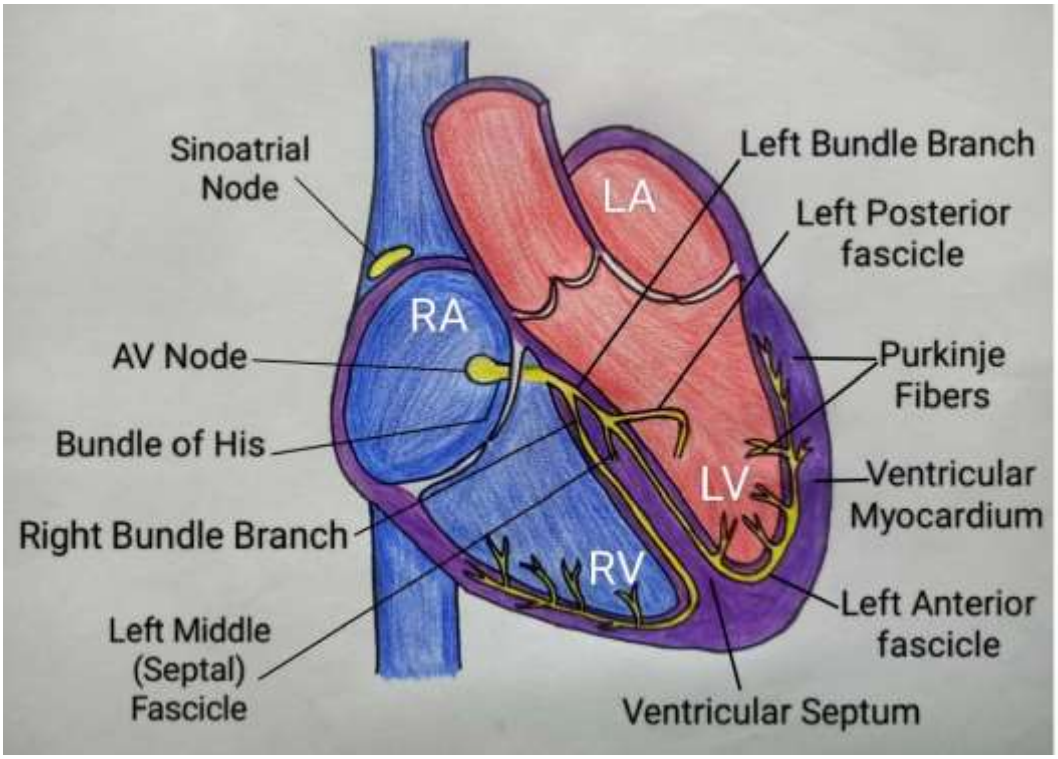

Figure 1.2 Cardiac Electrical Conduction [21]

It is a quick and painless treatment that can provide crucial details regarding the condition and performance of the heart. Electrodes are affixed to the skin of the arms, legs, and chest during an ECG. The electrodes pick up the heart's electrical signals and send them to a device that records them as a succession of waves on a graph. The different segments and intervals are explained as follows:

P wave- The electrical activity that takes place as the atria contract is represented by the P wave. Normally, it is a short, rounded wave that lasts 0.08 seconds.

PR Interval and Segment- A typical PR interval ranges from 0.12 to 0.20 seconds. From the P wave's completion to the start of the QRS complex, the P-R segment began.

Q wave- Q wave is the first downward deflection that lasts less than 0.03 seconds.

R wave- After the Q wave or after the PR interval, the R wave is the initial upward deflection. It symbolizes the electrical activity that takes place when the ventricles close. From the baseline to the wave's crest, the R wave's height is calculated.

RR Interval- The RR interval is the distance between two consecutive R peaks.

S wave- After the R wave, the S wave is the first downward deflection. There might not be a S wave in some leads. The S wave, if it exists, is usually brief and lasts less than 0.04 seconds.

QRS complex and interval- The electrical activity that takes place as the ventricles compress is represented by the QRS complex. Usually, the complex is tall and narrow and lasts for less than 0.12 seconds.

ST segment and interval- The time between the completion of the QRS complex and the beginning of the T wave is known as the ST segment. It stands for the period when the ventricles are getting ready for their subsequent contraction. Normally the regular ST segment is flat and level with the baseline.

T wave- Electrical activity that takes place as the ventricles rest and get ready for the subsequent contraction is represented by the T wave. The average waveform is rounded and less than 0.20 seconds long.

QT interval- QT interval stands for the amount of time needed for the ventricles to recuperate and contract. Age, sex, and heart rate all affect the normal QT interval, which is normally shorter than 0.44 seconds.

RST junction- It is the area of the electrocardiogram (ECG) where the QRS complex ends and the RST segment starts [1] [22-24]. All the mentioned waves, segments, and intervals of ECG have been shown in Figure 1.3 [25].

1.2.4 Heart Rate Variability

Heart rate variability (HRV) is a term used to describe the variation in the space between heartbeats. It illustrates the autonomic nervous system's capacity to adapt to changing needs, which regulates the heart rate and other body functions. It can be measured by subtracting the one RR interval from the previous RR interval which is depicted in Figure 1.4.

Electrocardiography (ECG) is an effective tool to measure HRV. HRV has been demonstrated to be predictive of many health outcomes and to provide insights into

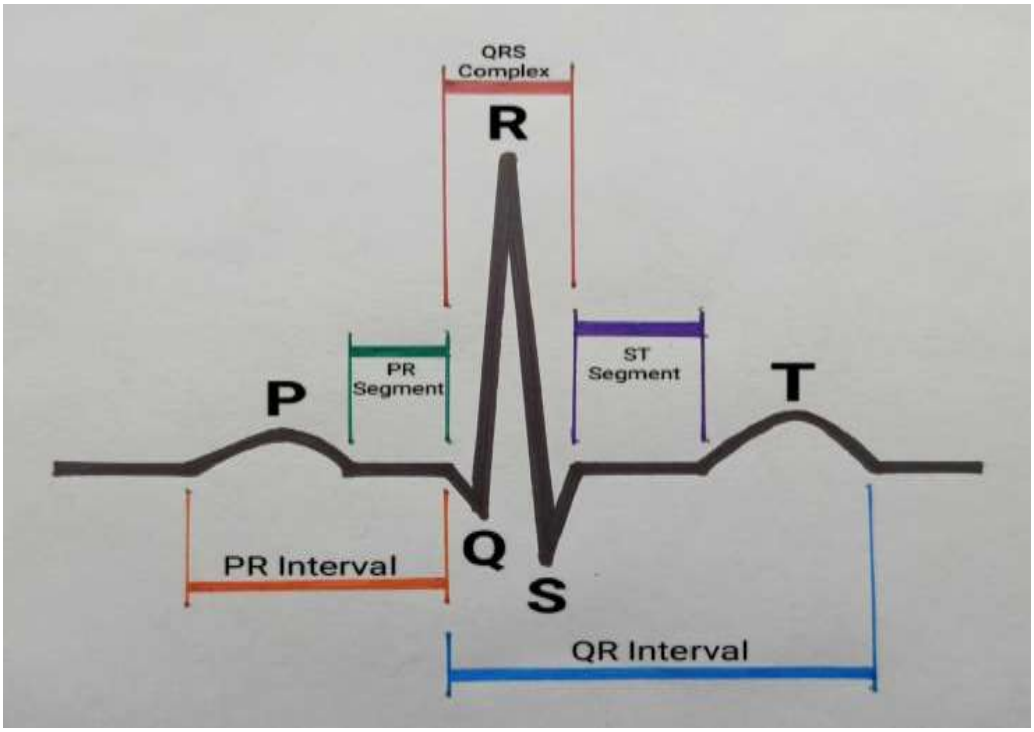

Figure 1.3 ECG waveform [25]

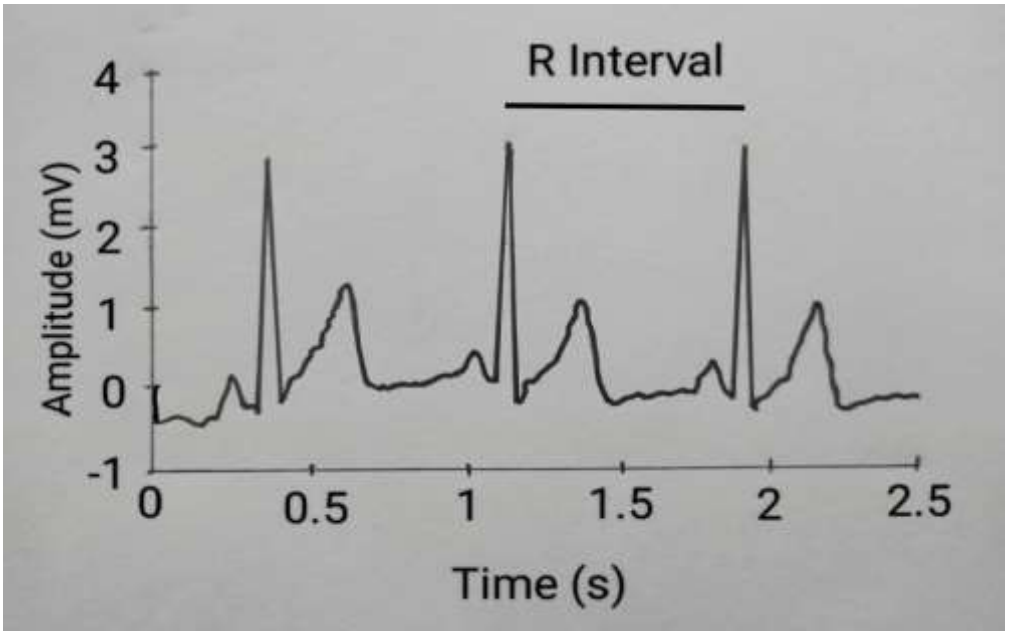

Figure 1.4 Heart rate variability [26]

monitoring autonomic function. High HRV is linked to improved health outcomes, including a lower risk of cardiovascular disease, while low HRV is linked to an increased risk of several health issues, including diabetes, depression, and heart disease.

Age, gender, physical activity, stress, and sleep are just a few of the variables that might affect HRV.

1.2.5 Skin Conductance Response

The skin's electrical conductance, which is correlated with the activity of the sympathetic nervous system, is measured by the skin conductance response (SCR). The sympathetic nervous system produces sweating when it is stimulated, such as during times of stress or arousal, which raises the skin's electrical conductance and is known as electrodermal activity (EDA). The rise in the skin's electrical conductance can be measured using electrodes applied to the skin and is known as the skin conductance response. SCR is frequently used in psychology and neuroscience to examine emotional processes and illnesses including anxiety and depression. SCR is used in marketing research to examine how consumers react to advertising and other stimuli. Figure 1.5 illustrates the skin conductance.

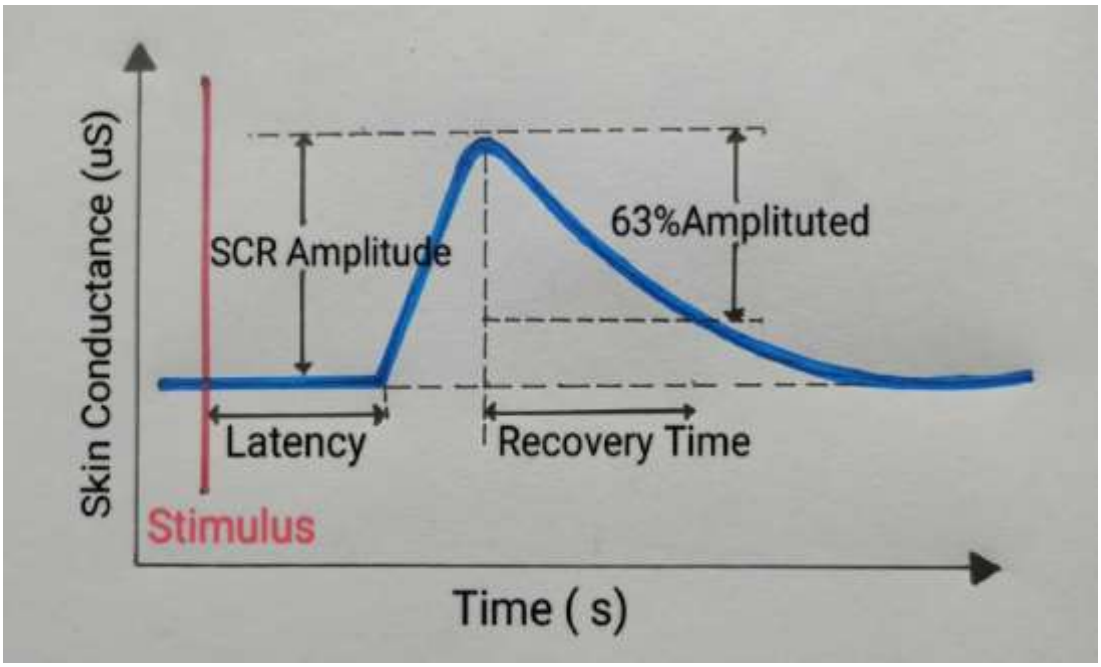

Figure 1.5 Skin Conductance [27]

Skin conductance measurements typically involve one of two primary categories: Tonic skin conductance and Phasic skin conductance [28-30].

(i) Tonic skin conductance (TSC): The term "tonic skin conductance" (TSC) describes the skin's normal level of electrical conductance, which is principally regulated by the activity of the eccrine sweat glands. By applying a steady, low-level electrical current to the skin and observing the resulting voltage, TSC can be measured. TSC is affected by many variables, including age, gender, and individual variations in sweat gland activity, and is generally stable over time.

(ii) Phasic skin conductance (PSC) refers to the transient changes in skin conductance that occur in response to external stimuli, particularly emotional or arousing stimuli. PSC can be measured by applying brief electrical pulses to the skin and measuring the resulting changes in voltage.

Skin conductance level (SCL) and skin conductance response (SCR) are two further subtypes of PSC. SCR stands for the brief fluctuations in skin conductance in reaction to stimuli, whereas SCL stands for the baseline level of skin conductance. SCR is frequently assessed in research on emotion and psychophysiology as a sign of emotional arousal and stress [31]. The SCR has been evaluated and analyzed for postural change activity in this research work. Figure 1.6 depicts EDA and SCR.

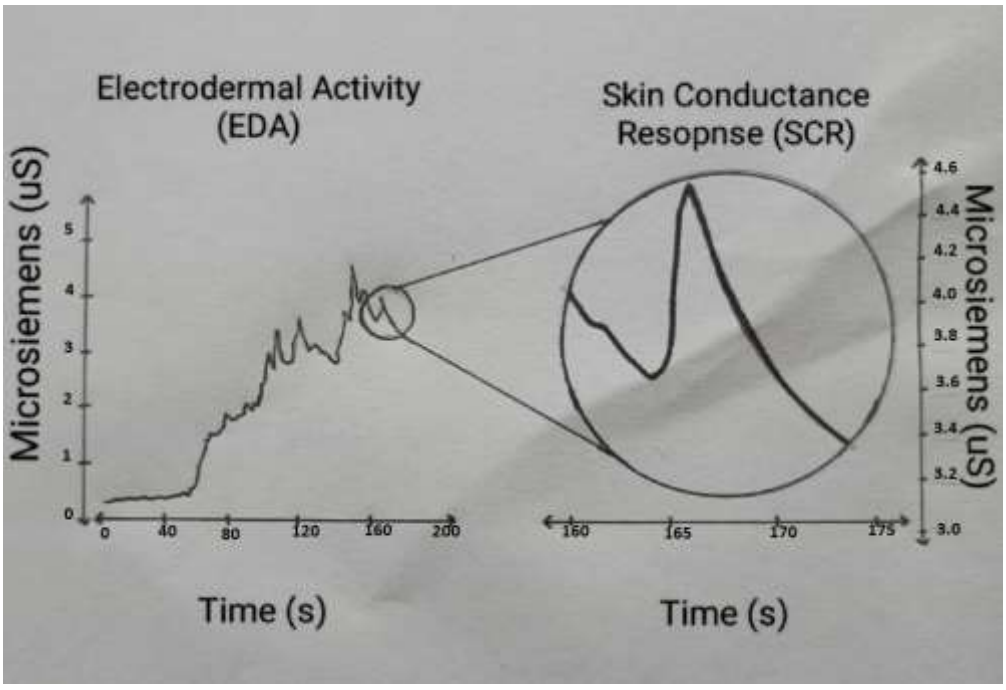

Figure 1.6 Electrodermal activity (EDA) and SCR [32]

1.3 Evolution of HRV and SCR

1.3.1 Autonomic Nervous System

The body's autonomic processes including digestion, blood pressure, breathing, and sweating are controlled by the autonomic nervous system (ANS), an intricate structure of nerve fibers and ganglia. In reaction to internal and external stimuli, it is in charge of preserving homeostasis or establishing equilibrium between diverse physiological processes.

The "fight or flight" response is controlled by the SNS and is characterized by increased heart rate, breathing, and blood pressure as well as decreased digestion and other non-essential activities when it is triggered by stressful or threatening events [33]. The SNS and PNS regulate a variety of physiological processes in a complementary way, and the activity of both systems is influenced by a variety of hormonal, neuronal, and feedback mechanisms that support homeostasis.

Numerous health issues, such as hypertension, cardiovascular disease, gastrointestinal disorders, and mental health conditions including anxiety and depression, can be brought on by ANS dysfunction or imbalance [34]. It is critical to understand the functioning and control of the ANS to maintain overall health and well-being.

1.3.2 History of HRV

Herophilos (335–280 BC), a Greek scientist, was the first to record heart rate around about 300 BC. Herophilos timed the pulse using a water clock. Galen of Pergamon (131–200 AD), a scholar and physician, first spoke of the pulse around 170 AD. He used the pulse to identify and forecast a variety of ailments. Stephen Hales was the first to note fluctuations in arterial pressure and the time between beats during the respiratory cycle in 1733. Carl Ludwig, the first person to create a smoking drum kymograph, utilized his invention in 1847 to record changes in amplitude and pressure. Anrep et al. [35-36] and their collaborators showed that both central and peripheral mechanisms contribute to heart rate variations. Hering [37] stated that breathing caused a reduction in heart rate in 1910. According to Hamlin et al. [38], RSA in dogs was caused by the activation of vagal nerves.

Using power spectrum analysis, numerous researchers [39–43] looked at heart rate changes in the 1970s. In 1985, DeBoer et al. [44] proved that HRV signals can be analyzed. Power spectral density was employed in 1986 by Myers et al. [45] to classify cardiac patients using HRV analysis. Additionally, Malik et al. [46] discovered that HRV can be analyzed using filtering methods. Schreibman et al. [47] proposed resampling in 1989 to address the non-uniform samples in HRV signal. For RR interval measurement, Merri et al. [48] proposed a minimal sample interval used in HRV. In 1990, Furlan et al. [49] demonstrated that throughout the early hours of the day, sympathetic activity increases and vagal tone decreases. In 1995, Malik and Camm [50] conducted a thorough study on the application of HRV and its clinical consequences. Lvanov et al. [51] employed wavelets for HRV analysis later on in 1996. For HRV analysis in 1997, Jasson et al. [52] employed time-frequency analysis techniques. A fresh approach to calculating HRV time series was developed by Laguna et al. in 1998 [53]. A thorough study of HRV analysis methods was provided in 1999 [55] [56]. Chan et al. [56] assessed the HRV variations associated with various physical activities in 2003. Fractal characteristics and support vector machines were utilized in 2004 to characterize the dynamics of the heart rate. [57] [58]. Further, neural networks are used for HRV signals [59]. Kheder et al. [60] carried out an HRV analysis in 2006 utilizing a nonlinear approach. The fractional Fourier transform was employed in 2008 by Zhang et al. [61] to find the biological signals.

In 2010, Bailon et al. [62] used respiratory data to investigate the low and high-frequency bands of HRV during exercise stress testing. Wavelets were employed for analyzing signals by Rafiee et al. in 2011 [63]. HRV analysis methods and their relationship were evaluated by Madhavi and Ananth in 2012 [64]. Karthikeyan et al. [65] employed a variety of nonlinear techniques in 2013 to detect stress using several physiological markers. In 2015, Silva et.al [66] used multiscale entropy for HRV analysis. In 2016, Rawal et al. [67] designed a tree-structured matched wavelet for HRV analysis. In 2017 and 2018, Porta et al. [68-69] applied various linear and nonlinear (i.e., sample entropy) approaches to analyze the complexity of short HRV series. In 2020, Verma et al. [70] used an optimization technique for ECG heartbeat classification.

In 2021, Rawal et al. [71] designed a matched wavelet using the genetic algorithm to efficiently analyze the HRV variation during the menstrual cycle.

1.3.3 History of SCR

Electrodermal activity (EDA) refers to the human body's ability to alter the electrical characteristics of the skin consistently. EDA has also gone under other names throughout history, including skin conductance, galvanic skin response (GSR), SCR, etc. Emil du Bois-Reymond was a German physiologist who is often credited with being the first to measure skin conductance. In 1848, du Bois-Reymond reported that the electrical resistance of the skin decreased when the skin was moistened. He called this phenomenon "galvanic skin response" and speculated that it might be related to the activity of sweat glands. Du Bois-Reymond's work on the electrical properties of living tissue laid the foundation for the development of modern skin conductance measurement [71]. SCR was shown to be a useful indicator of both cognitive and emotional processes by Hermann and Luchsinger in 1867 [71-72]. They discovered that SCR specifically increased in response to emotionally stimulating or attention-demanding stimuli. One of the first to show that SCR might be used as a gauge of cognitive and emotional processes, Hermann and Luchsinger's work opened the door for more study in this field [73-74].

Researchers like F.J. McGuigan and Carl W. Richter started using skin conductance in the 1920s and 1930s to examine autonomic nervous system activity and emotional reactions. The use of skin conductance measurement in research grew in the 1950s and 1960s because of the development of more advanced instrumentation and data analysis methods. Skin conductance became a popular tool for researchers like Roy John, J. Gruzelier, and M. Rosenfeld to examine a variety of phenomena, including stress, attention, and psychopathology. With the improvement of automated data collecting and processing tools in the 1980s and 1990s, the use of skin conductance measurement in research proliferated. [75-76]. To explore a variety of physiological and emotional events, skin conductance measurement and SCR analysis are still often employed in disciplines like psychology, neuroscience, and medicine today [77].

1.3.4 HRV, SCR, and Postural Change

The important factor that has been used to assess numerous changes in the body over the past three decades is Heart Rate Variability (HRV), which represents the parasympathetic and sympathetic nervous system activities that control the cardiovascular system. Thus, the activity of the ANS can be assessed with the measurement of HRV [78-79]. In addition to HRV, another physiological signal, i.e., Skin Conductance Response (SCR) (which is frequently used these days for assessing the effect of physical activities i.e., postural change) has been analyzed. It is also known as electrodermal behavior. When the amount of sweat is altered in ducts, variations are observed in SCR. Electro-dermal activity (EDA) is described as an indicator of variations in the skin's electrical conductance [80]. When the posture of the body is altered from a supine to a standing position, because of gravity, the blood pressure drops initially. To maintain the blood flow, the sympathetic nervous system activates which causes a decrement in the HRV and changes in skin conductance response [81-83].

1.4 Analysis method for HRV

Heart rate variability can be analyzed using various ways. Linear methods such as Time Domain and Frequency Domain methods have been used to measure the intervals between successive normal complexes of heartbeats [84-88]. Under usual physiologic conditions, HR is not periodic, and approaches based on linear HRV characteristics do not adequately convey the complexity of beat-to-beat variability. Nonlinear techniques are more suited to reveal the hidden dynamics of the HRV signal to get around the drawbacks of linear methods [89-91].

1.4.1 Analysis Using Linear Methods

Linear methods are divided into two parts: - Time domain analysis, and Frequency domain analysis.

(i) Time Domain Analysis

The simplest methods used for the analysis of HRV are time-domain measures [1]. Time domain methods include:

Statistical time domain measures include:

- SDNN: Normal to Normal (NN) interval's standard deviation.
- RMSSD: The successive difference between adjacent Normal to Normal interval's root mean square.
- SDANN: Averages of the normal-to-normal intervals' standard deviation.
- SDNNi: Mean of Standard Deviation from all Normal-to-Normal intervals.
- SDSD: Differences between adjacent normal to normal intervals' standard deviation.
- NN50: NN intervals with more than 50ms differences between them.
- pNN50: The percentage of successive NN intervals that have a difference of more than 50 ms.

(ii) Frequency Domain Analysis

The spectral analysis method referred to as frequency domain analysis dissects the total variability of a data series into its constituent frequency elements. These frequency components are depicted through a spectral density function that illustrates spectral strength concerning frequency. The integral of the spectral density function within the specified frequency range allows for the determination of spectral power within a specific frequency band. The Fast Fourier Transform (FFT) is a common method for spectrum analysis of HRV. Very low frequency (VLF), Low Frequency (LF), and High Frequency (HF) are the main notable components of the main spectrum [92].

1.4.2 Analysis Using Nonlinear Methods

In the last decades, a variety of nonlinear signal processing techniques have been developed to analyze nonlinear dynamics in novel ways.

Sample Entropy Analysis

Sample Entropy (SE) Sample entropy is commonly used to assess the predictability or irregularity of physiological signals in biomedical research. It compares patterns in time series data and measures the likelihood that similar patterns of a given length of data remain similar when the time series is extended by one data sample. SE was proposed by Richman and Moorman to address the limitations of Approximate Entropy (AE). SE

is not dependent on the length of the signals and is free from self-matches of vector pairs [68][93].

1.4.3 Analysis using Time-Frequency Methods

The underlying issue of not having enough data to do a reliable HRV analysis affects both linear and non-linear techniques for HRV analysis. Therefore, multi-resolution approaches are employed for HRV analysis.

The time and frequency resolution issues, regardless of the transform employed, are caused by a physical phenomenon (the Heisenberg uncertainty principle), yet it is feasible to analyze any signal using a different method called Multiresolution Analysis (MRA). A mathematical method called multi-resolution analysis (MRA) is used in signal and image processing to evaluate and depict data at various levels of detail or resolution. It entails breaking down a signal into several layers or levels, each of which captures a particular band of frequencies or scale component of the signal.

MRA's main principle is to represent a signal at many scales, enabling the investigation of both minute details and broad trends. A more thorough comprehension of the structure and characteristics of the signal is made possible by this decomposition [66] [94-95]. The MRA process typically involves applying a series of filters and down-sampling operations to decompose the signal. The down-sampling operation reduces the signal's sampling rate, maintaining the most relevant components [96-97].

1.4.4 Analysis using Matched Wavelets

Despite significant improvements in signal processing techniques, wavelets are still used in clinical research. Most of the studies employed wavelets from a library of common wavelets for this primary reason. The primary drawback of the currently available wavelets is that they might not closely resemble the signal of interest, which further reduces their capacity to identify the desired aspects of the signal. This restriction causes incorrect results interpretation, which in turn causes incorrect signal interpretation. Designing a wavelet that is appropriate for a specific signal is therefore necessary. Matching wavelets are therefore intended for numerous applications, including image compression, data compression, feature extraction, etc., to increase the analysis' accuracy and rigor [98-100].

1.5 Survey of Literature

Medical professionals and engineers continue to be intrigued by the recording and analysis of HRV and SCR signals after many years. So, during the postural change activity, a quick literature review in the fields of heart rate variability and skin conductance analysis was performed.

Various researchers have investigated that the response of HRV and SC can be affected by physical as well as mental activities such as exercise, public interactions, postural changes, depression, joy or anger, etc. Rawal *et al.* [101] discussed the role of HRV in medical diagnosis, as well as the experimental protocols and preprocessing of recorded ECG signals. Rawal *et al.* [66] [102] investigated that different body postures and activities like internal changes of the body (i.e., menstrual cycle), exercise, running, or aerobics, affect the sympathetic as well as parasympathetic activity. To test sympathetic behavior, some researchers have used EDA to analyze SC during exercise. In the context of physical exercise, cardiac autonomic control is described as a subsystem of the ANS. Vieluf *et al.* [103] found that physical activities are responsible for the sympathetic activation of ANS, While Molina *et al.* [104] investigated that there is a correlation between physiological parameters even after exercise. Posada-Quintero *et al.* [29] investigated in their research work that when participants perform any physical activity, they experience physical load, and the sweating rate is increased. EDA represents the changes in SC with a strong positive association with sweat production. It is found in various research that both HRV and SC are used for expressing the balance of the ANS. Although SC is only used to represent the fluctuations of sympathetic activities, as investigated by Posada-Quintero *et al.* [82]. Hnatkova *et al.* [105] explained in their research that the effect of the postural change varied according to the change in body position, also the HR increases to a higher value when a position is changed from supine to standing as compared to supine to sitting. Radhakrishna *et al.* [106] investigated that the value of HRV parameters is higher in the position of supine as compared to the standing position, while a decrement in the value of HRV parameters has been observed in the standing position investigated by Banskota *et al.* [107].

Rawal *et al.* [108] discussed in their research paper that several authors used time and frequency domain methods to investigate the influence of exercises on cardiovascular

metrics in both men and women. Ryan *et al.* [109] observed no significant change in the value of the frequency component of HRV when the position is changed from left supine to right supine position. Further, Cruz *et al.* [110] used time domain and frequency domain approaches of HRV to examine HRV in healthy people in supine and standing positions. The impact of change in HRV has also been observed in supine, sitting, and standing positions of the body [111.] Stefania *et al.* [112] used SC tonic or phasic variables and associated them with different features of linear methods. Alejandro *et al.* [113] estimated the Guided Coherence in a particular frequency range using a time-varying multivariate autoregressive model of EDA and HRV time series that integrates physiologically influenced assumptions.

There are various linear methods used by researchers to examine the variation in the HRV parameters [108]. However, linear methods have certain drawbacks which were discovered by Acharya et al. [114].

Linear methods are not ideal for identifying significant changes in heart activity because the cardiovascular system is complex. After gaining knowledge about the cardiovascular system's complexity, the authors found that the nonlinear methods of HRV analysis are best suited for this purpose [102]. For the analysis of non-linear signals i.e., HRV and SCR, nonlinear approaches discussed in the literature are Shannon entropy, Approximation entropy (ApEn), Sample entropy, Permutation entropy, Quadratic entropy, Quadratic sample entropy, DFA, etc. [91] [93] [115-125].

The SE was developed by Richman and Moorman [93] as a statistical measure to investigate the irregularity or complexity of time-series signals such as EEG and ECG. SE is the modified version of the AE. Because of AE's dependency on the data's length and the self-matching of the vector pairs, it is unsuitable for many applications. Furthermore, AE requires a certain amount of data to produce reliable results. AE may offer erroneous results or fail to deliver relevant insights if the data is too short [126]. There are various modified versions of SE, such as permutation entropy [121], multiscale entropy [127], Weighted multivariate composite multiscale sample entropy [128], local sample entropy (LSampEn) [129], cross-sample entropy [130], etc.

Byun et al. [131] investigated major depressive disorder by examining the HRV signal of 30 participants using SE, AE, FE, Shannon entropy, and some linear methods. The authors found that the entropy analysis of HRV signals can be a promising tool for such applications. Porta et al. [126] have investigated the HRV signals using two methods: the linear model-based approach and the nonlinear model-free approach. Baumert et al. [132] have investigated the variations in the entropy of RR and QT interval variability during two types of stress, i.e., orthostatic, and mental stress.

In this research paper, authors have applied SE and FE along with time domain parameters such as SDRR, RMSSD, and HF power for analyzing the complexity of the RR and QT interval variability. Wejer et al. [119] have transformed the HRV signals into patterns. The researchers have examined the complexity of the heart rhythms during the head-up tilt test using the entropy of these patterns. Porta et al. [133] have investigated the nonlinearity of short-term HRV under different physiopathological states using detrended fluctuation analysis (DFA), the recurrence plot base measure (RQA), and the surrogate data analysis (SDA). Ribeiro et al. [134] have investigated various nonlinear measures for their systematic review article for analyzing the fetal heart rate and found that measures based on entropies, such as SE and multiscale entropy, are the most effective measures for this. Time-domain indices involve measuring SDNN, RMSSD, and other statistical measures of HRV. The frequency-domain analyses of the power spectral density of HRV. It is usually categorized into low-frequency (LF), high-frequency (HF), and very-low-frequency (VLF) bands. Nonlinear methods assess the complexity of HRV by using SE, AE, FE, and QE methods.

In the last two decades, the use of multiresolution analysis (MRA) has been increased for the analysis of HRV signals. For the multiresolution analysis of HRV, the most used approaches are Wigner Ville distribution (WVD), short-time Fourier transforms (STFT) and wavelet transforms [14] [135-138]. The fundamental issue with the STFT is its constant lack of flexibility in resolution. The WVD spectrum has various artifacts and negative values that correspond to negative energy. Therefore, the wavelet transform is the most effective method for presenting non-stationary data.

As stated in previous works, numerous wavelet basis functions exist in the wavelet toolkit. Adopting current wavelets would have the fundamental issue that their selection

would be largely dependent on the signal being studied. Therefore, because of their non-signal-specific nature, existing wavelets cannot be used to correctly fetch the fluctuations of heart rate variability in various postures. The choice of the right wavelet is an essential part of evaluating HRV fluctuations from an analytical standpoint. These customized wavelets are known as matched wavelet that matches the properties of the signals that need to be analyzed.

A matched wavelet has been created by Rawal et al [66] for the analysis of menstrual cycle HRV data. Toth and Toth [139] developed an innovative wavelet for the identification of fault bearings, whereas Deak K et al [140] chose the optimum wavelet for predicting the size of manufacturing flaws for the tapered roller bearing. Quellec et al [141-142] used optimum wavelet for microaneurysm detection in retina graphs as well as content-based picture retrieval in medical databases. In the Musical Sounds, Duraipandian M [143] used Adaptive Algorithms for Signature Wavelet Recognition, whereas a band-limited orthonormal wavelet is also developed for a given signal [99]. Strela et al [144] have employed multiwavelets in the filter bank for image and signal processing of discrete-time signals. Shark et al. [145] developed an optimal method for matching arbitrary transient signals using wavelets. Rawal et al [70] have designed a matched wavelet based on a genetic algorithm for the analysis of HRV.

Based on the extensive survey of literature for analyzing the HRV variation for postural change activity and its relationship with SCR in young adults using signal processing analysis methods, the following are the drawbacks spotted in the literature survey-

1. Most of the work is based on analyzing the HRV only for the postural change, however, its relationship with SCR is not analyzed.
2. Also, no prior study has examined HRV variations between the supine and standing postures in conjunction with skin conductance response.
3. For a majority of subjects, linear methods were unable to distinguish the difference in HRV between supine and standing postures.
4. Additionally, nonlinear, and multi-resolution techniques can identify many anomalies and minor modifications in the behavior of the heart rate in a variety of pathological diseases. However, these techniques have not shown to be reliable in

identifying HRV fluctuations for the activity of postural change in the maximum number of individuals. They are not as accurate in detecting HRV fluctuation as would be anticipated for physiological signals.

Therefore, there is a pressing requirement to create HRV analysis techniques that can precisely detect the HRV differences between various body positions in young adults and pinpoint their relationship with SCR.

1.6 Objective of this research work

In young, healthy individuals, HRV and SCR analyses are effective tools for examining the physiological impacts of physical activity, such as postural movement from one posture to another. There are already several tools available for HRV measurement and assessment, but the methods currently in use are not enough accurate. Numerous researchers have come up with some new techniques for HRV analysis, although the results from the traditional techniques are inconsistent. Therefore, it is necessary to standardize the methods that are used to assess and analyze the signals associated with cardiovascular variability. The field of HRV research is still expanding and actively being researched. Despite this ongoing development and exploration, a few issues are still unresolved. To ascertain an individual's health problems, it is important to decode HRV fluctuations utilizing signal processing techniques as the body shifts from one position to another and to correlate this response with skin conductance.

So, the main objectives of this research work are-

1. To create a Heart Rate Variability (HRV) and Skin Conductance database at various body points.
2. To apply Linear methods of HRV analysis and find the relationship between Skin Conductance and HRV.
3. To propose a Non-Linear method for HRV analysis and then establish the correlation between Skin Conductance and HRV.
4. To develop the Multi-Resolution method for HRV analysis and further explore the relation between Skin Conductance and HRV.

1.7 Proposed Methodology

To achieve the above-mentioned objective, the methodology has been proposed as shown in Figure 1.7.

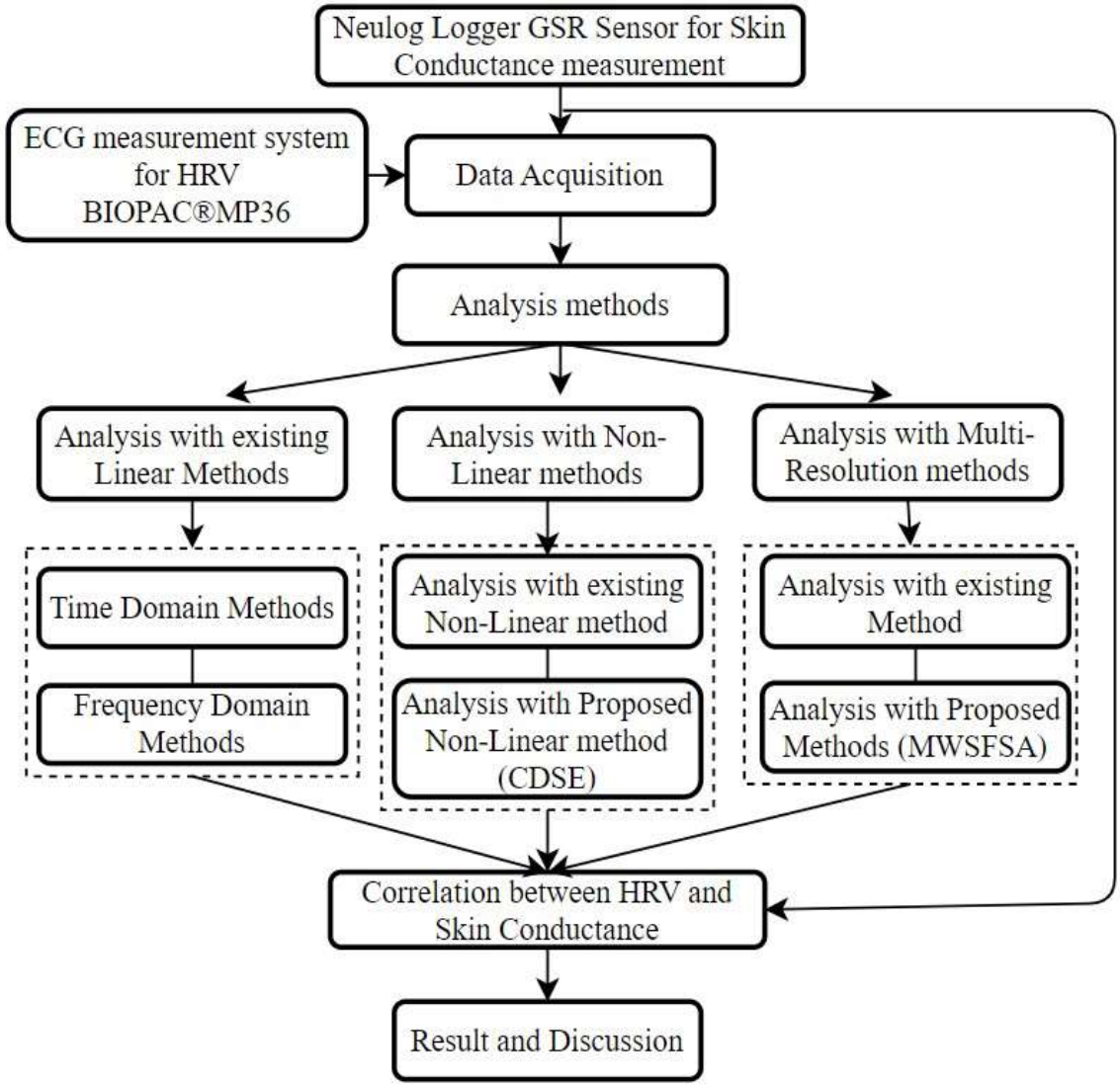

Figure 1.7 Flowchart of the Methodology

1.8 Thesis Organization

The structure of the thesis has been organized into 6 chapters as follows:

Chapter 1: An overview of the cardiac system, a summary of the physiological background, and information on the procedures for HRV, SCR, and HRV analysis are

all covered in the chapter. The objectives and a literature review are also presented in this chapter, along with the necessity for further research in this field.

Chapter 2: In this chapter, numerous recording-related concerns are covered in detail, including the protocols used in the recording as well as information about the experimental procedures utilized for this study.

Chapter 3: Chapter 3 reviews time domain and frequency domain linear HRV analysis techniques. It is critical to investigate the usefulness of various linear time domain and frequency domain approaches in detecting HRV changes between postures and their relationship to SCR.

The investigation of the linear HRV methods on the recorded dataset revealed that they were unable to distinguish between the sympathetic and parasympathetic control of the heart in various positions for a large number of participants.

Chapter 4: Chapter 4's primary goal is to use sample entropy analysis to circumvent the drawbacks of traditional linear HRV analysis techniques.

After Analysing the HRV signal using sample entropy analysis, it is found that the accuracy of detecting the postural variation is increased but not as much as expected. In traditional SE, some limitations have been identified by the authors: firstly, the distance is calculated using only the Chebyshev distance function which limits the use of sample entropy to decode the deeper information of the time series data. Secondly, the relative inconsistency occurs in the case of small data length. To eliminate these problems of SE, a novel method is developed in this paper in which different distance functions are used for the maximum extraction of information from the biological signal.

Chapter 5: Following a review of the available research, multiresolution analysis (MRA) techniques have become a potent tool in clinical applications relating to cardiovascular health. However, the best wavelet to use depends on the HRV signal. Determining which one produces the optimal wavelet for a given application is thus fundamentally problematic. This can occasionally result in a condition being misdiagnosed.

Conventional wavelets were initially applied and displayed limited efficacy in accurately capturing the desired trend. To address this limitation, matched wavelets were developed for each subject's HRV signal, considering its unique characteristics and properties. These specifically matched wavelets- Matched wavelets using the Stochastic fractal search algorithm (MWSFSA) were developed for each HRV signal in supine and standing postures.

The wavelet filter coefficients were meticulously optimized, and the HRV signals were reconstructed using these optimized coefficients. Subsequently, the LF/HF ratio of the reconstructed signals underwent meticulous evaluation, both in the supine and standing postures.

Further, the LF/HF ratio was calculated for the developed matched wavelets and conventional wavelets (db2 to db6), and there comparative analysis was performed. Among all the methods tested, MWSFSA demonstrated superior performance.

CHAPTER 2

METHODS AND MATERIALS

The electrocardiogram (ECG), which provides the cardiac input data used in HRV analysis, is by far the most crucial component. Numerous electrical heart abnormalities can be found using the ECG signal. Similarly, skin conduction response which is also known as electrodermal behavior is analyzed to evaluate the impact of different physiological activities on ANS. When the amount of sweat is altered in ducts, variations are observed in the response of SCR. Electro-dermal activity (EDA) is described as an indicator of variations in the skin's electrical conductance. This chapter presents several challenges that arise when recording an ECG and SCR, including the type of recording device, different noise sources, artifacts, and environmental electrical interference.

2.1 Overview

HRV is the phrase used to describe the variations that occur between heartbeats. The autonomic nervous system is responsible for these variations. The skin conductance response is the electrical conductivity of human skin. Numerous recording-related concerns are covered in detail, including the protocols used in the recording as well as information about the experimental procedures utilized for this study.

2.2 Technical and Clinical Procedures

There are a few requirements that must be met to accurately capture an ECG signal, and they are as follows:

- The selection of sampling frequency is an important point for the recording of the ECG signal. The recommended range is 250 to 500 Hz. A very low-frequency range can cause a jitter while estimating the R-wave fiducial point. This jitter problem can be fixed using an interpolation algorithm [1].

- The accurate selection of the QRS fiducial point is crucial. It is recommended to utilize a thoroughly validated QRS fiducial point detection algorithm.
- The recorded HRV time series are not equally spaced in time due to physiological and technical disturbances. Therefore, to remove these artifacts, and improve the signal quality, interpolation can be used for preprocessing of the recorded signal.

There are a few requirements that must be met to accurately capture an SCR signal, and they are as follows [71]:

- The skin should be prepared before placing the electrodes. The skin of that particular area must be dry, and clean.
- The electrodes must be properly placed in the recommended area.
- The Sensor that is going to be used for the recording of SCR must be properly calibrated.
- The recommended sampling rate for SCR is a minimum of 10 Hz to capture the changes in the skin conductivity.
- The participants must be aware of the experiment. Their consent must be taken before the recording begins.
- A comfortable environment must be provided to relax the participants before the recording of SCR to avoid the effect of stress.
- The personal information of the participants must be kept confidential.

2.3 Recording Setup and Related Data

Data collection was carried out in two different bodily positions, namely, lying down and standing, with each position maintained for 10 minutes. The rest before and in between the recording is provided to settle the hemodynamic parameters of the body. For ECG recording the BIOPAC®MP36 system has been used at 500 Hz sampling frequency while the recording of SCR has been done using a Neulog Logger GSR sensor at 20 Hz sampling frequency. For ECG recording, the authors have used the Lead II derivation. For Lead II derivation, the electrodes are attached to the

corresponding points (lower left rib and right clavicle) on the wrist and ankles. Three Ag-AgCl electrodes were put on each participant's arms and legs. For SCR recording, the electrodes were attached to the first two fingers of the left hand of each participant. To ensure the best recording circumstances, each participant was given ample rest of approximately ten minutes in a supine posture to keep the disturbances minimal, following that the Participants' ECGs and SCRs were recorded for ten minutes in the supine posture. Afterward, the participant is relaxed for 10 minutes before commencing another 10 minutes of recording in a standing position. The RR intervals for all the ECG recordings were directly received from the BIOPAC®MP36 system. All subjects were given instructions to refrain from talking, coughing, or moving their hands, legs, or bodies during recording. Additionally, they were told not to eat or drink anything, previous to the recording. The recording procedure along with the attachments of the electrodes have been shown in Figure 2.1 and Figure 2.2.

2.4 Source of Interference in ECG and SCR Recording

For the recording of both signals, the electrodes placed on the human body externally can cause some interference. Other than this power line interference, muscle noise, artifacts due to the motion of the body, baseline wander, and radio frequency interferences can affect the quality of the recorded signal while recording the ECG and SCR signals [71] [146-147].

2.5 Self-Recorded Data of ECG and SCR

To achieve the objectives of this research work, the authors have recorded the ECG dataset of 70 participants using the BIOPAC®MP36 system at a 500 Hz sampling frequency and SCR using a Neulog Logger GSR sensor at a 20 Hz sampling frequency in different postures and examined the effect of postural shift on HRV. Recording was done in supine and standing postures for 10 minutes, for each posture. A flowchart of the recording of HRV and SCR is shown in Figure 2.3. The participating candidates are healthy young adults from the age groups of 18-25 years including both male and female participants. Before the recording, the authors obtained written consent from participants, and they were advised not to eat or drink for 2 hours before the recording

began. Table 2.1 represents the primary characteristics such as age, height, weight, BMI, and health status of the participants who participated in this research.

Figure 2.1 The Electrode placement for ECG and SCR recording

Figure 2.2 The Instrumental setup for ECG and SCR recordings

Table 2.1 Physical characteristics of participants

Characteristics of participants	**No.**	**Age in years**		**Height in cm**		**Weight in Kg**		**BMI**		**Health Status**
		Mean	SD	Mean	SD	Mean	SD	Mean	SD	
All participants	70	23.24	1.78	166.84	9.17	63.85	11.78	22.56	2.52	No medical history

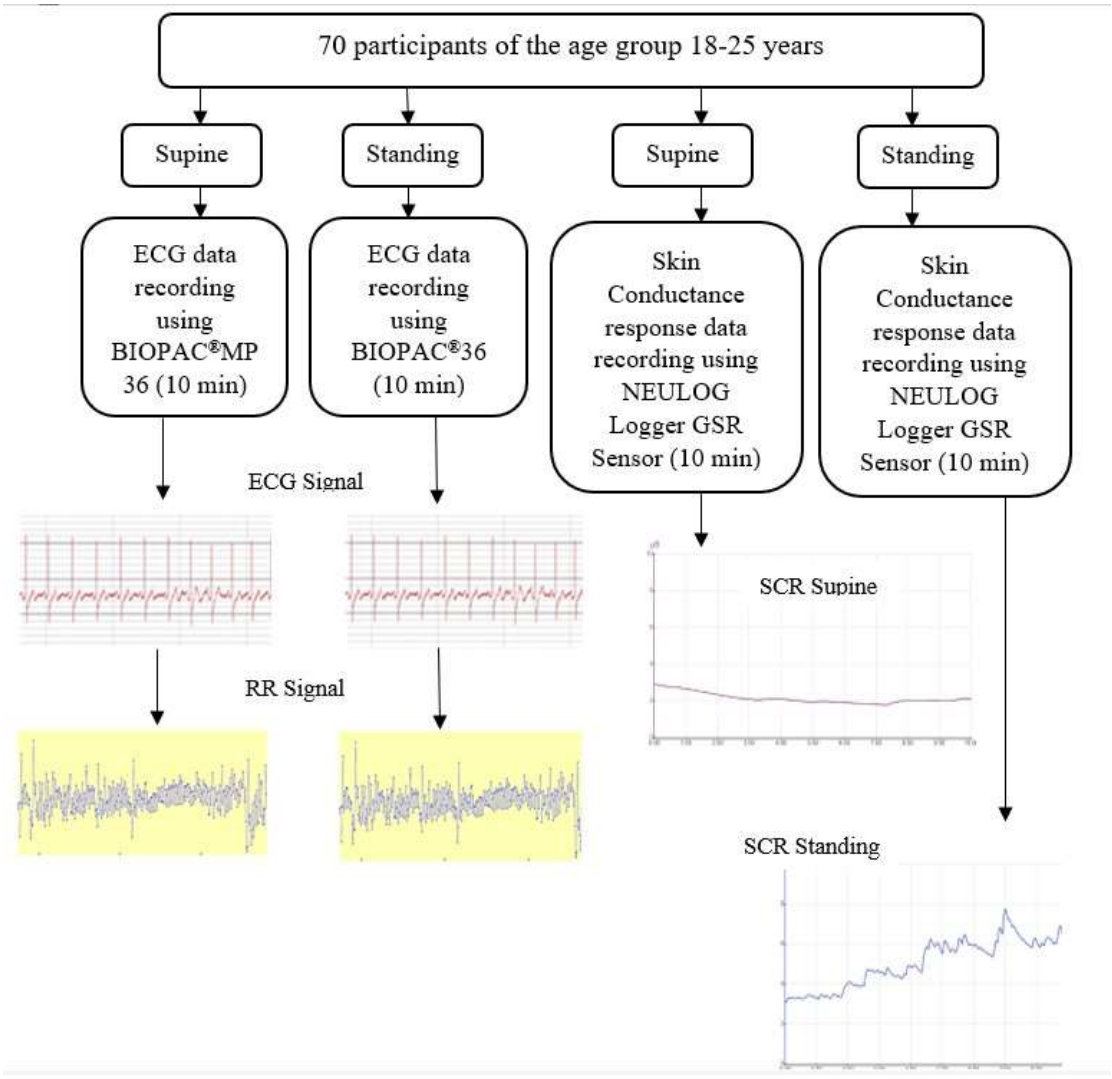

Figure 2.3 Flowchart of HRV and SCR data acquisition for different postures

2.6 Preprocessing of HRV

During the recording of the physiological signals i.e., ECG and SCR, various technical and manual disturbances occurred and caused the degrading of the quality of the recorded signal. There are various reasons for these artifacts such as poorly fastened electrodes, motion artifacts, susceptible noise, line interference, etc. These artifacts can cause the missing RR interval or sudden peak in SCR recording. As both HRV and SC are not equally spaced signals in time, to transform them into evenly spaced signals and enhance their physiological information, preprocessing is required. In the preprocessing of a time series two main approaches have been followed by researchers, one is the deletion of the ectopic beats by deleting some beats or samples [148], and another is the substitution of a better matching value by adding the substitute value through interpolation [149-151].

Interpolation

Interpolation is the process of creating new data points to equalize the distance between the original signals. It is a technique that is frequently used to lessen signal artifacts. Even though there are many interpolation techniques documented in the literature, the most popular ones include Linear [152-154] [14], Spline [14, 155-156], Berger [92, 157], and Cubic interpolation [158, 159, 160].

(i) **Linear Interpolation**

The easiest way of interpolating the data points into a straight line between two nearby data points is through the use of linear interpolation. The position along the line is then used to estimate the value at an intermediate point [161].

(ii) **Cubic Spline Interpolation**

In this method of interpolation, the data has been broken down into smaller subintervals, and each subinterval has been interpolated with a different cubic polynomial. By using this interpolation method, a continuous, smooth curve that traverses all of the data points is produced [162-163].

(iii) **Cubic Interpolation**

Each pair of neighboring data points in a cubic interpolation is interpolated using a single cubic polynomial. Each data segment is turned into a single cubic polynomial, and these individual polynomials are then joined to create the final curve. Using the cubic interpolation the resulting curve passes over every data point, but smoothness and continuity throughout the full dataset may not be guaranteed [159] [164].

2.7 Conclusion

The initial step in computer-aided diagnostics is to capture the important ECG characteristics. Additionally, a detailed explanation has been given of the precautions and procedures that need to be followed during the recording of the physiological signals. This chapter explained the technical and clinical recommendations for recording, the description of the recording instruments, the sources of interference during the recording, and the preprocessing of the recorded signals before analysis.

CHAPTER 3

TIME DOMAIN AND FREQUENCY DOMAIN ANALYSIS

The purpose of this chapter is to assess the currently used linear time and frequency domain HRV analysis techniques. It is crucial to assess the effectiveness of traditional methods of linear signal processing methods in detecting HRV fluctuations during the transitioning *i.e.*, supine to a standing posture.

3.1 Overview

Medical professionals and engineers have maintained an ongoing interest in recording and analyzing HRV signals over the years. In the field of biomedical engineering, two crucial physiological signals are HRV and SC. The autonomic nervous system regulates HRV [1].

A variety of both physical and emotional actions, including activities like physical exercise, jogging, aerobic exercises, social interactions, stressors, alterations in body position, moments of enthusiasm or irritation, and more, influence both sympathetic and parasympathetic responses. These effects can be evaluated through the measurement of SC and HR [11] [88]. During postural shifts, the heart's autonomic controls change. To get a deeper understanding of how the heart works, a variety of physiological techniques have been explored, including changing one's posture. Several tools are already available for HRV measurement and assessment, but the methods currently in use are not considered accurate. To understand how the postural change from supine to standing affects the body's autonomic regulation, it is important to

decode HRV variations using signal processing techniques. This chapter assesses the effectiveness of linear computation techniques that combine time domain and frequency domain methods for identifying HRV changes between the supine and standing positions.

To analyze the HRV, the time domain methods were first applied to the dataset of 70 participants in supine postures, the same time domain methods were then implemented for the standing postures dataset. In this work, the implemented time domain methods are SDNN, RMSSD, NN50, and pNN50. The effects of postural variation on heart function were then investigated using frequency domain techniques. Afterward, the correlation between HRV and SCR has been explored.

3.2 Conventional Linear HRV Analysis Methods

The regulation of cardiac functioning under both healthy and pathological circumstances depends strongly on the heart rate's variability. This chapter presents the linear analysis of HRV.

3.2.1 Time Domain Methods

To measure the intervals between successive normal complexes of heartbeats, time-domain methods are used. It is based on the statistical analysis of the NN interval [1] [165].

SDNN

SDNN stands for the NN interval's standard deviation. It measures the overall variability of the RR intervals between successive heartbeats over a specific period. SDNN measures the short-term and long-term variability of HRV. It can be calculated using eq. (3.1).

$$\text{SDNN} = \sqrt{\frac{1}{N}\sum_{i=1}^{N}(RR_i - RR_{av})} \tag{3.1}$$

Here, N = Sum of consecutive RR intervals,

RR_i = i^{th} *RR* intervals,

RRav = Average value of RR intervals.

RMSSD

The RMSSD can be calculated by using eq. (3.2). It reflects the parasympathetic modulation of ANS.

$$\text{RMSSD} = \sqrt{\frac{1}{N-1}\sum_{i=1}^{N-1}(RR_{i+1} - RR_i)^2} \tag{3.2}$$

Here, N = the total number of consecutive RR intervals,

RR_i = i^{th} *RR* interval,

RR_{i+1} = i^{th+1} number of *RR* intervals [165].

NN50

Neighbouring NN interval pairs which are greater than 50 milli seconds during the entire recording is known as NN50. It can be calculated by using eq. (3.3).

$$\text{NN50} = \sum_{i=1}^{N}\{|RR_{i+1} - RR_i| > 50ms\} \tag{3.3}$$

N = Overall number of RR intervals in the section that was chosen [165].

pNN50

It measures the percentage of RR interval differences longer than 50 ms in comparison to the total number of examined RR intervals. It can be calculated by using eq. (3.4)

$$\text{pNN50} = \frac{NN50}{N} \times 100 \tag{3.4}$$

N = Overall number of RR intervals in the section that was chosen [165].

3.2.2 Frequency Domain Methods

Fast Fourier Transform is the mathematical tool to break the signal in frequency components of a time series signal. The main spectral components of frequency domain analysis are the following [1].

Ultra-low frequency (ULF) The frequency range of this component is between 0.0001-0.003Hz

Very low frequency (VLF): 0.003-0.004Hz is the frequency range of this component.

Low Frequency (LF)

This band is used to represent the sympathetic and parasympathetic activity of ANS. 0.04-0.15Hz is the frequency range of the LF band [1].

High Frequency (HF)

This band represents the PNS activities. The range of the HF band lies between 0.15 to 0.40 Hz [1].

LF/HF

The balance between sympathetic and parasympathetic activity is represented by the LF/HF ratio [165-167].

3.3 Experimental Findings and Related Discussion

In this chapter, the linear analysis of HRV has been done using time and frequency domain methods. The performance measure of applied methods is represented by the 'Accuracy' and 'mean value'. The performance of the applied methods cannot be evaluated only by one metric 'mean value' if the evaluation is related to human health. In such instances, it is crucial to conduct evaluations on an individual basis for each subject. This is important since the reliability of the mean value may not always be sufficient in research with a large number of participants.

As a result, accuracy has been employed in this work as a performance indicator to assess the effectiveness of applied approaches, which were founded on the capacity to identify variations in HRV in a particular subject.

In plainer terms, accuracy is the proportion of individuals among all subjects for which the method can reliably identify HRV fluctuations.

$$\text{Accuracy} = \frac{Number\ of\ \ Subjects\ having\ correct\ relationship\ of\ HRV\ variation\ for\ postural\ variation}{Total\ number\ of\ subjects}$$

The relationship of HRV variation for the postural change is said to be correct if the HRV variation in standing is less than the supine posture as shown in eq. (3.5) [108] [168-169].

$$HRV_{ST} < HRV_{SU} \quad (3.5)$$

Where HRV_{SU} stands for the value of HRV parameter in supine posture, while HRV_{ST} stands for the value of HRV parameters in standing posture. It suggests that a person's HRV in a standing posture is lower than a person's HRV in a supine posture. The deployed algorithms are deemed accurate if they successfully identify each subject's HRV fluctuations between postures as described in (3.5). If the HRV analysis methods successfully identify each subject's HRV fluctuations between postures as described in equation (3.5), they are said to be 100% accurate. Therefore, by calculating subject-specific HRV fluctuations rather than the mean of all individuals, our study gives another dimension of heart rate variation analysis which will be more believable and appropriate for our investigation. In this research work, the performance parameter accuracy is employed to describe the subject-specific fluctuations in HRV between the phases. One significant advantage of using accuracy as a measure for HRV analysis rather than mean values is that accuracy provides a precise depiction of any HRV analysis method's performance.

The findings are presented as a comparative analysis of several linear algorithms and their performance has been evaluated using accuracy as a performance parameter. Time domain approaches such as RMSSD, SDNN, NN50, and pNN50 are used in this thesis work. The frequency domain analysis has been performed by LF, HF, and LF/HF ratio.

3.3.1 Results of Linear Methods

The results have been presented as a mean value of 70 subjects in supine and standing postures and their performance has been analyzed by the performance metric ‘Accuracy’ in a subject-wise manner as shown in Figure 3.1.

(I) Time Domain Methods

The examination of time domain parameters, specifically SDNN, RMSSD, NN50, and pNN50, is used in the linear assessment of HRV in a group of 70 participants. The goal is to assess the impact of posture changes on HRV and calculate the corresponding significance levels (p-values), as shown in Table 3.1.

Table 3.1 Time domain analysis of HRV in supine and standing postures

S. No.	Time Domain parameters	Supine Posture	Standing Posture	p-value
1	SDNN	46.35 ± 18.61	39.82 ± 18.89	1.08E-06
2	RMSSD	40.39 ± 23.29	23.84 ± 19.97	5.52E-12
3	NN50	131.7 ± 109.9	44.12 ± 57.87	4.57E-11
4	pNN50	19.76 ± 17.38	5.7 ± 8.38	4.73E-12

From Table 3.1, it is found that the time domain metrics of HRV have higher values in the supine posture, and their value drops when the postural change activity is taken from the supine to the standing position. This means that the sympathetic dominance of ANS increased in standing posture. The higher value of RMSSD in the supine indicates that the parasympathetic activation is higher in the supine posture. A significant difference between the value of supine and standing posture has been found. Accuracy of the time domain methods has been calculated to capture the postural variation of HRV correctly, and it is found that the pNN50 and NN50 can detect this variation with 81.42% accuracy. On the other hand, the accuracy of RMSSD is 78.57%, and SDNN is 76.87% as shown in Figure 3.1.

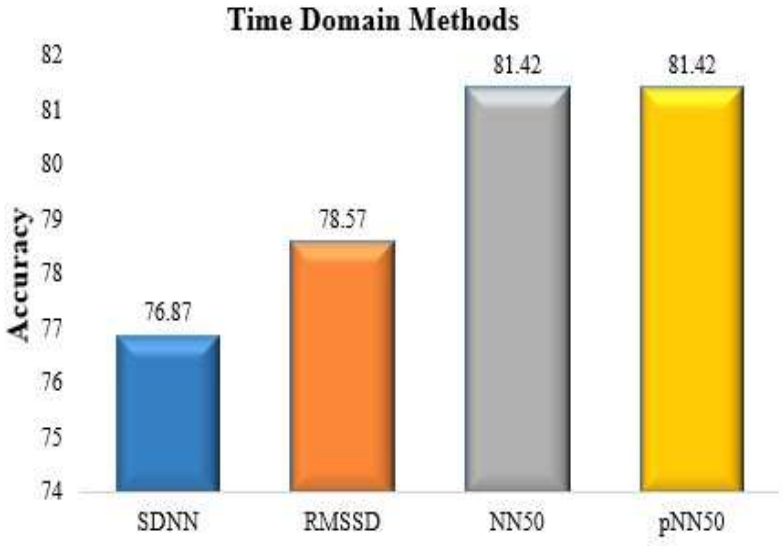

Figure 3.1 The Performance analysis of time domain methods

(II) Frequency Domain Methods

After the Time-domain analysis of HRV, the spectral analysis has been performed for chasing better accuracy. For the frequency domain analysis of HRV signals of 70 subjects, the parameters- LF, HF, and LF/HF ratio have been evaluated as shown in Table 3.2. The value of frequency domain parameters has been presented as the mean value of 70 subjects along with the standard deviation. The significant difference between the postures has been analyzed by t-test analysis.

Table 3.2 Frequency domain analysis of HRV in supine and standing postures

S. No.	Frequency Domain Parameters	Supine Posture	Standing Posture	p-value
1	Low Frequency	559.92 ± 499.88	665.25 ±636.38	0.0278
2	High Frequency	716.13 ± 676.10	273.58 ±402.34	2.29E-10
3	LF/HF ratio	1.23 ±1.07	3.53 ±2.82	6.44E-10

The obtained results indicate that there is a momentous increment in the LF component when the position has been changed from supine to standing. The high-frequency component decreases when the position transition takes place. The LF/HF ratio increases in the standing postures. A conclusion can be made from the results, that the sympathetic influence of the ANS increased when posture is changed from supine to standing. The increased value of LF in standing posture indicates the sympathetic dominance of ANS in this posture, while higher HF in supine posture shows that parasympathetic dominance is higher in supine posture. Since LF/HF represents the equilibrium between the sympathetic and parasympathetic nervous systems, its larger value in the standing position denotes a higher sympathetic dominance relative to the parasympathetic dominance of the ANS. In Table 3.2, the *p*-value indicates that the values of HF and LF/HF ratio are significantly different for supine and standing postures.

For accurately detecting the postural variation of HRV, the accuracy of the applied methods has been calculated to assess the performance of the frequency domain

methods, and it has been discovered that the LF/HF ratio is capable of detecting this variation with 85.71% accuracy.

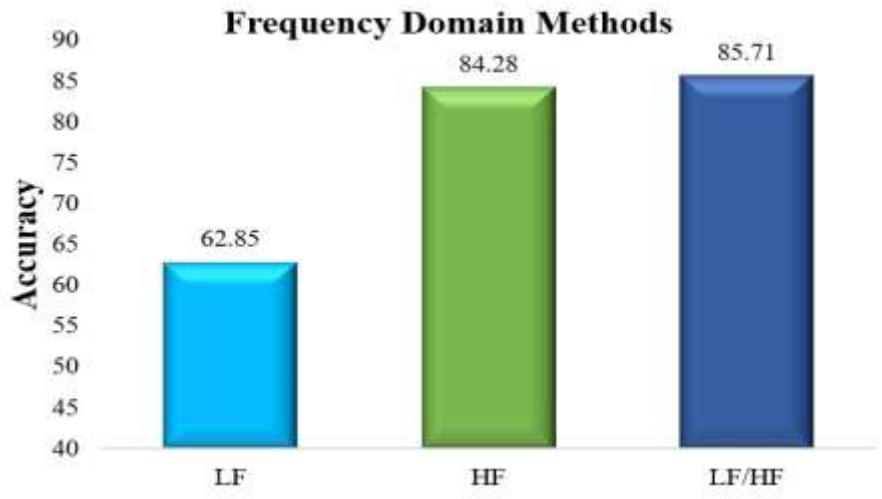

Figure 3.2 The Performance analysis of frequency domain methods

However, as shown in Figure 3.2, LF's accuracy is 62.85% and HF's accuracy is 84.28%.

3.3.2 The Comparative Analysis of Performance between Linear Methods for Postural Change Activity

As discussed earlier, in this research work, SDNN, RMSSD, NN50, and pNN50 for time domain analysis and LF, HF, and LF/HF metrics have been used as frequency domain analysis of HRV for evaluating the effect of postural change on HRV. For performance analysis of the applied methods, the accuracy of each method has been calculated to evaluate which method is more efficient in detecting subject-specific HRV fluctuations for postural variation activity. The performance graph of applied linear methods has been shown in Figure 3.3.

The subject-specific analysis shows that NN50 and pNN50 can identify postural variation correctly is higher than RMSSD and SDNN. The accuracy of pNN50 and NN50 is 81.42 %, while the accuracy of SDNN and RMSSD is 76.87% and 78.57% respectively. Also, the frequency domain metric, LF/HF ratio outperforms other linear methods. The accuracy of the LF/HF ratio for correctly identifying the postural change

from supine to standing posture is highest at 85.71% as it can detect the HRV variation for postural alteration in the maximum number of subjects.

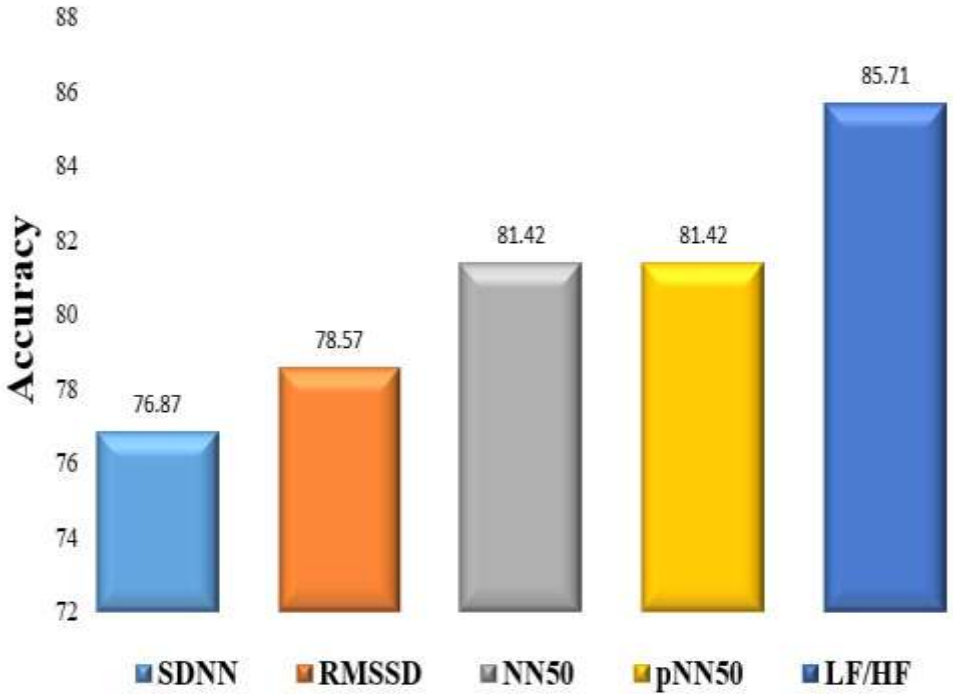

Figure 3.3 Performance analysis of Linear methods

3.3.3 Impact of postural change on HR and SCR and its relationship with HRV

The influence of postural variation on SCR and heart rate of 70 subjects has been analyzed and presented in Table 3.3 as mean value and SD. The significant difference between the values of different postures has been evaluated by performing a statistical analysis and given as a p-value.

The mean value of skin conductance and heart rate has been given for the two body positions. As we can see from the results the value of SCR and HR has been increased when the posture of the body is changed from a supine to a standing position. Table 3.3 concluded that the mean value of skin conductance and HR is higher in the standing position which implies lower HRV in this position.

Table 3.3 Effect of Postural Change on SCR and HR

S. No.	Physiological Signals	Supine Posture	Standing Posture	p-value
1	SCR	1.79 ±2.03	2.44 ±2.35	4.00E-05
2	HR	76.80 ± 11.01	93.94 ±12.93	3.67E-27

These obtained results indicate that the increment of the SCR and HR in the position of standing regulates the sympathetic activation in this position. It also indicates that both SCR and HR have a positive correlation for the postural change from supine to standing.

3.4 Conclusion

This chapter presents the linear evaluation of the HRV signal of 70 subjects which is recorded in the supine and standing posture. For this purpose, time domain and frequency domain methods have been implemented on the recorded dataset to evaluate the postural variation of HRV during postural changing activity from the supine position to the standing position. It is found that the frequency domain method (LF/HF ratio) is more accurate in detecting the postural variation of HRV between postures than all the applied time domain methods. However, the accuracy of the LF/HF ratio is not sufficient when the analysis is related to the physiological signal. So, there is a need to develop a method that can more precisely detect the HRV variation accurately between postures.

The relation between SCR, HR, and HRV is also evaluated. A positive correlation is observed between SCR and HR, while an inverse relation has been found between SCR and HRV.

Chapter 4

Sample Entropy Analysis

This chapter provides information on the Sample Entropy (SE) analysis which is used to identify changes in HRV signals caused by activity that involves postural adjustment. In this chapter, a novel approach called CDSE for identifying HRV variations as well as SCR between the two body positions to overcome the shortcomings of sample entropy analysis has been proposed. To validate the proposed method, a comparative study of the new method and traditional SE utilizing statistical parameters has been presented in this chapter. Afterwards, the correlation between HRV and SCR has been discussed.

4.1 Overview

The autonomic nervous system regulates HRV and SCR. The impact of physical activity on the ANS can be assessed by evaluating the response of skin conductance and HRV [1] [170-171]. A wide range of physical and emotional behaviors, including activities like working out, running, engaging in aerobics, social interactions, stressors, alterations in body position, moments of enthusiasm or agitation, and so forth, influence both sympathetic and parasympathetic activity. These influences can be gauged by monitoring SC and Heart HR [11] [88] [172].

In the previous chapter, the analysis of HRV has been performed using linear methods, but their accuracy for detecting the postural variation is low. Various researchers suggested that HRV is a nonstationary signal, so the nonlinear analysis of HRV would be more accurate for the detection of postural variations between different body postures [102]. Thus, in this chapter, an attempt has been made to analyze the HRV using two nonlinear methods called approximation entropy (AE) and sample entropy (SE). Afterward, a novel nonlinear method based on sample entropy analysis was developed for the analysis of HRV.

4.2 Existing Nonlinear Methods of HRV Analysis

Numerous nonlinear signal processing techniques have been developed during the past few decades to examine the nonlinear dynamics from a novel perspective. The nonlinear methods which are implemented in this research work are approximation entropy and sample entropy.

4.2.1 Approximation Entropy Analysis

Pincus S. M. [120] introduced AE, which is a tool for quantifying anomalies in HRV time series. It is used to assess the consequences of pathological signal abnormalities. The values of AE have been calculated using 3 variables, embedding dimension '*m*', length of signal '*N*', and tolerance '*r'*. The complexities in the HRV signal indicate the higher value of AE [108]. The use of AE for calculating complexity has become outdated, especially when dealing with short data sequences and extensive embedding dimensions, as the adverse effects of bias become increasingly evident. In its place, a significantly less biased assessment of conditional entropy, known as S.E., has taken over. [126]. Although authors found that AE is less sensitive to short-term fluctuations and reflects better signal's overall complexity. Authors discovered that AE is more resilient and robust when dealing with distorted signals or missing data points. However, AE should be used in conjunction with other methods for a more comprehensive evaluation of the HRV signal.

4.2.2 Sample Entropy Analysis

Richman and Moorman have proposed SE to overcome the flaws of AE. SE does not depend on the length of the signals and is free from self-matches of vector pairs. Embedding, dimension *'m'*, tolerance value *'r'*, and the signal *'N'* length are the three fundamental parameters for evaluating the values of SE analysis. The SE is calculated for physiological signals using conditional probability and by evaluating its negative logarithm of the consecutive template vector pairs E and F [93]. The value of SE can be calculated as Eq. (4.1)

$$SE = -\log E/F \tag{4.1}$$

Where $Q_{m+1}(i)$, and $Q_{m+1}(j)$ are the two vectors. E represents the vector pairs that having maximum distance as calculated in Eq. (4.2)

$$d\,[Q_{m+1}(i), Q_{m+1}(j)] < r \tag{4.2}$$

Similarly, $Q_m(i)$, and $Q_m(j)$ are the two vectors. F represents the vector pairs having maximum distance as calculated in Eq. (4.3)

$$d\,[Q_m(i), Q_m(j)] < r \tag{4.3}$$

4.3 Limitation of Existing Sample Entropy

In traditional Sample entropy, only a single distance function has been used to calculate the distance between two template vectors. It is based on a single distance function which does not provide sufficient features when analyzing the postural change. Further, it is also inconsistent for small-data length signals [173]. It is also not focused on increasing the accuracy of detecting postural differences accurately by analyzing the HRV. Also, various modified versions of SE have been developed in the literature, dealing with signal complexity and short data length. However, these methods are not focused more on evolving the dimension of using a multi-distance function. Because calculating the distance between vector pairs is essential in SE estimation.

4.4 Objective of the proposed SE method

So, this research work is based on overcoming the limitations of the existing research work. The objectives of this proposed work are as follows:

- To develop a method that can extract the maximum information from the signal and is compatible with the analysis of short data length and long data length signals.
- To develop a method compatible with synthetic signals and real-time data such as HRV.
- To develop a method that can accurately detect the postural difference between supine and standing postures for a large number of participants.

4.5 Proposed Method

To address the limitations of conventional SE, a novel approach measured by composite distance function was proposed for the full extraction of information from biological

signals such as HRV and SC. Afterward, different noise signals with different data lengths were used to demonstrate the efficacy of the proposed method. To overcome the relative inconsistency of evaluated entropy for short data length signals. For this purpose, HRV and SCR signals have been acquired. After that, the successive R peaks have been taken from the ECG signal, which is known as the RR signal.

Step 1: Let the original RR Signal (q) be represented by Eq. (4.4) and shown in Figure 4.1-

$$q = \{q_1, q_2, \ldots\ldots\ldots\ldots\ldots\ldots\ldots q_N\} \tag{4.4}$$

where N= Total number of samples.

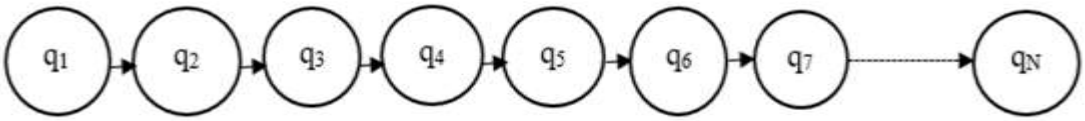

Fig. 4.1 Original RR Signal

Step 2: It is difficult to analyze the whole signal in one go and extract the maximum information from the data. To extract the maximum information from the signal, different combinations and methods need to be explored. So we divided the signal into two series and named them as odd-numbered and even-numbered sample series.

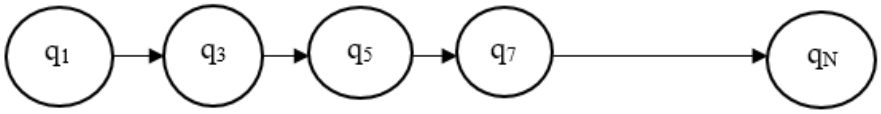

Fig. 4.2 Odd Sample Series

Odd sample series- Here odd series is created with the odd-numbered samples from the original RR signal as shown in Figure 4.2. Let the odd series be denoted as q (o) as shown in Eq. (4.5). Where 'o' varies from 1 to N1 sample. When the number of the sample is odd, N1 will be equal to N. While the number of samples is even, N1 will be equal to N-1.

$$q\,(o) : 1 \leq o \leq N1, \tag{4.5}$$

Where, N = Odd, N1 = N

N = Even, N1 = N-1

Even sample series- Here even series is constructed by selecting the even-numbered samples from the original RR signal as shown in Figure 4.3. Let even series be denoted as q (e) as given in Eq. (4.6), where 'e' varies from 2 to N2 sample. When the number of samples is even, N2 will be equal to N. While the number of samples is odd, N2 will be equal to N-1.

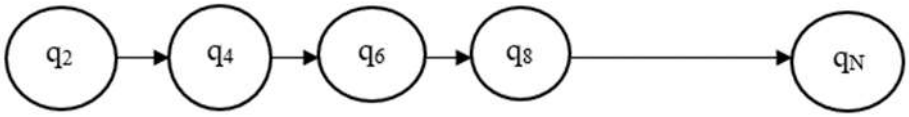

Fig. 4.3 Even Sample Series

$$q\ (j) : 2 \leq e \leq N2, \tag{4.6}$$

Where, N = Odd, N2 = N-1

N = Even, N2 = N

Step 3: *Construction of vector pair*- Construct template vector based on embedding dimension 'm' for q (o) (odd sample). The embedding dimension determines how many samples are contained in each vector pair. Where $y_m(i)$ is the vector of 'm' data points from q(i) to q(i+m-1) as given in Eq. (4.7).

$$y_m(i) = q(i+\varphi) \tag{4.7}$$

where φ is, $0 \leq \varphi \leq m-1$

and i is, $1 \leq i \leq N- m+1$

Step 4: ***Composite Distance function***- The match of the vector pair $[y_m(i), y_m(\varphi)]$ occurs whenever the distance between two template vectors is less than a predefined tolerance 'r'. In conventional sample entropy, the distance is calculated using the Chebyshev distance method (d_1), and only the largest element-wise difference between the two-state vectors is considered in this method. However, there are several methods for determining the distance between two template vectors [173]. In the proposed method, the distance is calculated using the composite distance function to obtain the maximum information from the signal.

The composite distance function in this proposed method is made up of three distance methods that are used to measure the distance between two vectors, and these three distances are denoted as d_1, d_2, and d_3. where-

d_1= is the maximum difference between individual template vectors. (As used in conventional SE)

d_2= is the absolute relative distance between two individual template vectors.

d_3= is the straight-line distance between two individual template vectors.

All three distances [174] can be calculated as given in Eq. (4.8), Eq., (4.9) and Eq. (4.10)-

$$d_1\,[y_m(i),\, y_m(\varphi)] = max\{\ |q(i+j) - q(\varphi+j)|\ :\ 0 \le j \le m-1\ \} \tag{4.8}$$

$$d_2\,[y_m(i),\, y_m(\varphi)] = \sum_{j=1}^{m-1} |\,q\,(i+j) - q\,(\varphi+j)\,| \tag{4.9}$$

$$d_3\,[y_m(i),\, y_m(\varphi)] = \sqrt{\sum_{j=1}^{m-1}(q(i+j) - q(\varphi+j))^2} \tag{4.10}$$

Step 5: *Matched vector pair count*- If the distance between two vector pairs is less than or equal to a tolerance 'r', then [y_m(i), y_m(φ)] is called an m-dimensional matched vector pair. Here we have calculated three matched vector pair counts as B_1, B_2, and B_3 using '*m'* and different distances d_1, d_2 and d_3 respectively.

(a). If $$B_i = \begin{cases} 1 & when \quad d_1[y_m(i), y_m(\varphi)] \le r \\ 0 & when \quad d_1[y_m(i), y_m(\varphi)] > r \end{cases} \tag{4.11}$$

After the calculation of Bi for the value of 1 or 0 based on d_1, m, and tolerance r as given in Eq. (4.11), B_1 will be calculated as shown in Eq. (4.12)-

$$B_l = \sum B_i \tag{4.12}$$

Where B_1 is the sum of all the values of Bi.

(b). Let B_2 be the count of all matched vector pairs for distance d_2 as given in Eq. (4.13)-

$$\text{If } B_j = \begin{cases} 1 & when \quad d_2[y_m(i), y_m(\varphi)] \le r \\ 0 & when \quad d_2[y_m(i), y_m(\varphi)] > r \end{cases} \tag{4.13}$$

Based on the value of d_2, embedding dimension, and tolerance r, Bj is calculated as 1 or 0. Then B_2 will be calculated as in Eq. (4.14) -

$$B_2 = \sum B_j \tag{4.14}$$

Where B_2 is the sum of all the values of B_j.

(c). First, we calculated B_z for the value of 1 or 0 using distance d_3 as given in Eq. (4.15)

$$\text{If } B_z = \begin{cases} 1 & when \quad d_3[y_m(i), y_m(\varphi)] \leq r \\ 0 & when \quad d_3[y_m(i), y_m(\varphi)] > r \end{cases} \tag{4.15}$$

B_3 will be calculated as given in Eq. (4.16)-

$$B_3 = \sum B_z \tag{4.16}$$

Where B_3 is the sum of all the values of B_z.

Step 6: Similarly, repeat step (3) to step (5) to obtain m+1 dimensional matched vector pairs that will give A1, A2, and A3. Where A1, A2, and A3 are the three matched vector pair counts as given in Eq. (4.18), Eq. (4.20), and Eq. (4.22) respectively.

$$\text{(a). If } A_i = \begin{cases} 1 & when \quad d_1[y_{m+1}(i), y_{m+1}(\varphi)] \leq r \\ 0 & when \quad d_1[y_{m+1}(i), y_{m+1}(\varphi)] > r \end{cases} \tag{4.17}$$

After the calculation of Ai as given in Eq. (4.17), A_1 will be calculated as shown in Eq. (18) -

$$A_1 = \sum A_i \quad , \tag{4.18}$$

Where A_1 is the sum of all the values of A_i.

$$\text{(b). If } A_j = \begin{cases} 1 & when \quad d_2[y_{m+1}(i), y_{m+1}(\varphi)] \leq r \\ 0 & when \quad d_2[y_{m+1}(i), y_{m+1}(\varphi)] > r \end{cases} \tag{4.19}$$

Then A_2 will be calculated as shown in Eq. (4.20), Where A_2 is the sum of all the values of A_j.

$$A_2 = \sum A_j \ , \tag{4.20}$$

$$\text{(c). If } \quad A_z = \begin{cases} 1 & when \quad d_3[y_{m+1}(i), y_{m+1}(\varphi)] \leq r \\ 0 & when \quad d_3[y_{m+1}(i), y_{m+1}(\varphi)] > r \end{cases} \tag{4.21}$$

Now A_3 will be calculated as a sum of all the values of A_z as shown in Eq. (4.22)-

$$A_3 = \sum A_z \,, \tag{4.22}$$

Step 7: In the conventional method [93], SE is defined as the negative logarithm of the ratio of A to B. Here, A is the count of the m+1 dimensional matched vector pair and B is the count of the m-dimensional matched vector pair as given in the following Equation.

$$\textit{Conventional Sample Entropy (x, m, r)} = S.E._{conventional} = -\log \frac{A}{B}$$

According to the above equation, the Odd sample entropy using different distances (d_1, d_2, and d_3) can be calculated as given in Eq. (4.23) to Eq. (4.25),

$$SE_{1_{odd}} = -\log \frac{A_1}{B_1} \tag{4.23}$$

Where $SE_{1_{odd}}$, the sample entropy of odd sampled series is calculated using distance d_1 and

$$SE_{2_{odd}} = -\log \frac{A_2}{B_2} \tag{4.24}$$

Where $SE_{2_{odd}}$, the sample entropy of odd sampled series is calculated using distance d_2.

$$SE_{3_{odd}} = -\log \frac{A_3}{B_3} \tag{4.25}$$

Where $SE_{3_{odd}}$.is the sample entropy of odd sampled series calculated using distance d_3.

Step 8: The sample entropy of the odd sample series can be calculated by taking the average of all the separately calculated sample entropies $SE_{1_{odd}}$, $SE_{2_{odd}}$, and$SE_{3_{odd}}$ using composite distance function is shown in Eq. (4.26).

$$\textit{Odd Sample Entropy-} \quad S.E._{odd} = \frac{SE_{1_{odd}} + SE_{2_{odd}} + SE_{3_{odd}}}{3} \tag{4.26}$$

Step 9: Repeat steps (3) to (6) for even-numbered samples q(e) and calculate $SE_{1_{even}}$, $SE_{2_{even}}$, and $SE_{3_{even}}$ from step (6) to (7).

Step 10: The sample entropy of an even sample series can be calculated by taking the average of all the separately calculated sample entropies $SE_{1_{even}}$, $SE_{2_{even}}$, and$SE_{3_{even}}$ using composite distance function is given in Eq. (4.27).

$$\textit{Even Sample Entropy-} \quad S.E._{even} = \frac{SE_{1_{even}} + SE_{2_{even}} + SE_{3_{even}}}{3} \tag{4.27}$$

Step 11: In the proposed composite distance sample entropy, the RR signal is first divided into odd and even sample series. For both series, the SE is separately calculated using different distance methods which are termed as $S.E._{odd}$ and$S.E._{even}$. The proposed sample entropy is calculated by taking the average of $S.E._{odd}$ and$S.E._{even}$ as given in Eq. (4.28).

$$\textit{Proposed Sample Entropy} = SE_{proposed} = \frac{S.E._{odd} + S.E._{even}}{2} \tag{4.28}$$

The proposed method's flowchart is depicted in Fig. 4.4 in a step-by-step format.

4.6 Experimental Results and Discussion

In this chapter, a new method has been introduced for the analysis of non-linear signals. The performance of the proposed method is validated, by implementing it on the different synthetic signals along with the conventional method. Then both methods have been implemented on the self-recorded data set. To get better results, the value of embedding dimension ‘m’ and tolerance ‘r’ have been selected as ‘2’ and ‘0.2’ respectively. Synthetic data of different noise signals are analyzed to validate the supremacy of the proposed method over the conventional method. The effect of signal length is also evaluated in both methods. Afterward, a comparative study is performed between the conventional and proposed methods. For this purpose, the effect of body postures has been analyzed on HRV and SCR by applying conventional SE and proposed SE methods.

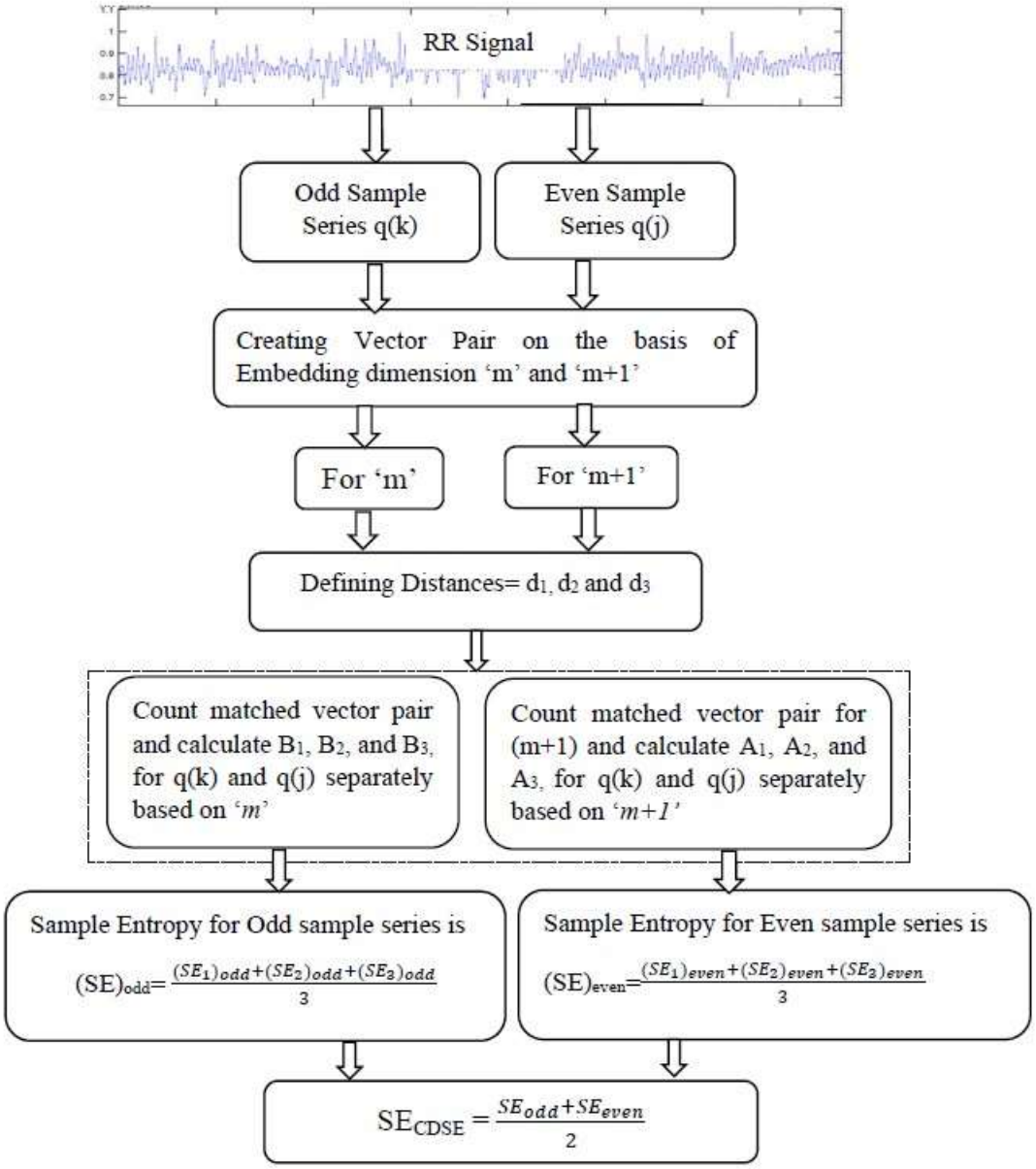

Figure 4.4 Flowchart of proposed 'CDSE' method

4.6.1 Sensitivity to the length of the data using synthetic signals.

We simulated four different noises i.e., pink, red, blue, and brown [127] [173]. For each noise, the data length has been taken with an increment of 10 points starting from 50 points to 1000. Each data length has been realized 100 times and their corresponding error bar have been plotted. For a graphical representation of data variability, an error bar has been used.

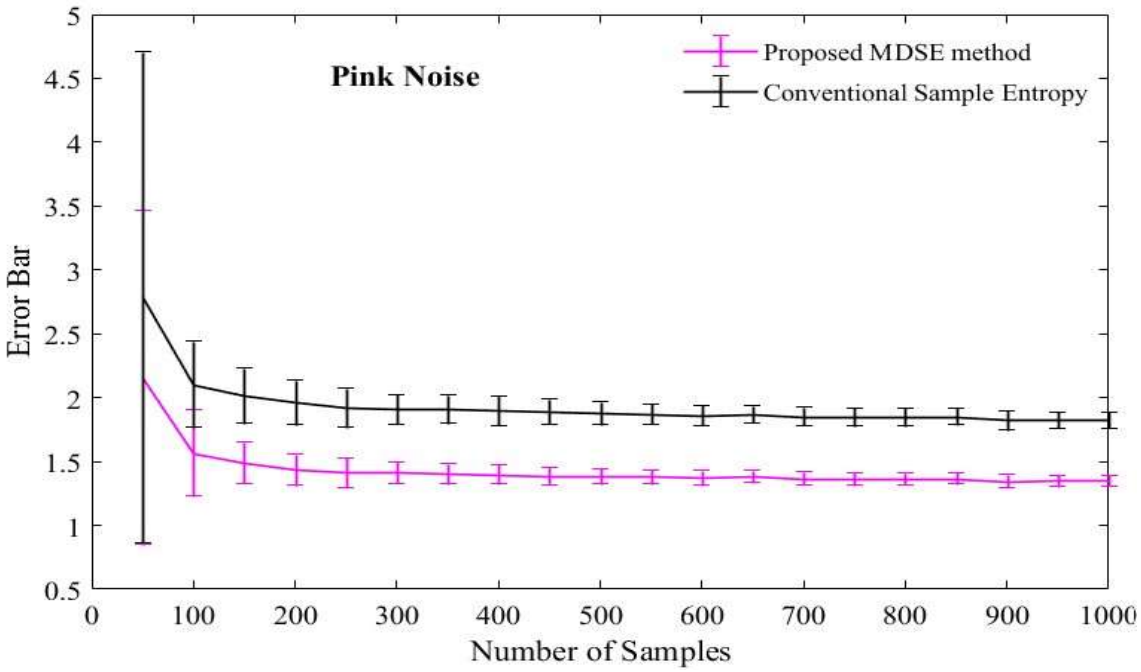

Figure 4.5 (a) Pink Noise

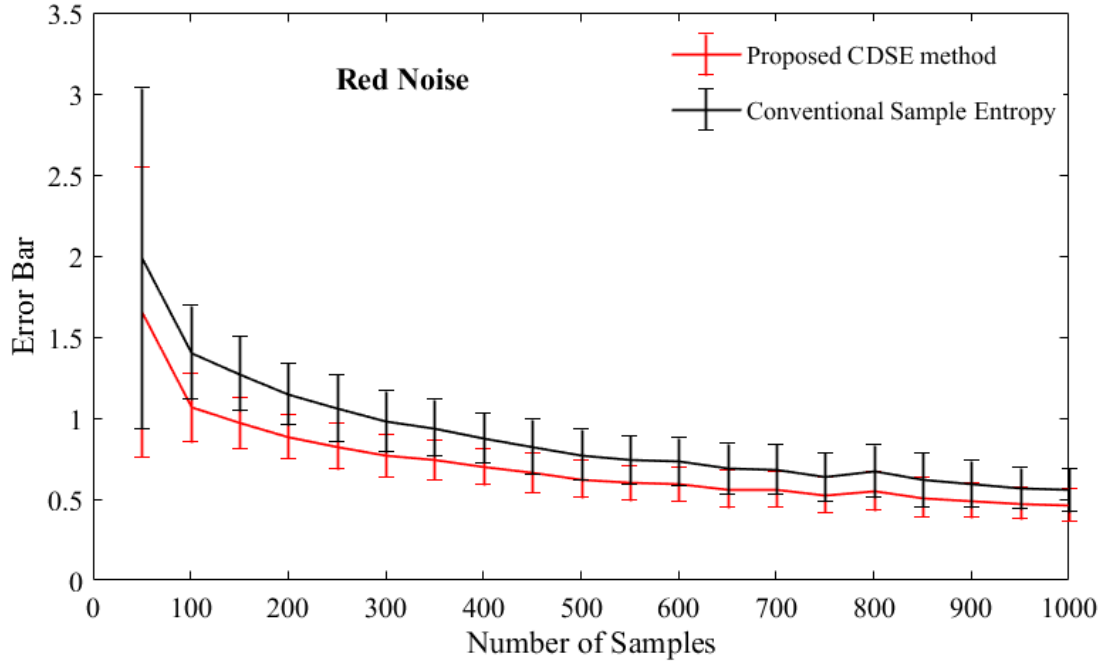

Figure 4.5 (b) Red Noise

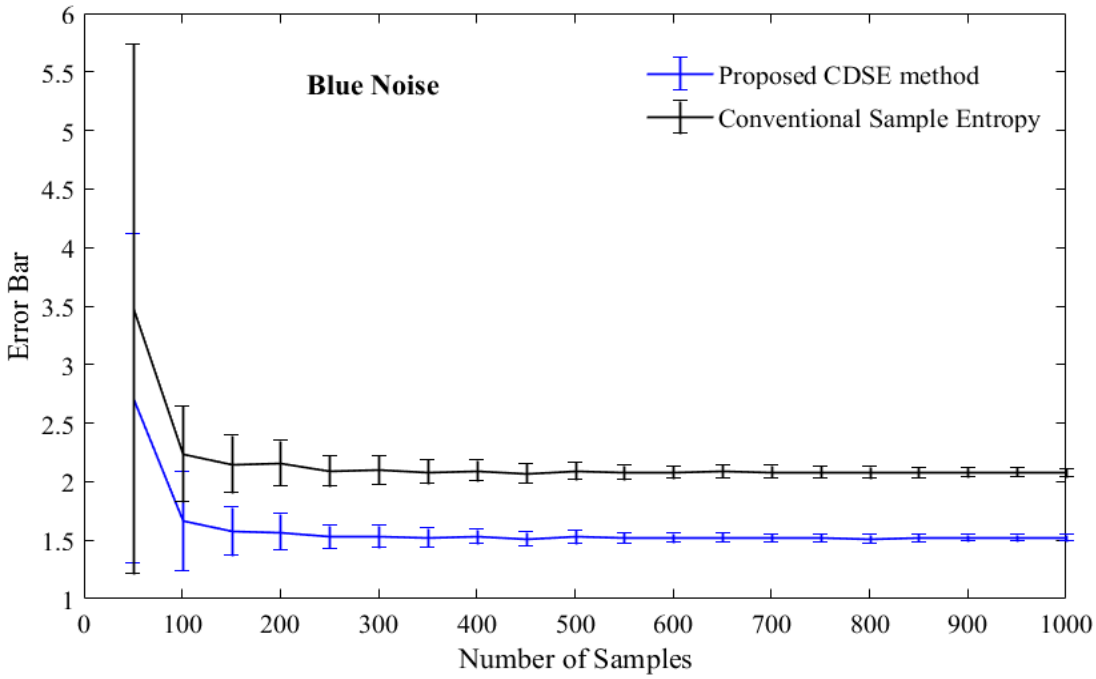

Figure 4.5 (c) Blue Noise

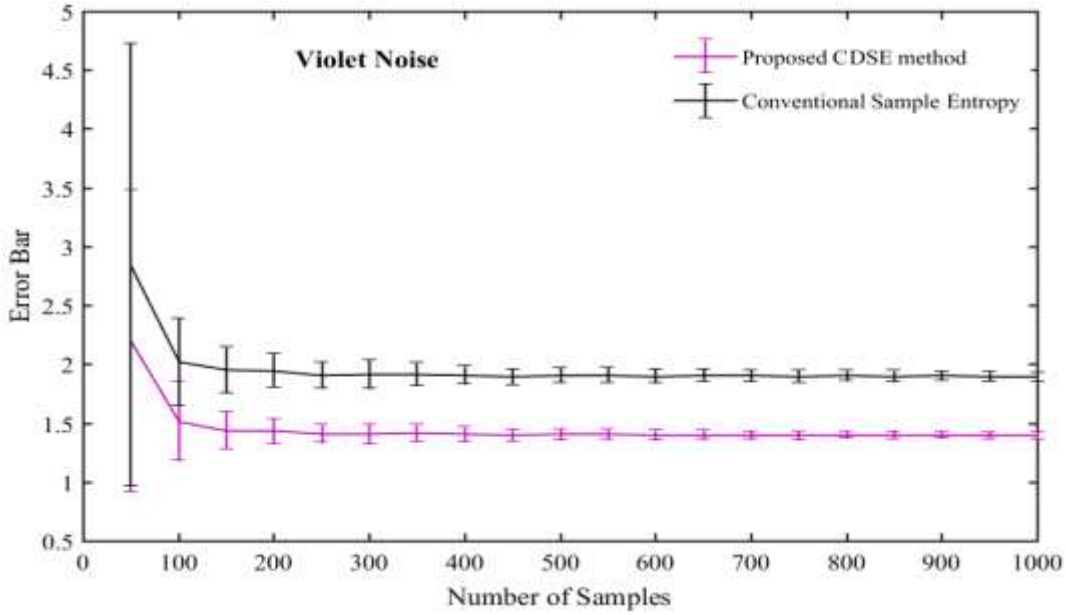

Figure 4.5 (d) Violet Noise

Figure 4.5 The Error Plot of Colour noises (a), (b), (c), and (d) of Proposed and Conventional SE analysis for (x-axis represents the signal length, the y-axis represents error plot of mean and SD).

To confirm the superiority of the proposed method these noise signals are realized 100 times at each sample size. Sample entropy using the conventional and proposed method

is calculated for these simulated noise signals with embedding dimensions m=2 and r=0.2. After the calculation of SE for the conventional and proposed method, the error bar graphs have been plotted for each noise type. In Figure 4.5, the colored error bar represents the error plot of the proposed CDSE method, while the black color represents the error plot of the conventional SE. The number of samples of the simulated signals has been shown on the x-axis, while the y-axis represents the mean value of applied methods along with their standard deviation. We used noise signals in our research work. The error bars were employed to visually compare the performance of our proposed method with the conventional SE method. This methodology is based on a long-standing research practice in which noise signals have been widely used by different researchers over the last several years to analyze and distinguish the usefulness of various analytic approaches.

From Figures 4.5(a), 4.5(b), 4.5(c), and 4.5(d), the variations in the mean value are higher for the conventional sample entropy and low for the proposed method for different data lengths.

Figure 4.5(a) represents the error bar graph of 'Pink noise', which is generally known as 1/f noise. It is the most commonly used noise in physiological signals. The error plot of pink noise for the proposed CDSE shows less deviation of the mean value compared to conventional SE. In Figure 4.5(b), the error bar of the 'Red noise' has been represented. Red noise is also known as brown noise and is represented as 1/f2. It shows higher intensities at lower frequencies. The error bar of 'Blue noise' is shown in Figure 4.5(c). Blue noise also known as high-frequency white noise, is used to evaluate the conventional and proposed methods. In the figure, the proposed SE shows a smaller deviation around its mean value compared to the conventional SE. We used noise signals as our research. Here, the deviation in the mean value of the error plot is higher for the conventional SE compared to the proposed SE.

4.6.2 The Effect of Postural change on Skin conductance response and Heart Rate using paired t-test on the mean value of 70 subjects

The comparative analysis is also done on the data set of SCR and heart rate using a paired t-test. In Table 4.1, the results are expressed in the form of the mean value along

with the standard deviation. The level of significance is considered as $p < 0.05$. The interpretation of the obtained results is also given in below Table 4.1.

Table 4.1 Mean and p-value of Skin conductance response and Heart rate for n=70 subjects with Interpretation

Parameters	Supine (Mean±SD) (n=70)	Standing (Mean±SD) (n=70)	*p*-value	SC and HR variations in Supine and Standing positions	Interpretation
SCR	1.79±2.03	2.44± 2.35	4.00E-05	$SCR._{st} > SCR._{su}$	The mean value of SCR is higher in the standing position as compared to supine implying that sympathetic activation is higher in the standing position.
Heart rate	76.80±11.01	93.94±12.93	3.67E-27	$HR._{st} > HR._{su}$	The mean value of HR is smaller in the supine position as compared to standing implying that the parasympathetic activity is higher in the supine position.

Both SCR and heart rate show higher mean values during the postural transition (from supine to standing). From the results, it is clear that the change in body posture affects the mean value of skin conductance response and heart rate. Initially when the body is in a rest position the mean value is low but when the body position is changed from supine to standing, the mean value is increased.

4.6.3 Performance Evaluation of Proposed Method and Conventional Sample Entropy on HRV and SCR Dataset

The performance of the proposed method has been analyzed by evaluating the accuracy of obtained results which are based on the correct detection of HRV and the response of SC variation in supine and standing positions. The Accuracy of the conventional and proposed method is calculated using equation (4.29) for HRV and SC signals based on entropy trend in the position of supine and standing.

$$Accuracy = \frac{N_{s1}}{N_s} \times 100 \tag{4.29}$$

Where N_s is the total number of subjects and N_{s1} is the number of subjects having higher sample entropy in the supine position than in the standing position $(SE._{su} > SE._{st})$.

The accuracy using the proposed method is *94.28%* as 66 out of 70 subjects show higher sample entropy in the supine position for HRV signal while using the conventional method, it is *88.57%* as 62 out of 70 subjects show higher sample entropy in the supine position as shown in Figure 4.6. Analyzing the effect of position change on SCR using the proposed method, the accuracy is obtained at *71.42%* percent while in the case of the conventional method, its percentage is *65.71%* as depicted in Figure 4.7.

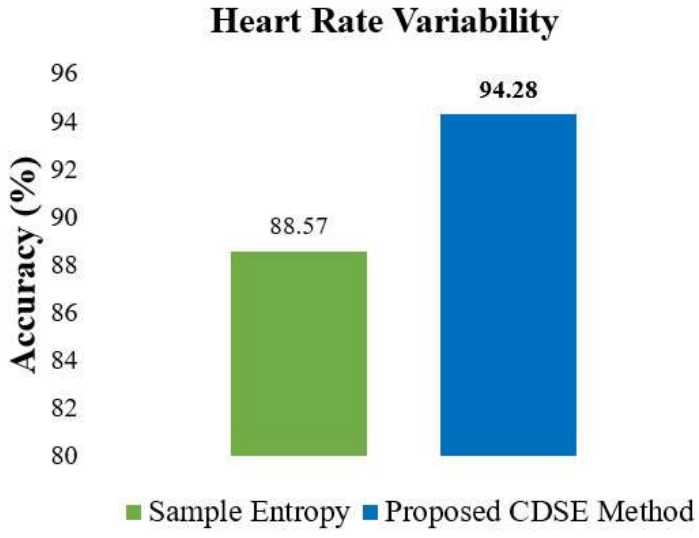

Figure 4.6 Performance analysis of conventional SE and proposed method for the analysis of HRV

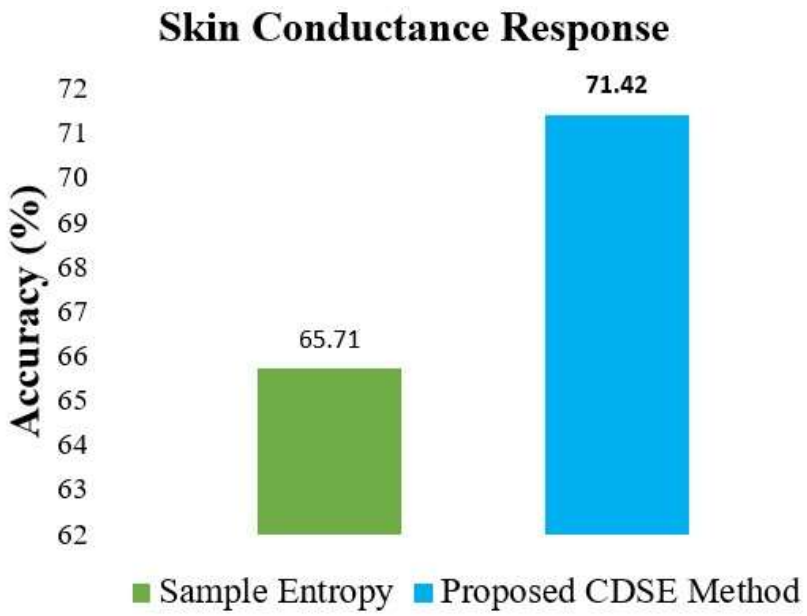

Figure 4.7 Performance analysis of conventional SE and proposed method for analysis of SCR

The trend of HRV obtained using the proposed and conventional method is shown in Figures 4.8(a) and 4.8(b), while the trend of SC is shown in Figures 4.9(a) and 4.9(b).

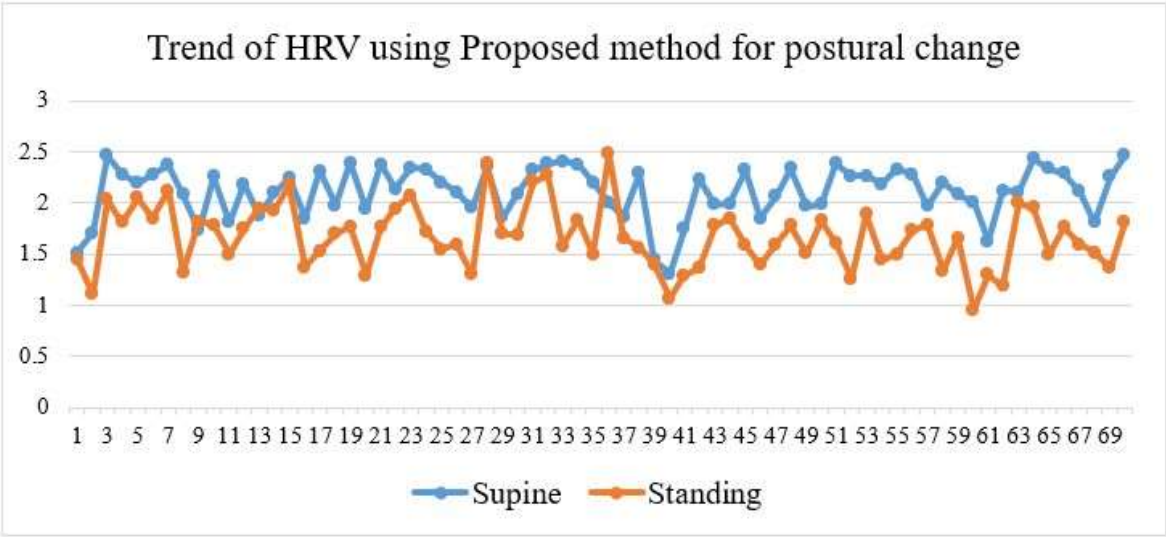

Figure 4.8 (a)

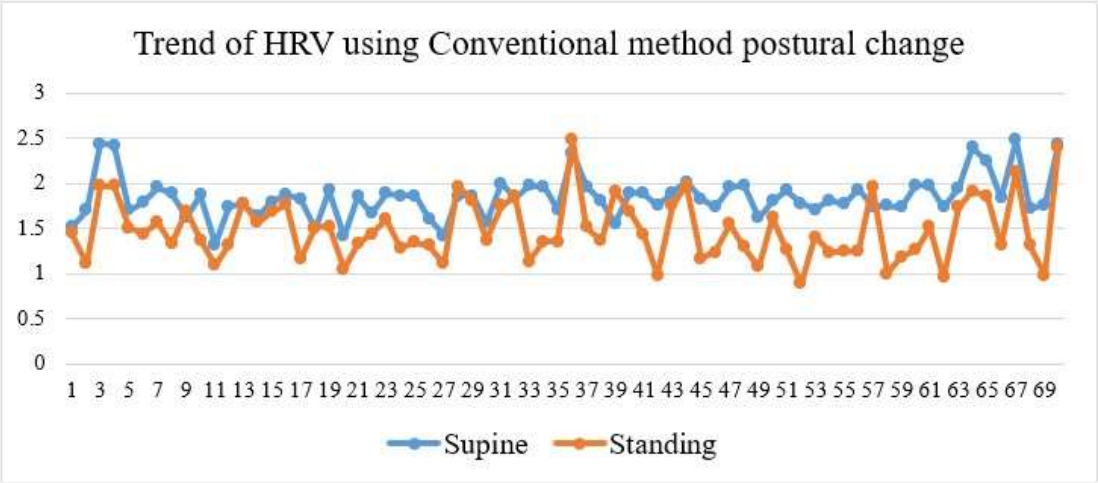

Figure 4.8 (b)

Figure 4.8 Number of Subjects out of 70 subjects showing SE.su > SE.st trend for HRV

Here Figure 4.8(a) and Fig. 4.8(b) show the trend of SE for HRV in the position of supine and standing using proposed and conventional methods. The blue color indicates the supine position while the orange color shows standing. In Figure 4.7, the number of subjects that follow the sample entropy trend in supine and standing positions (i.e. *SE.su* > *SE.st*) is higher for the proposed method as compared to the conventional method which implies higher accuracy of the proposed method.

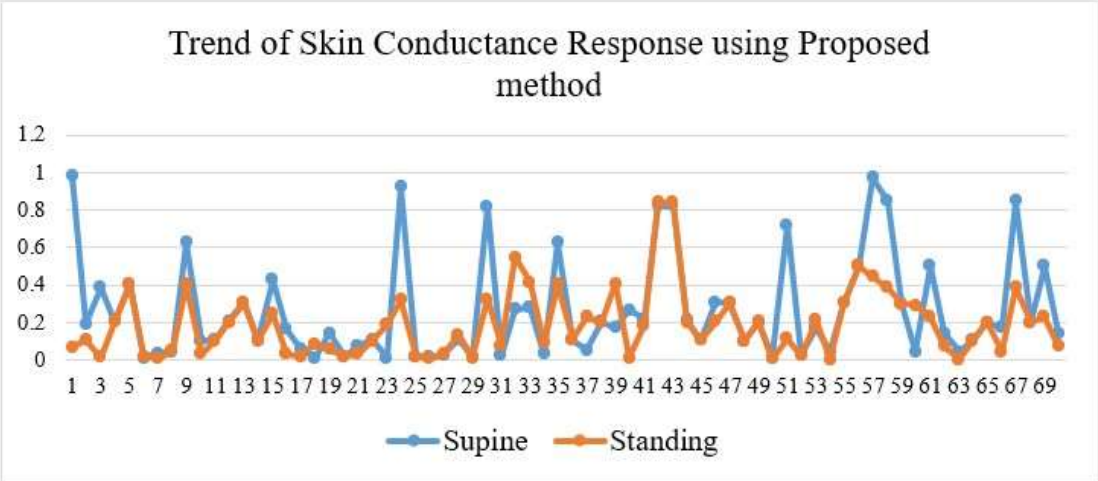

Figure 4.9 (a)

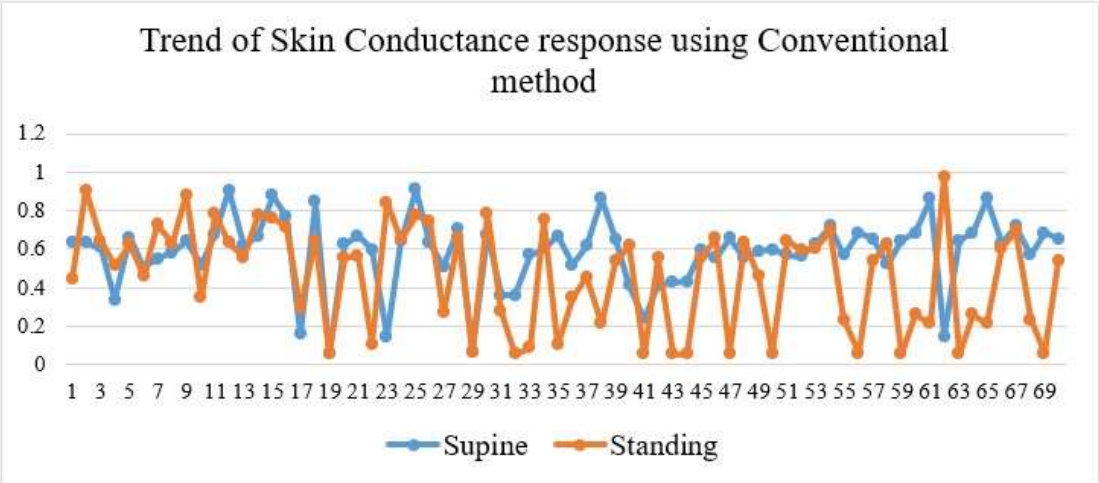

Figure 4.9 (b)

Figure 4.9 Number of Subjects out of 70 subjects showing SE.su > SE.st trend for Skin conductance response.

In Figures 4.9(a) and 4.9(b), the trend of SE has been shown for skin conductance response. From the figure, a higher number of subjects follow the *SE.su* > *SE.st* trend using the proposed method as compared to the conventional methods, which indicates the higher accuracy of the proposed method.

4.6.4 Comparative analysis of different nonlinear methods applied to the HRV dataset.

Furthermore, the HRV of 70 subjects was analyzed using the proposed CDSE and the existing nonlinear techniques. The results of the applied nonlinear methods in the form of mean value were presented in Table 4.2, while Table 4.3 interpreted these findings. From Table 4.2 and Table 4.3, the authors found that the obtained results using nonlinear methods such as AE, SE, FE, QE, and CDSE are in the desired trend as mentioned in the literature [66, 102, 108, 175]. The proposed CDSE and existing methods can detect the expected trends of heart rate variability for the body's postural changing activity. Results indicate that the values of HRV decreased when participants switched their posture from supine to standing. The decreased HRV implies that the sympathetic activity of the autonomic nervous system increased in the standing position of the body, while parasympathetic activation is higher in the supine posture. The authors have evaluated the performance of the applied methods with the idea of accurate

measurements of the obtained Postural trend. For this purpose, the authors have implemented proposed and existing nonlinear techniques to the recorded signal of different postures and found that only the CDSE method can detect the desired trend of HRV correctly in a more significant number of participants compared with other methods. Fig. 4.10 presents the accuracy graph of applied approaches.

Table 4.2 HRV Analysis in Supine and Standing Body Postures Using Different Methods

S. N.	**Methods (mean for n=70)**	**Supine**	**Standing**	***P-Value***
1.	AE	1.3600 ± 0.1192	1.2240 ± 0.1580	6.92E-11
2.	SE	1.6782 ± 0.2512	1.3058 ± 0.2672	1.82E-16
3.	FE	-0.0075 ± 0.0014	-0.0065 ± 0.0009	1.50E-07
4.	QE	0.0019 ±0.0003	0.0015 ± 0.0002	2.32E-09
5.	Proposed C**DSE** Method	2.1331 ± 0.2499	1.6793 ± 0.3093	1.57E-18

Table 4.3 Interpretation of Increment and Decrement of the value of HRV in different postures

Methods	**HRV trend in supine and standing position**	**Interpretation [102] [108]**
AE	$AE_{su} > AE_{st}$	The lower value of AE indicates a higher Heart rate and lower HRV in the standing position [61]. It indicates that the regulation and coordination of ANS are greater in the standing posture. It also indicates that the sympathetic and vagal modulation of the sympathetic nervous system is higher in standing posture [176].
SE	$SE_{su} > SE_{st}$	A higher value of SE in the supine position indicates higher HRV and low heart rate [111] [175]. It also indicates that the HRV signal is more irregular in supine posture than standing. The reason behind higher HRV and large irregularity in the supine posture is the increased vagal modulation in the supine posture.
Fuzzy Entropy	$FE_{su} > FE_{st}$	In the supine posture, the body is in relaxed mode So, the ANS is skewed towards parasympathetic modulation which results in more irregular HRV and reflects the higher value of FE. When posture switches to standing mode, the sympathetic activation of ANS increases. Which results in more regular HRV signals, and the value of entropy decreased [131] [132].
Quadratic Entropy	$QE_{su} > QE_{st}$	The small value of QE in standing posture suggests that the parasympathetic modulation is higher in the supine posture, when

		body posture changes from supine to standing, the parasympathetic activation decreases, and sympathetic activation increases in standing posture [125].
Proposed **CDSE** method	$CDSE_{su} > CDSE_{st}$	A decrement in SE value after the change in position from supine to standing implies decreased HRV. In the supine posture, the cardiovascular system is in a relaxed state as the gravity force is not acting against blood flow. So, the ANS is skewed towards parasympathetic modulation which results in complex and more irregular HRV and reflects the higher value of entropy. When posture switches to standing mode, it increases cardiovascular activity and in response, the sympathetic activation of ANS increases. Which results in more regular HRV signals, and the value of entropy decreased.

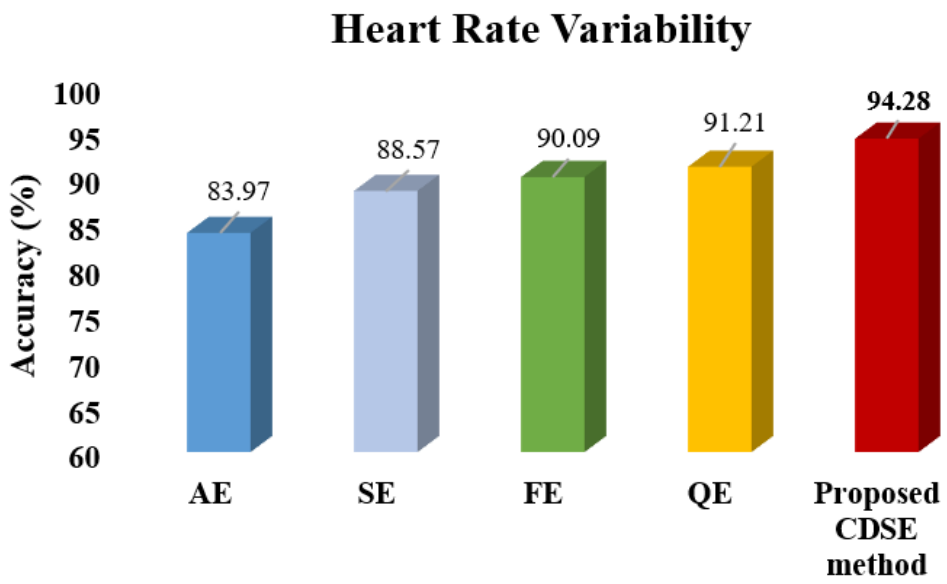

Figure 4.10 Comparison of the proposed method with other existing methods for detecting the accurate trend of HRV for postural change.

4.6.5 The Correlation between HR and SCR

The value of SE for both HRV and SC signal is decreased for the conventional and proposed method in the standing posture indicating that the parasympathetic activity is higher in the supine position and higher sympathetic activation in the standing position. The effectiveness of the proposed method has been compared with the conventional

method using accuracy as a performance parameter. The accuracy obtained using the proposed method is much better than the conventional method.

The mean value of 70 subjects of skin conductance response and heart rate is increased when the position is changed from supine to standing, which suggests that both parameters have a positive correlation for the postural change activity. The increment of the mean value in the standing position indicates the sympathetic dominance in this position.

4.7 Conclusion

Within this research chapter, we delve into the impact of altering one's posture on Heart Rate Variability (HRV) and Skin Conductance (SC). An analysis of HRV and SC involves the application of non-linear methods, among which Sample Entropy (SE) stands out. However, conventional SE exhibits sensitivity to limited signal lengths, employing a single distance function for matched vector pairs. This sensitivity renders the analysis insufficient for establishing a clear connection between HRV and SC.

As a solution, we introduce a novel approach called "composite distance sample entropy" for matched vector pairs, aiming to mitigate the sensitivity associated with short signal lengths. In this proposed method, the distance between two template vectors is determined using a composite distance function. To validate the efficacy of this method, we simulate various noise signals of varying lengths for sample entropy computation. Subsequently, we perform a comparative analysis, employing accuracy measures and paired t-tests, between the proposed method and the conventional approach. This evaluation is conducted on a self-recorded dataset comprising data from 70 subjects in both supine and standing positions.

The results demonstrate that the proposed method yields higher accuracy compared to the conventional SE method, and it appears to be less influenced by signal length. Furthermore, our research uncovers a positive correlation between HR and SC across different body postures.

CHAPTER 5

MATCHED WAVELETS

The right wavelet must be used to accurately measure the HRV changes. A matched wavelet that accurately depicts the characteristics of an HRV signal during postural change activity from a supine position to a standing position is therefore necessary. This chapter uses the stochastic fractal search algorithm to create matched wavelets in response to the drawbacks of conventional wavelets analyzing HRV. Further, the correlation between the HRV and SCR has been established for postural change activity.

5.1 Introduction

HRV and SCR have been commonly utilized in research to explore non-invasively the impact of diverse physical activities on heart activity and electrical conductivity of skin [1] [170-171]. HRV indicates the variation in time intervals between consecutive heartbeats caused by dynamic autonomic nervous system (ANS) activities. The reason is that as a predictor of mortality and multiple risk factors, HRV is used here for the assessment of ANS. Thus, the activity of the ANS can be assessed with the measurement of HRV [78-79]. In addition to HRV, another physiological signal, i.e. Skin Conductance Response (SCR) (which is frequently used these days for assessing the effect of physical activities i.e. postural change) has been analyzed. It is also known as electrodermal behavior. Electro-dermal activity (EDA) is described as an indicator of variations in the skin's electrical conductance [80]. To maintain the blood flow, the sympathetic nervous system activates which causes a decrement in the HRV and changes in skin conductance response [81-83]. A wide range of physical and emotional behaviors, including activities like working out, running, engaging in aerobics, social interactions, stressors, alterations in body position, moments of enthusiasm or agitation, and so forth, influence both sympathetic and parasympathetic activity. These influences can be gauged by monitoring SC and Heart HR [11] [88] [172]. During postural shifts,

the heart's autonomic controls change. To get a deeper understanding of how the heart works, a variety of physiological techniques have been explored, including the change in posture.

In the literature, it is mentioned that the autonomic balance is different for different postures, which implies that the sympathetic nervous system activity is higher for standing or sitting postures (vertical postures) and vagal or parasympathetic activity is dominant for supine posture (recumbent posture) [171] [177-179].

Conventional HRV assessments are often classified as linear or non-linear. First, HRV is measured using linear approaches. Time domain techniques are the most basic technique to compute HRV; they are determined statistically using successive inter-beat intervals, whereas frequency domain measures are more comprehensive indexes based on spectrum analysis of HRV [91] [180]. However, non-linear measures that are devoid of the non-stationary features of HRV are developed using a mathematical approach. In comparison with the linear approach, the nonlinear approach is very well known for identifying the smallest fluctuations of ANS [181]. There is no time resolution present in linear methods of HRV analysis. So, it can't be told which incident happened at what time.

There are various multiresolution techniques used for the analysis of HRV [14] [135-138]. The fundamental issue with the STFT is its constant lack of flexibility in resolution. The WVD spectrum has various artifacts and negative values that correspond to negative energy. Therefore, the wavelet transform is the most widely used technique for the analysis of HRV.

In adopting current wavelets, the fundamental issue is that their selection is largely dependent on the signal being studied. Therefore, existing wavelets cannot be used to correctly fetch the fluctuations of heart rate variability in various postures. Analytically assessing HRV variations requires careful consideration of the wavelet to be used. The choice of the right wavelet is an essential part of evaluating HRV fluctuations from an analytical standpoint. As a result, choosing a wavelet according to the characteristics of the signal is the most requirement.

A Matched wavelet that correctly depicts the characteristics of an HRV signal in diverse body postures (supine and standing postures) is required for this research. Thus, in this chapter, a new wavelet has been developed for each HRV signal in supine and standing positions. The developed matched wavelet accurately describes the behavior of the HRV signal in each posture. Afterward, the correlation between the HRV, SCR, and HR have been analyzed.

5.2 Type of wavelets

The analysis is made using the wavelet's function, which is more localized in time and space than Fourier analysis. Wavelets are mathematical computations that can be used to examine signals and data. A group of wavelets created by sizing and translating a single fundamental wavelet function is known as a family of wavelets. Typically, a function with zero average, like the Mexican hat or the Haar function, is referred to as the fundamental wavelet function [19]. The various types of wavelets used in signal processing are-

Daubechies wavelet: The Daubechies wavelets are highly suited for the analysis of signals with sharp transitions or discontinuities because they possess a large number of advantageous characteristics. Their capacity to conduct a multi-resolution analysis of signals is one of their primary characteristics. They can so divide a signal into various frequency bands that each reflect various scales or resolutions.

Coiflet wavelet: Coiflet wavelets are orthogonal wavelets. These are the wavelets that have limited length and are zero outside of a small interval.

Coiflet wavelets are frequently employed in image processing applications like image compression and denoising because they can shrink the size of the picture file without affecting the quality. The coiflet wavelet has a filter length of 6N and a support width of 6N-1.

Symlet wavelet:

Similar to Daubechies wavelets, the Symlet wavelet family can be used in signal and picture processing. Symlet wavelets are compactly supported, like Daubechies wavelets, which means that they have finite lengths and are zero outside of a finite interval. They also have high localization characteristics and orthogonal in the time and

frequency domains. The abbreviation for these wavelets is symN, where N denotes the order of values 2, 3, 4…etc. It has a support width of 2N-1 and a filter length of 2N.

Haar wavelet:

It is discontinuous, symmetric, and compactly supported: the Haar wavelet. The filter length is 2 and the support width is 1, making this wavelet identical to db1.

Meyer wavelet:

An endlessly regular, symmetric orthogonal wavelet is referred to as a meyer (meyr) wavelet.

5.3 Properties of Wavelet Function

Different wavelets have various characteristics. Here is a description of these attributes [19] [182].

i. *Orthogonality:*

Wavelets are implied to be orthogonal to one another by the orthogonal property of wavelets. The coarser scaling function and each wavelet detail function are orthogonal to each other. Some wavelets, such as biorthogonal wavelets, don't have the orthogonal property of wavelets.

ii. *Smoothness*:

For many applications, the wavelet function should be sufficiently smooth to effectively capture the properties of the underlying signal. The number of derivatives that exist for a given wavelet is used to determine how smooth it is. The Haar wavelet is an example of a wavelet that lacks smoothness since it is discontinuous and non-differentiable.

iii. *Support Width*

The wavelet's smoothness quality and support breadth are inversely connected. The wavelet with the largest support width is smoother.

iv. *Symmetry*:

Since wavelet coefficients are symmetric, phase shifts are prevented, and they do not stray from the original signal. The biological wavelets can be symmetric or antisymmetric.

v. *Vanishing Moments*:

The smoothness of a wavelet is directly correlated with its vanishing moments. Wavelets with a higher number of vanishing moments are better at capturing higher-degree polynomial signals.

vi. *Localisation*:

The wavelet's characteristics are time- and frequency-specific. In smoother wavelets, the frequency localization characteristics are better.

5.4 Continuous Wavelet Transform

The continuous wavelet transform is described by using equation (5.1) [183].

$$CWT_x^{\psi}(b,a) = \psi_x^{\psi}(b,a) = \frac{1}{\sqrt{|a|}} \int x(t)\psi^* \left(\frac{t-b}{a}\right) dt \quad (5.1)$$

where x(t) is the original signal, b and a are the translation and scale parameters, ψ is the mother wavelet-style converting function and '*' stands for the complex conjugate. In the transfer domain, the time information is given by translation parameter b, and the 'a' corresponds to the scales in maps. In the context of maps, a smaller scale indicates a detailed perspective of the signal whereas a greater scale indicates a non-detailed global picture. When it comes to frequency, low frequencies (high scales) offer the signal's overall information, whereas high frequencies (low scales) correspond to the signal's intricately buried information. Scaling, however, can either expand or contract a signal mathematically [184]. The signal is compressed and stretched more when the scale is increased or decreased.

5.5 Discrete Wavelet Transform

A potent technique for multiscale representation and analysis of nonstationary HRV signals is the discrete wavelet transform (DWT) [185]. The Quadrature Mirror Filter (QMF) bank is used in DWT to split the signal in the frequency plane [186].

The signal is divided into an approximation $a_{j,k}$ (low pass component) and detail $d_{j,k}$ (high pass component) coefficients at each scale and then down-sampled. At the ideal cut-off frequencies, the frequency axis is recursively split in half at each scale using equation (5.2).

$$f_j = 2^{-j}\frac{1}{2T} \tag{5.2}$$

The low-pass filter is represented by the scaling function *Ø(t),* and the high-pass filter is represented by the wavelet function *ψ(t)* [11]. Using equations (5.3) and (5.4), the approximation $a_{j,k}$ and detail coefficients $d_{j,k}$ are provided.

$$a_{j,k} = \text{x(t)},\emptyset_{j,k}(t) \tag{5.3}$$

$$d_{j,k} = \text{x(t)},\psi_{j,k}(t) \tag{5.4}$$

where $\emptyset_{j,k}(t)$ and $\psi_{j,k}(t)$ are the scaled and dilated versions of basis functions and are defined using equations (5.5) and (5.6), wherein j and k are the scale and translation, respectively.

$$\emptyset_{j,k}(t) = 2^{-j/2}\,\emptyset(2^{-j}t\text{-}k) \tag{5.5}$$

$$\psi_{j,k}(t) = 2^{-j/2}\,\psi(2^{-j}t\text{-}k) \tag{5.6}$$

The scaling and wavelet functions are given in equation (5.7)

$$\text{x(n)} = \sum_{j=1}^{J}\sum_{k} d_{j,k}\;\psi_{j,k}(n) + a_{j,k}\,\emptyset_{j,k}(n) \tag{5.7}$$

In a DWT, specific frequency bands are linked to various regulatory processes, particularly for the HRV signals. Therefore, the sub-band decomposition is required to comprehend the underlying physical processes in biological signals like HRV. The results obtained using the sub-band decomposition depend upon the type of wavelet used for the HRV analysis [19].

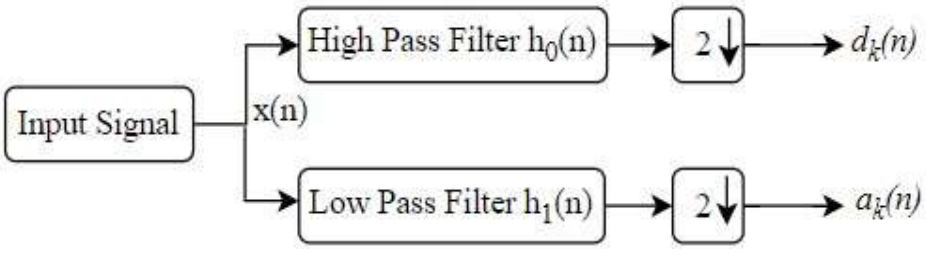

Figure 5.1 Discrete wavelet transform

5.6 Wavelet and filter banks

Signal processing methods like analysis and synthesis filter banks are employed for signal analysis and reconstruction when a signal has been broken down into several

frequency bands. The HRV signal is often extracted and reconstructed from its frequency components for Heart Rate Variability signal analysis using decomposition and reconstruction filter banks. By employing a decomposition (analysis) filter bank, the HRV signal is divided into numerous frequency bands. By running the HRV signal through a series of filters, each of which isolates a particular frequency range or band from the signal. Each filter's output corresponds to the energy of the signal for that frequency range [187] [188]. In most cases, the resulting frequency bands are selected to match the physiological processes that contribute to the HRV signal. The inverse filters are used to combine the frequency bands that were produced from the analytical filter bank. The resultant signal is a close representation of the initial HRV signal.

5.7 Implementation of Daubechies wavelets on the recorded data set of HRV

Daubechies wavelets (db2 to db4) were employed for multiresolution analysis of HRV, on the recorded dataset of HRV. To examine each subject's HRV signal, it is decomposed into different frequency ranges, and subsequently, the LF/HF ratio is computed as part of the analysis. The calculated values obtained from this process are significantly different for supine and standing positions, and higher in the standing position as compared to the supine position for each calculated wavelet (db2 to db6). An increase in the LF/HF ratio when transitioning from the supine to the standing position suggests a reduction in HRV during standing. This shows an elevation in sympathetic activity within the ANS in the upright posture. The efficiency of accurately detecting the HRV variation in the postural change activity is used to assess each wavelet's performance. Figure 5.2 represents the performance graph of applied wavelets.

5.8 Mean Square Error

In several disciplines, including signal processing, mean square error (MSE) is a regularly employed metric for assessing the accuracy of a reconstruction or prediction. The MSE is utilized to determine the average squared deviation between the reconstructed signal and the original signal.

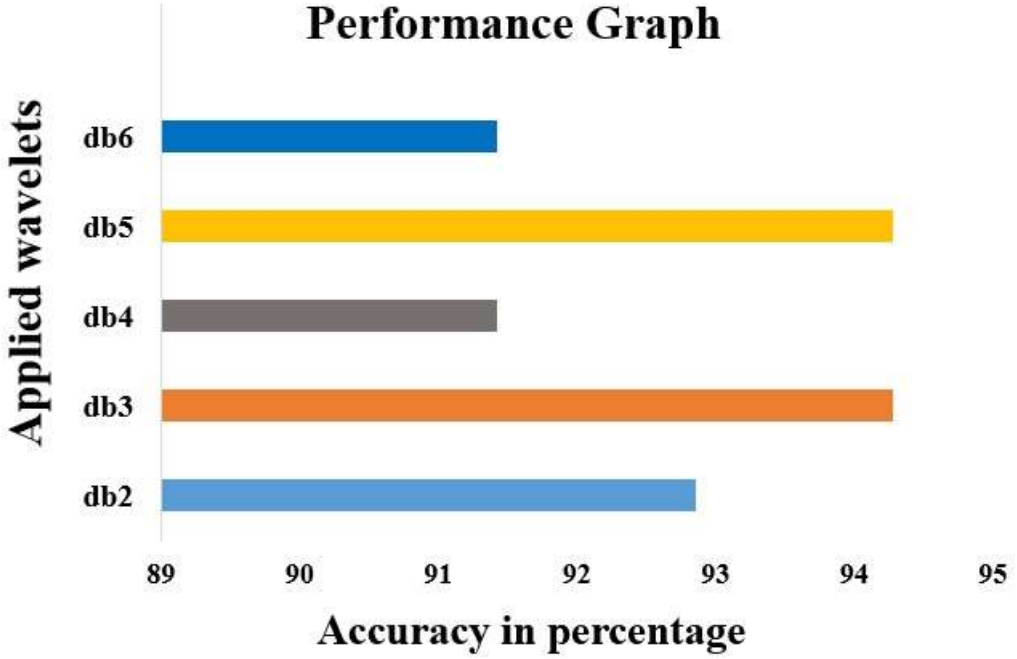

Figure 5.2 Performance Graph of applied wavelets

5.9 Mean square Error calculation of applied wavelets (db2 to db6)

After the calculation of LF/HF, the original signal has been reconstructed with the decomposed frequency bands. The mean square error between the original signal and the reconstructed signal has been calculated to find out the performance of the applied wavelets for the recorded HRV signal. The MSE has been plotted using the box plot in Figure 5.3 and Figure 5.4.

Figure 5.3 represents the mean square error between the original and reconstructed signal in the supine posture for different wavelets, while Figure 5.4 shows the MSE in the standing posture for applied wavelets.

From Figure 5.3 and Figure 5.4, it is visible that the reconstructed signal using db4 is much closer to the original signal in both postures. This implies that the db4 wavelet is superior compared to other wavelets for better reconstruction of the signal using decomposed frequency bands.

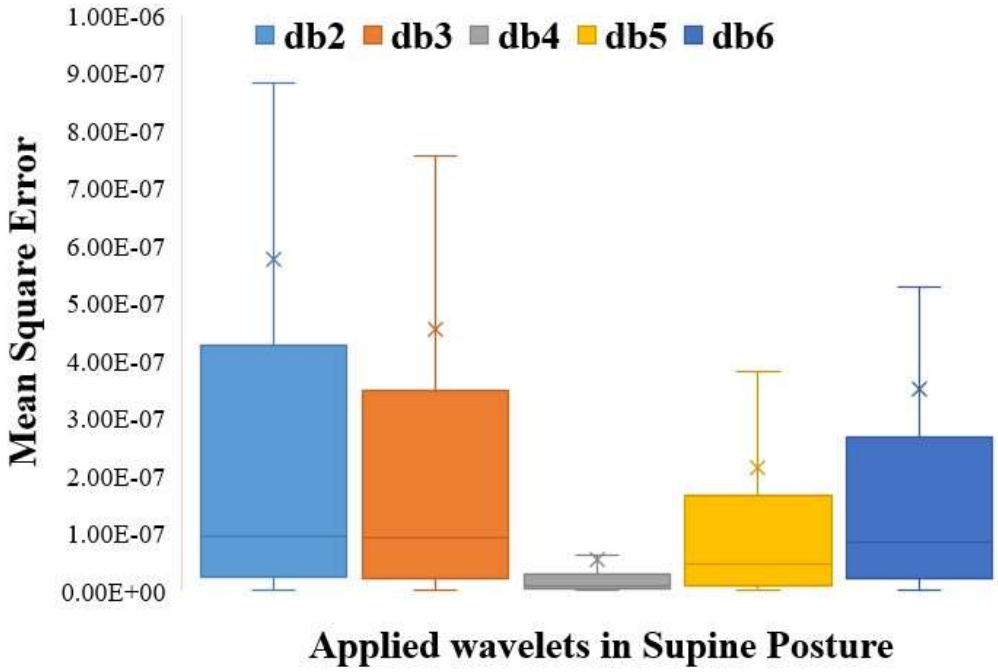

Figure 5.3 Comparative analysis based on MSE in Standing Posture

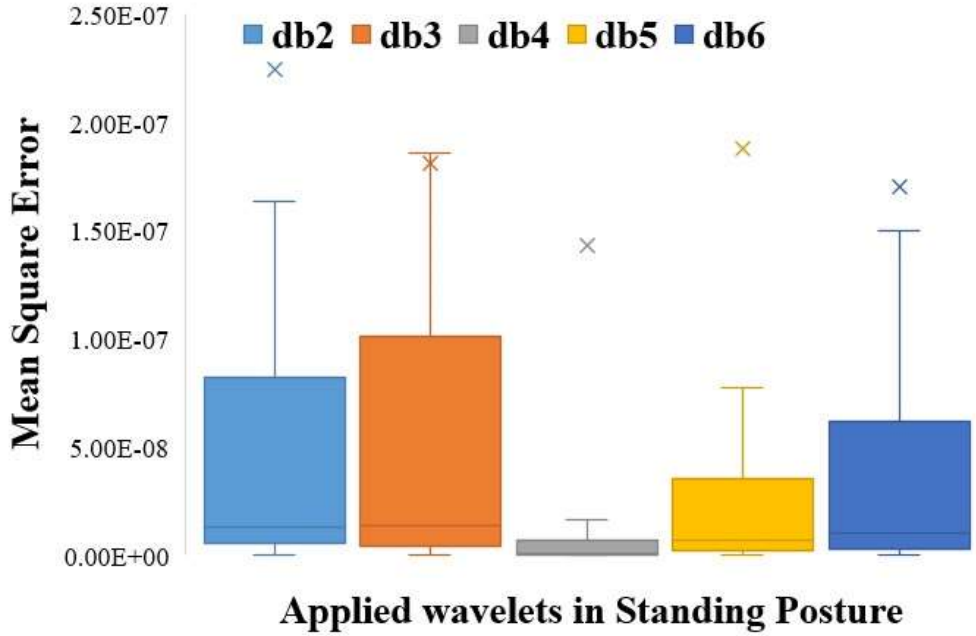

Figure 5.4 Comparative analysis based on MSE in Standing Posture

When the different wavelets i.e., db1 to db6 have been applied to the recorded data set of 70 subjects, an increment in the value of LF/HF has been found in the standing posture as compared to the supine posture. The evaluated accuracy in a subject-to-

subject manner has been shown in Figure 5.2. Using db3, db5, and db2, the maximum number of subjects follow this trend as compared to other applied wavelets. After all these evaluations, some contradictory results have been found, this means that on one hand db4 can reconstruct the signal in a better way than other applied wavelets. On the other hand, the accuracy of db4 using the LF/HF ratio is not as good as it has been obtained with db3, db5, and db2. In addition, the reconstruction of the HRV signal is not that good with db3, db2, and db5, as good as with db4.

So, there is a need to optimize the wavelet filter coefficients that match the characteristics of the original signal and reconstruct the signal with minimum MSE and higher accuracy.

5.10 Limitation of Existing Wavelets

The signal is divided into a series of frequency channels with equal bandwidth using the wavelet transform. Wavelets have several uses because there is an endless variety of basic functions that can be used. By dilating and translating the mother wavelet $\psi(t)$ (an appropriate function), several basis functions are created.

In the past, wavelets have been employed to analyze biological signal data. The goal of the ongoing research is to identify a wavelet that can accurately estimate a given signal. Therefore, the wavelet that depends on the unique characteristics of the signal under inquiry is anticipated to be the best [189]. Although wavelets are widely used in many applications, their usage in clinical applications including HRV has been constrained by the choice of the best mother wavelet.

5.11 Need for a Matched Wavelet

For fundamental investigations and clinical diagnostics, it is vital to analyze and record physiological signals like HRV. In some cases, the traditional wavelets may be unable to recover the hidden data from the extremely complicated HRV signals. Such concealed information relates to fundamental mechanisms of normal and pathologic function and has clinical relevance in the prediction of sudden cardiac death, stress analysis, etc. Based on the aforementioned research, it is evident that the analysis of a specific signal's dynamic behavior necessitates the utilization of a waveform that closely aligns with the signal. Therefore, this study requires a tailored wavelet that is

capable of accurately capturing the dynamics of an HRV signal across various body postures, including supine and standing positions.

5.12 Developed Method

In this research work the new matched wavelet has been developed for analysis of the HRV signals of each participant. The matched wavelet has been optimized using the Stochastic fractal search (SFS) algorithm so that the developed matched wavelet (MWSFSA) can reconstruct the signal that depicts similar characteristics as the original signal. The frequency content and temporal properties of the HRV signal are matched by matched wavelets, which can enhance the analysis's signal-to-noise ratio (SNR).

5.12.1 Overview of Stochastic Fractal Search Algorithm (SFSA)

Stochastic fractal search is a bioinspired approach [190]. This method employs the mathematical concept of fractals to mimic growth patterns observed in various natural entities such as tree leaves, peacock wings, and electrical discharge formations in the sky. The SFSA algorithm conducts an exploratory search within the problem domain by employing fractals. The algorithm revolves around two fundamental processes: diffusion and updating.

This clustering process involved in the SFSA algorithm promotes exploitation by leveraging the proximity of each point to its present position. The updating process consists of two steps that modify the position of each solution. It involves mutating the elements and then involves a comprehensive transformation of the solution. The updating process is executed based on assigned probabilities for each solution. Consequently, superior solutions possess lower probabilities of modification and a greater likelihood of remaining unchanged [191] [192].

(i) Diffusion Process:

To bolster the algorithm's exploitation potential and enhance the likelihood of discovering local minima, coefficients are generated within the search space. Gaussian walks are utilized to generate different solutions, denoted by solution A and solution B, as described by equations (5.8) and (5.9).

Coefficient A (CA) is calculated as follows:

$$CA = Gaussian(\mu\_X, \sigma) + \varepsilon \times X - \grave{\varepsilon}' \times w_i \quad (5.8)$$

Coefficient B (CB) is obtained using the Gaussian distribution:

$$CB = Gaussian(\mu\_Y, \sigma) \quad (5.9)$$

In this context, ε and ἐ symbolize randomly generated numbers uniformly distributed within the range of 0 to 1. The ith coefficient is denoted as w_i, while X represents the optimal coefficients. μ_X and μ_Y refer to the absolute values of X and w_i, respectively. The standard deviation, σ, is determined using the formula illustrated in equation (5.10):

$$\sigma = \log(G) / G \times (w_i - X) \quad (5.10)$$

As the simulation progresses and the iteration (G) increases, the factor log(G)/G reduces the magnitude of the Gaussian jumps.

(ii) Updating Process

Following the initialization phase, the fitness of all coefficients within the search space is assessed, and the optimal coefficient (OC) is determined. The OC is then diffused around its initial position, yielding diverse coefficients using either Equation (5.8) or Equation (5.9).

Subsequently, a ranking procedure is conducted to evaluate the fitness of all coefficients. Each coefficient is assigned a uniform probability based on its fitness, as determined by equation (5.11).

The rank (ranki) of coefficient w_i among the other coefficients in the group is calculated as:

$$ranki = rank(w_i) / n \quad (5.11)$$

Here, $rank(w_i)$ represents the rank of coefficient w_i, and n is the total number of coefficients in the group.

For each coefficient w_i in the group, the jth component of w_i is updated according to the following equation if the condition ranki < ε is satisfied; otherwise, it remains unchanged:

$$w_i' = w_r(j) - \varepsilon \times (w_t(j) - w_i(j)) \quad (5.12)$$

Here, w_i' represents the newly modified position of coefficient w_i, while w_r and w_t denote randomly selected coefficients.

In the second updating phase, the positions of all coefficients are adjusted based on the positions of other coefficients in the group. This process helps improve the quality of exploration.

Once again, the coefficients obtained from the initial updating process are ranked using equation (5.11). If the condition ranki < ε is satisfied for the ith position of the new coefficient w_i', the current position of $w_i'(i)$ is adjusted using equations (5.13) and (5.14) depicted below. Otherwise, it remains unaltered.

$$w_i'' = w_i' + \varepsilon' \times (w_t' - X) \quad \text{if} \quad \varepsilon' \leq 0.5 \quad (5.13)$$

$$w_i'' = w_i' + \varepsilon' \times (w_t' - w_r') \quad \text{if} \quad \varepsilon' \geq 0.5 \quad (5.14)$$

During the initial updating process, random points, w_t' and w_r', are selected, and ε' is generated using a Gaussian distribution. If it is established that the fitness of the new solution is superior, only then is the value of w_i'' substituted with w_i'.

5.12.2 Developed matched wavelet MWSFSA: Matched wavelet using the stochastic fractal search algorithm.

In this research work the new matched wavelet has been developed for analysis of HRV signals of each participant. The matched wavelet has been optimized using the Stochastic fractal search (SFS) algorithm so that the developed matched wavelet (MWSFSA) can reconstruct the signal that depicts similar characteristics as the original signal. The frequency content and temporal properties of the HRV signal are matched by matched wavelets, which can enhance the analysis's signal-to-noise ratio (SNR). This may lessen the effect of noise on HRV characteristics.

5.12.2.1 Problem formulation

(a) *Initialization of filter coefficients.*

1) Initialize the analysis scaling filter coefficient '$w_0(n)$'.

2) Determine the analysis wavelet filter coefficients w1(n) as specified in equation (5.15).

$$w_1(n) = (-1)^n w_0(n) \quad (5.15)$$

3) Compute the synthesis filter coefficients '$h_0(n)$' and '$h_1(n)$' using equations (5.16) and (5.17).

$$h_0(n) = (-1)^n w_1(n) \quad (5.16)$$

$$h_1(n) = (-1)^{n+1} w_0(n) \quad (5.17)$$

(b) *Reconstruction of the HRV signal: S_{recon}*

Reconstruct the HRV signal 'S_{recon}' using the filter coefficients initialized in equations (5.15), (5.16), and (5.17).

(c**) *Calculation of Mean square error***

The MSE has been calculated using equation (5.18).

$$\mathbf{MSE} = \frac{\sum_{i=1}^{n}(S_{org} - S_{recon})^2}{N} \quad (5.18)$$

Where S_{recon} is the reconstructed signal, while S_{org} is the original signal.

(d) *Equality Constraints*

1) Orthogonality: The orthogonality is explained in the equation (5.19).

$\sum(w) = \sqrt{2}$

Hence, $g1 = \sum (w) - \sqrt{2}$ (5.19)

2) Normality: The scaling function is bound to have a norm of 1, which means that its energy is retained, by the normalcy requirement. The normality condition is given in the equation (5.20).

$\sum (w.\hat{}2) = 1$

Hence, $g2 = \sum (w.\hat{}2) - 1$ (5.20)

(e) Fitness function.

Fitness function = MSE + K * penalty (5.21)

Here K= 100, and the penalty can be calculated as –

Penalty = |g1| + |g2|

5.12.2.2 Application of SFSA in Optimization of the Filter Coefficients

To minimize the discrepancy between the reconstructed and original signal, the search methodology of fractals has been implemented to find the best filter coefficient for the best possible reconstruction of the signal. The implementation of SFSA for the optimization of filter coefficients and evaluating the best possible results is explained in the following steps and the methodology of optimized matched wavelet MWSFSA has been explained in the flowchart shown in Figure 5.5.

Step 1: All the random coefficients (points) have been evaluated between -1 and 1, in this step, as per equation (5.22)

$$\text{Points} = w_{min} + \text{rand}\,(w_{max} - w_{min}) \quad (5.22)$$

Where, w_{min} = -1 * ones (1, order)

w_{max} = 1 * ones (1, order)

Step 2: Load the original signal '*f*'.

Step 3: Constraint definition- equality constraints

g1 = Sum(w) - √2

g2 = Sum(w.^2) - 1

Step 4: Generation of wavelet using $w_0(n)$, $w_1(n)$, $h_0(n)$, and $h_1(n)$ as given in equations (5.15), (5.16), and (5.17).

Step 5: Reconstruction of the signal based on the generated wavelets as explained in step 4.

Step 6: Calculate the MSE between the signal generated in Step 6 and the original signal as loaded in Step 2.

Step 7: Decision making: Is iteration count < Maximum iteration?

(i) If NO, then results will be saved, and the LF/HF ratio will be calculated.

(ii) If YES, then diffusion will be started as explained in equations (5.8) and (5.9). Afterward, the first updating process begins as explained in equation (5.12). After the completion of the first updating, the second updating process started as mentioned in equations (5.13), and (5.14).

Step 8: After the second updating process completion, it is required to check whether the termination criterion is met or not.

(i) If YES – then results will be saved and the filter coefficients at which the minimum MSE is obtained will be used to reconstruct the signal.

(ii) If NO – then the process will start again from step 4.

5.13 Experimental Results and Discussion

In this research work, new matched wavelets have been developed to analyze each HRV signal. For this matched wavelet, the filter coefficients have been optimized using the stochastic fractal search algorithm. Using these optimized filter coefficients, signal reconstruction has been performed. For the comprehensive evaluation of HRV signals, the new matched wavelet has been developed using SFSA (MWSFSA) and compared with conventional wavelets (db2 to db6). Further, the filter coefficients have been optimized using SFSA, and these optimized filter coefficients have been used for the reconstruction of the signal. Also, MSE has been calculated between this reconstructed signal and the original signal.

5.13.1 Mean Square Error Calculation

In several disciplines, including signal processing, mean square error (MSE) is a regularly used metric to assess the accuracy of a reconstruction or prediction. MSE has been calculated using the equation (5.18). To verify the supremacy of the developed matched wavelet MWSFSA, a comprehensive comparative analysis has been performed in Table 5.1 and Table 5.2.

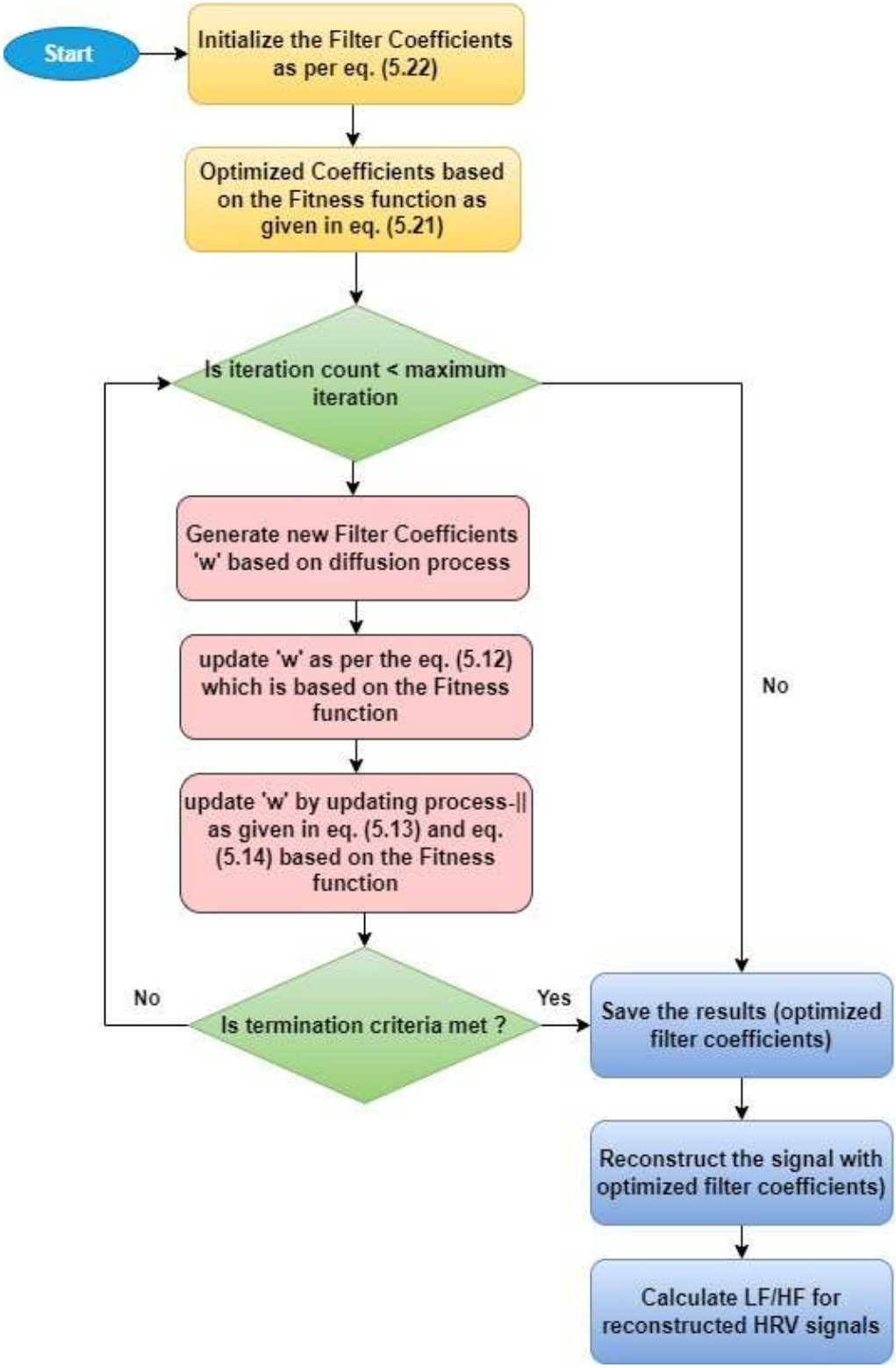

Figure 5.5 Flowchart of the matched wavelet MWSFSA for optimizing filter coefficients.

The comparative analysis between the matched wavelet MWSFSA, and conventional wavelets (db2 to db6) has been performed in this chapter based on MSE. The comparative analysis of MSE is given in Table 5.1 and Table 5.2.

Table 5.1 Comparison of MSE for applied methods for n=5 subjects in supine posture

Implemented Methods	**Comparison of MSE between the original and reconstructed signal for applied methods (n=5)**				
	Subject1	**Subject2**	**Subject 3**	**Subject4**	**Subject5**
db2	5.78E-07	6.40E-06	1.88E-08	4.95E-07	8.46E-07
db3	1.78E-07	5.14E-06	1.30E-09	3.85E-07	1.42E-06
db4	4.40E-09	7.04E-08	7.74E-09	3.02E-09	1.34E-08
db5	7.60E-08	2.43E-06	1.01E-09	1.80E-07	6.89E-07
db6	3.38E-08	3.91E-06	2.73E-08	2.64E-07	1.97E-06
MWSFSA	**1.72E-10**	**3.26E-10**	**9.77E-11**	**9.55E-13**	**1.89E-12**
Filter coefficients for each developed MWSFSA	W= [0.78099 0.00026 0.00831 0.62456]	W= [0.09474 0.91746 0.38556 0.01682]	W= [-0.18913 0.61665 0.27631 0.71162]	W= [0.02516 0.56528 0.82450 -0.00072]	W= [0.00115 0.05152 0.49504 0.86704]

The results show that when using the developed matched wavelet MWSFSA, the MSE value is significantly lower compared to the other utilized methods. This indicates a higher quality of signal reconstruction achieved by the MWSFSA method in comparison to the other approaches. Table 5.1 and Table 5.2 show the filter coefficients for five subjects in supine and standing posture which have been used in the signal reconstruction. Thus, MWSFSA is the most effective matched wavelet as it has less MSE in comparison to other wavelets.

5.13.2 Comparative analysis of MSE using box plot

As discussed above, the developed matched wavelet MWSFSA demonstrates the lowest MSE values as compared to the conventional wavelets (db2 to db6).

Table 5.2 Comparison of MSE for applied methods for n=5 subjects in standing posture

Implemented Methods	**Comparison of MSE between the original and reconstructed signal for applied methods (n=5)**				
	Subject1	**Subject2**	**Subject 3**	**Subject4**	**Subject5**
db2	3.00E-07	2.27E-07	3.10E-07	5.16E-11	6.93E-09
db3	3.16E-07	2.65E-07	1.18E-07	3.38E-10	1.36E-08
db4	1.18E-09	1.08E-10	7.74E-10	9.12E-11	1.02E-10
db5	1.51E-07	1.25E-07	5.31E-08	2.05E-10	7.92E-09
db6	3.11E-07	2.69E-05	3.69E-08	7.43E-10	8.08E-09
MWSFSA	**3.38E-10**	**8.17E-14**	**6.16E-13**	**1.36E-12**	**9.55E-13**
Filter coefficients for each developed MWSFSA	W= [0.16506 -0.11217 0.81107 0.55005]	W= [0.03913 0.02603 0.46664 0.88291]	W= [0.03913 0.02603 0.46664 0.88291]	W= [0.89831 0.40286 0.16754 -0.05482]	W= [0.02516 0.56528 0.82450 -0.00072]

This highlights the superior performance of the MWSFSA method in terms of signal reconstruction quality for all five subjects. So, it is necessary to evaluate the value distribution of MSE of 70 subjects in both body postures with all the applied methods using box plots. Figure 5.6 and Figure 5.7 represent the box plot of MSE in supine and standing posture respectively.

Figure 5.6 and Figure 5.7 show that the developed matched wavelets MWSFSA have a minimum deviation in the mean square error value between the original and reconstructed signal of HRV in both body postures compared to the other applied methods. The value distribution of MSE is at a lower scale for MWSFSA in supine and standing postures, which implies that the MWSFSA can optimize and generate the best optimal filter coefficients for each HRV signal that reconstructs the signal with maximum characteristics of the original signal intact with it.

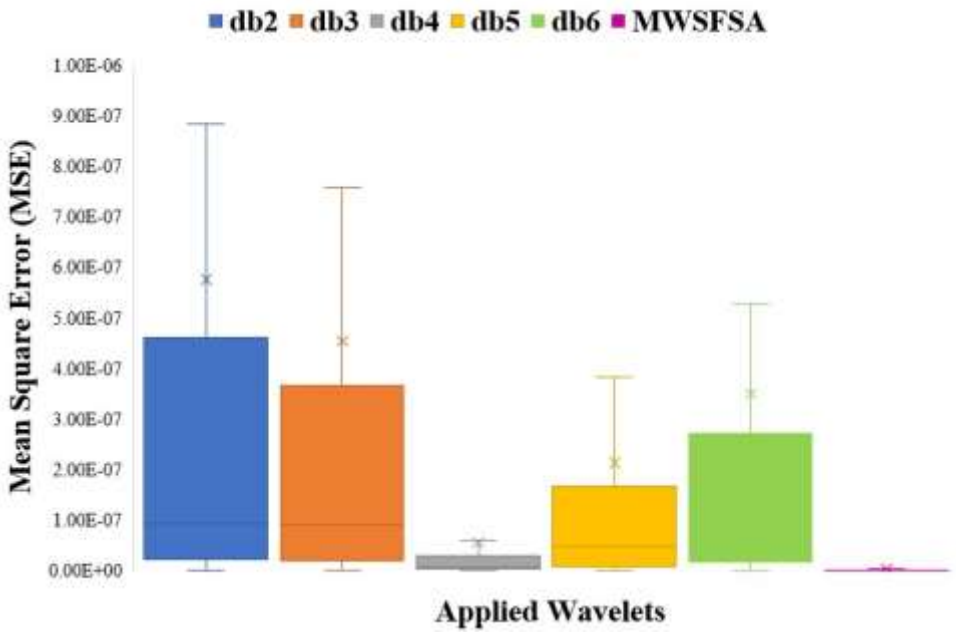

Figure 5.6 Comparison of Mean Square Error in Supine posture for 70 subjects between developed matched wavelet MWSFSA and conventional wavelets (db2 to db6).

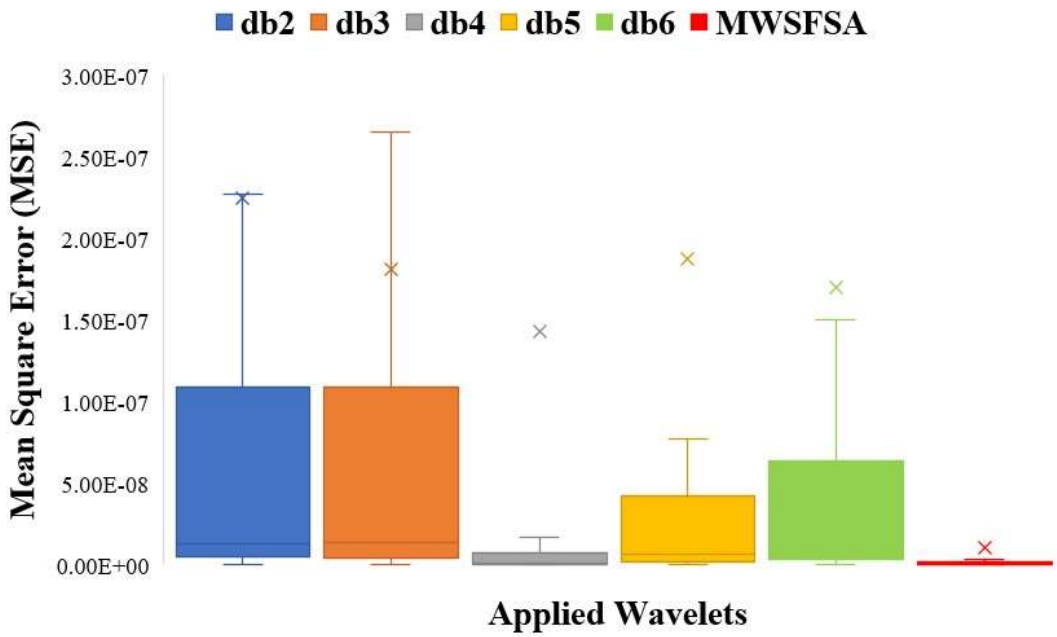

Figure 5.7 Comparison of Mean Square Error in Standing Posture for 70 subjects between developed matched wavelet MWSFSA and conventional wavelets (db2 to db6).

After MWSFSA, the existing wavelet db4 shows the minimum deviation of the MSE in both body postures. As the developed wavelet MWSFSA shows less deviation in the values of MSE in supine and standing posture, this makes MWSFSA superior to consider for the analysis of the LF/HF ratio of HRV for the reconstructed signal. The variation in LF/HF ratio represents the activation of the sympathetic or parasympathetic nervous systems in different body postures. The desired trend of the LF/HF ratio for the different postures and its interpretation has been explained in Table 5.3.

Table 5.3 The Interpretation of the Variation HRV in Supine and Standing Posture Using LF/HF Ratio

Parameter	**The Desired HRV trend in supine and standing position**	**Interpretation [108]**
LF/HF ratio	$LF/HF_{su} < LF/HF_{st}$	A rise in the value of the LF/HF ratio in standing posture indicates the activation of the sympathetic nervous system in this posture, while the decrease in supine posture implies the parasympathetic increment in this posture.

5.14 Comparative analysis of existing wavelets and developed matched wavelet MWSFSA using LF/HF ratio.

In this chapter, the HRV signal of 70 subjects has been analyzed for the postural variation effect using the developed and conventional wavelets. As mentioned in the section above, the optimized filter coefficients by developed matched wavelets MWSFSA are the most effective ones as compared to the other methods based on MSE. So, for each participant, an MWSFSA has been developed to generate the best possible filter coefficients for better signal reconstruction. In this way, for the HRV signal of 70 subjects, in supine and standing postures, the total number of developed matched wavelets is 140. The HRV signals were reconstructed using these optimized filter

coefficients, and subsequently, the LF/HF ratio was computed for each participant. When analyzing Heart Rate Variability (HRV), a commonly utilized parameter is the LF/HF ratio, which reflects the balance between low and high-frequency components. The "fight or flight" reaction activates sympathetic activity, which is predominantly linked to the low-frequency (LF) component of HRV. The parasympathetic response, sometimes known as the "rest and digest" response, is connected to the high-frequency (HF) component of HRV. This ratio, which reflects the entire autonomic nervous system activity, is frequently employed as a measure of sympathovagal balance.

The average value of the LF/HF ratio is given in Table 5.4. The level of significance between the value of supine and standing postures has been calculated using a paired t-test.

Table 5.4 Comparative analysis between applied methods using LF/HF ratio

S. No.	**Applied Wavelets**	**LF/HF Ratio**	
		Supine posture (n=70)	Standing posture (n=70)
1	db2	$1.31 \pm 0.89^{*}$	$3.66 \pm 2.11^{*}$
2	db3	$1.46 \pm 1.14^{*}$	$4.24 \pm 2.70^{*}$
3	db4	$1.50 \pm 1.27^{*}$	$4.59 \pm 3.08^{*}$
4	db5	$1.49 \pm 1.20^{*}$	$4.80 \pm 3.42^{*}$
5	db6	$1.56 \pm 1.38^{*}$	$4.85 \pm 3.44^{*}$
6	Developed matched wavelet MWSFSA	$0.73 \pm 0.30^{*}$	$1.32 \pm 0.83^{*}$

*Note: * represents the significance level $p < 0.0001$*

According to the data presented in Table 5.4, the LF/HF ratio value is lower in the supine posture and increases during the transition from supine to standing posture, indicating a shift in postural activity. This significant change in the value of the LF/HF ratio is noticed for all the applied wavelets. The higher value of the LF/HF ratio in the standing posture indicates that the heart rate variability is decreased in this posture, while the lower value of the LF/HF ratio represents the higher value of HRV in the supine posture.

5.15 Performance Analysis

The evaluation of the methods used in this study focused on their accuracy in detecting the HRV postural shift trend between supine and standing positions. The accuracy of the developed method was assessed individually for each subject, and the majority of subjects exhibited a higher LF/HF ratio in the standing posture as compared to the supine posture, as depicted in Figure 5.8. This observation can be explained by the following factors.

(i) *Consistency of results:* The developed method (MWSFSA) has consistently produced the expected trend of LF/HF ratio in 68 out of 70 subjects, indicating a high level of consistency in capturing the autonomic response to postural shifts. Most subjects displayed the anticipated pattern of a larger LF/HF ratio in standing and a lower LF/HF ratio in the supine posture, demonstrating the robustness and dependability of the developed method. This level of agreement demonstrates the reliability of the method on a subject-to-subject basis.

(ii) *Robustness of the developed method:* The developed method (MWSFSA) not only has a minimum MSE between the original and reconstructed signal for 70 subjects as shown in Figure 5.6 and Figure 5.7, but it also outperforms based on detecting accurate LF/HF ratio trend for the maximum subjects. This makes the developed method more robust compared to other methods because it performs well on both parameters, whether it is MSE or the trend of LF/HF ratio trend.

(iii) *Clear differentiation:* The stark difference between the two postures indicates that the developed method (MWSFSA) successfully captures the autonomic alterations brought on by postural variations. Understanding the autonomic response to postural changes depends on this differentiation.

(iv) *Clinical implications:* The ability to accurately detect changes in the LF/HF ratio during postural shifts for maximum subjects can provide valuable information about the autonomic function and potentially aid in diagnosing or monitoring certain conditions. This highlights the practical significance of the method's accuracy.

(v) *Accuracy measurement:* The accuracy of the developed method (MWSFSA) has been measured using the equation (5.23).

$$\text{Accuracy} = \frac{\begin{array}{c} No.of\ subjects\ having\ \frac{LF}{HF}\ ratio\ in \\ supine\ posture < No.\ of\ subjects\ having\ \frac{LF}{HF}\ ratio\ in \\ Standing\ posture \end{array}}{Total\ number\ of\ subjects} \tag{5.23}$$

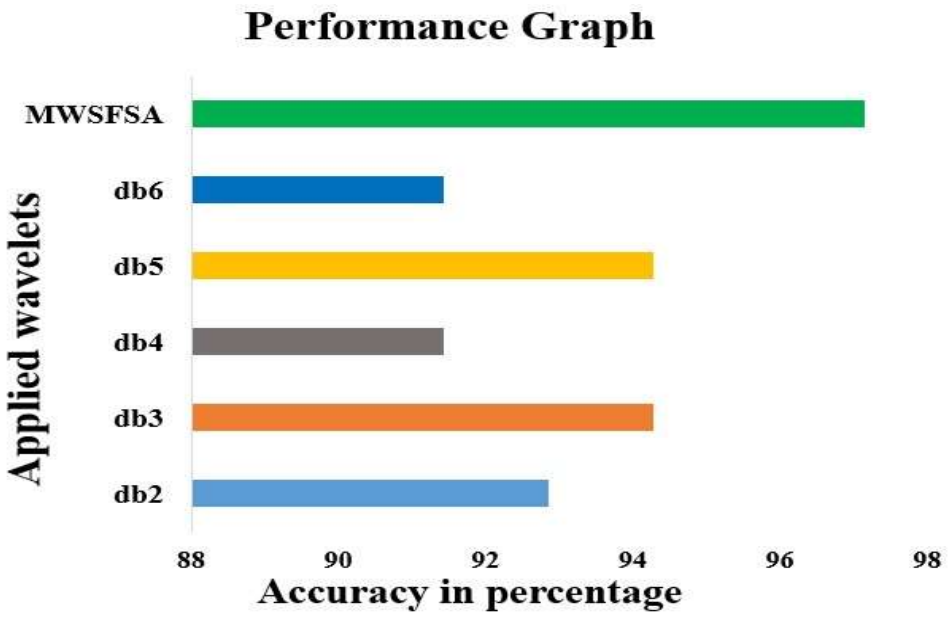

Figure 5.8 Accuracy of the developed matched wavelet MWSFSA along with db2 to db6 for correctly detecting the LF/HF ratio for postural change.

5.16 The Correlation between HRV, HR and SCR

As mentioned in the previous chapters, in this research work the skin conduction response of 70 subjects has been recorded along with HR in both the posture (supine and standing) for analyzing the impact on ANS activity. In Table 5.5 the mean value of SCR, HR, and LF/HF ratio of HRV have been given along with the standard deviation. The significant difference between the values of different postures has been evaluated by performing a statistical analysis and given as a p-value.

From Table 5.5 it is evident that the mean value of LF/HF ratio, SCR, and HR increased in the postural change activity from supine to standing. This implies that the activity of the sympathetic nervous system increased in the standing posture.

Table 5.5 Correlation between LF/HF ratio, SCR, and HR for postural change from supine to standing position.

Parameters	Supine (Mean ± SD)	Standing (Mean ± SD)	*p*-value	Parameter variations in Supine and Standing positions	Interpretation
LF/HF ratio	0.73±0.30*	1.32±0.83*	4.0190e-08	**LF/HF_{su} < LF/HF_{st}**	A rise in the value of the LF/HF ratio in standing posture indicates the activation of the sympathetic nervous system in this posture, while the decrease in supine posture implies the parasympathetic increment in this posture. An elevated LF/HF ratio during posture changes suggests a shift in the sympathovagal balance towards a predominance of sympathetic activity.

SCR	1.79±2.03	2.44± 2.35	4.00E-05	**$SCR._{st}$ > $SCR._{su}$**	The mean value of SCR is higher in the standing position as compared to supine implying that sympathetic activation is higher in the standing position.
Heart rate	76.80±11.01	93.94±12.93	3.67E-27	**$HR._{st}$ > $HR._{su}$**	The mean value of HR is smaller in the position supine as compared to standing implies that the parasympathetic activity is higher in the supine position.

The elevated values of these three parameters during posture changes suggest a shift in the sympathovagal balance towards a predominance of sympathetic activity in the standing position. This also represents a positive correlation between HR, LF/HF ratio, and SCR for postural change activity.

5.17 Conclusion

In this chapter, the influence of postural transitions, specifically from supine to standing has been explored on heart rate variability (HRV) using different wavelets. The study aimed to improve the accuracy of HRV analysis by developing and applying the matched wavelet named MWSFSA obtained through optimization algorithms. Furthermore, this work has been focused on analyzing the LF/HF ratio as an indicator of autonomic nervous system activity, specifically the balance between sympathetic and parasympathetic activity.

The findings of this study demonstrate that the MWSFSA wavelet is more accurate in capturing the effects of postural changes on HRV parameters, particularly the LF/HF ratio. The superior performance of the MWSFSA wavelet, indicated by the minimum mean squared error (MSE) between reconstructed and original signals, suggests its efficacy in capturing the intricate interplay between sympathetic and parasympathetic activity. The LF/HF ratio serves as an essential marker of autonomic balance, representing the relative contributions of sympathetic and parasympathetic branches of the autonomic nervous system to cardiac activity. The accurate determination of LF/HF ratio trends in response to postural changes enables a deeper understanding of autonomic regulation during orthostatic challenges. The ability to reliably assess sympathetic and parasympathetic activity through accurate LF/HF ratio analysis has broad implications. It can aid in evaluating cardiovascular health, identifying subjects at risk for autonomic dysfunction, and developing targeted interventions for various clinical conditions, including orthostatic intolerance, cardiovascular diseases, and autonomic disorders.

In conclusion, developing and implementing the MWSFSA wavelet, optimized for HRV analysis during postural changes, offers a valuable contribution to the field. The enhanced accuracy of the LF/HF ratio assessment is 97.14 % which is the highest compared to other wavelets, for capturing the complex dynamics of sympathetic and parasympathetic activity, providing valuable insights into autonomic control of the cardiac system. Further, a positive correlation between HR, LF/HF ratio, and SCR for postural change activity is found. This research has the potential to advance our understanding of autonomic regulation and facilitate more precise assessment of cardiovascular health, which pave the way for future studies in investigating the impact of postural changes on ANS function.

CHAPTER 6

CONCLUSION AND SCOPE FOR FUTURE WORK

The research of cardiovascular variability and skin conductance has gained popularity as a result of major technological developments in measurement instruments and processing capabilities. This dissertation is no exception. At the end of each chapter, we share numerous study findings that are specific to that chapter's content. In this chapter, we explain the thesis's significant contributions and evaluate its prospects for further extension.

6.1 Conclusion

Changes in cardiovascular rhythms and their impact on the autonomic nervous system (ANS) have been linked to a variety of physiological issues and medical interventions, such as changes in posture, exercise, mental stress, etc. The study of Heart rate patterns has a long history, there has been a surge of interest in the last three decades. There is a rising emphasis in current research on investigating skin conductance response and its impact on ANS. HRV and SC have both been linked to an assortment of health issues, including diabetes, myocardial infarction, hypertension, physical activity, and stress. As a result, HRV signals and SCR data have been collected to acquire physiological information during postural changes in this research work. This enables research into the dynamic shifts in individuals' cardiovascular regulation in tandem with electrodermal activity.

In this thesis work, the effect of postural change has been examined on HRV and SCR. To achieve this, the HRV and SCR data of 70 young healthy participants have been acquired in supine and standing postures.

This thesis delves into several established linear and nonlinear methods for analyzing HRV, as well as introducing new HRV analysis techniques to address the stated objectives." Furthermore, the relationship between HRV and SCR (Skin Conductance Response) has been studied.

The following are the key conclusions:

1. At the beginning of this study, established linear HRV analysis methods were used. On the recorded dataset, time-domain (SDNN, RMSSD, NN50, pNN50) and frequency-domain (LF, HF, LF/HF ratio) approaches were employed to analyze the variation of HRV postural transitions from supine to standing position. Findings show that the frequency-domain approach, specifically the LF/HF ratio, is more effective than time-domain methods at detecting HRV differences between postures with 85.71% accuracy. However, when assessing HRV in the context of physiological data, the LF/HF ratio alone may not give sufficient precision.

2. Due to the inefficient performance of the linear HRV analysis methods, and considering the nonlinear nature of HRV, nonlinear analysis of HRV has been performed using the existing method- Sample entropy. This study also attempted to investigate the relationship between HRV and SCR for postural change activities. From the analysis results, it is found that sample entropy is 88.57% accurate in detecting the postural variation of HRV from supine to standing postures correctly. Nonetheless, the conventional SE technique exhibits a susceptibility to short signal lengths, relying on a single distance function for matching vector pairs, which renders the analysis insufficient for establishing the connection between HRV and SC. Consequently, a novel approach called "composite distance sample entropy (CDSE)" has been introduced to mitigate the impact of short signal lengths. In the proposed CDSE method, the calculation of the distance between the two template vectors is conducted utilizing the composite distance function. The proposed method demonstrates an accuracy of 94.28%, which is approximately 6% more precise in detecting postural variations in HRV.

Furthermore, to substantiate the superiority of the CDSE method we propose, various noise signals of differing lengths were simulated. The results affirm that the proposed method outperforms the conventional SE method in terms of accuracy and appears to be less influenced by signal length variations. Additionally, our research uncovers a positive correlation between HR and SC across various body postures.

3. However, employing standard linear and nonlinear HRV methodologies to investigate and analyze long-term nonlinear heart rate fluctuations has intrinsic problems. To address this, these short variations in heart rate using wavelet transforms are examined. In this investigation, discrete wavelet transform is used to deconstruct HRV signals obtained during postural shifts. Following that a comparative analysis of other wavelet families, notably db2-db6 is performed. The results of using these distinct wavelets revealed that the LF/HF ratio in standing postures is larger than in supine postures. However, it is important to highlight that for the majority of research participants, these wavelets were unable to discern between the two body postures' HRV variations.
4. To overcome the drawbacks of the current conventional wavelets, a new matched wavelet using the stochastic fractal search algorithm has been developed. The fundamental drawback of employing existing wavelets is that their selection is frequently made without consideration of the signal under investigation. The changes of a particular HRV signal cannot be decoded using these wavelet basis functions. In terms of analysis, picking the right wavelet to measure HRV changes is a crucial step.
5. It is found that the new matched wavelet “MWSFSA” which is developed using a stochastic fractal search algorithm can accurately capture the effects of postural changes on HRV parameters, particularly the LF/HF ratio. The superior performance of the MWSFSA wavelet, indicated by the minimum mean squared error (MSE) between reconstructed and original signals, suggests its efficacy in capturing the intricate interplay between sympathetic and parasympathetic activity. The accurate determination of LF/HF ratio trends in response to postural changes enables a deeper understanding of autonomic regulation during orthostatic challenges. Thus, developing and implementing the MWSFSA wavelet, optimized for HRV analysis during postural changes, offers a valuable contribution to the field. The enhanced accuracy of the LF/HF ratio assessment is 97.14 % which is as highest compared to others, for capturing

the complex dynamics of sympathetic and parasympathetic activity, providing valuable insights into autonomic control of the cardiac system. A positive correlation between HRV's spectral parameter, LF/HF ratio, and SCR for postural change activity is found.

6.2 Limitations of this work and Scope for future work

HRV and SCR measurements are being used in a variety of applications. The measurements of HRV and SCR not only offer a basic connection between psychological processes and physiological processes but also allow for the analysis of the skin's electrical activity and the cardiac autonomic state. There are still certain concerns that must be handled because standardizing HRV techniques and response of skin conductance entail doing so. The following are some of the issues covered**:**

1. In this work, the effect of postural change has been analyzed from a supine position to a standing position to investigate the response of HRV and its relationship with SCR. Further, a sitting position will be desired to be included to investigate the deep analysis of the postural change effect.
2. In this work, HRV and SCR are the only two parameters considered to find the difference between postural change variation on the activity of ANS. For further analysis, other parameters such as respiration rate, blood pressure, etc., may contribute to a comprehensive investigation.
3. Within this study, an examination was carried out on a range of established algorithms aimed at identifying accurate HRV variations during postural changes. Given the constraints and shortcomings observed in these conventional algorithms, a set of innovative algorithms was subsequently introduced. These algorithms were further used to evaluate the accurate HRV fluctuations that occurred during the postural change activity on a self-recorded HRV dataset of 10 min duration and its association with SCR. However, the recording time of 10 minutes needs to be increased to determine its true relevance in identifying HRV changes and their association with SCR based on physiological behavior
4. In this work, a dataset of young people between the ages of 18 and 25 has been used. The population of middle-aged and older people needs to be taken into account to generalize the postural effect on physiological signals for further research.

5. For additional research, a gender-based study of postural change activity may be added.
6. The key emphasis of this work is based on analyzing the HRV variation for postural change activity and its association with the response of skin conductance. Skin conductance response needs to be analyzed deeply for further research using signal processing methods.
7. In this research work, a limited set of standard analysis methods was used to analyze the HRV dataset. Further, other existing methods may also be used for a comprehensive investigation of the HRV.
8. This research work primarily focuses on a deeper understanding of HRV analysis. However, the skin conductance analysis may be explored in further work in detail.

It is envisaged that the current work will make a significant addition to the field of HRV analysis approaches in detecting HRV changes and its link with SCR during postural change activity. The research presented in this thesis will also advance non-invasive HRV and SCR analysis techniques for efficient healthcare provision.

References

[1] M. Malik, “Heart rate variability: Standards of measurement, physiological interpretation, and clinical use.” *European Heart Journal*, vol. 17, no. 3, pp. 354-381, 1996, doi: 10.1093/oxfordjournals.eurheartj.a014868.

[2] T. Chaspari, A. Tsiartas, L. I. Stein, S. A. Cermak, and S. S. Narayanan, “Sparse Representation of Electrodermal Activity with Knowledge-Driven Dictionaries.” *IEEE Transactions on Biomedical Engineering*, vol. 62, no. 3, pp. 960-971, 2015, doi: 10.1109/tbme.2014.2376960.

[3] H. F. Posada-Quintero, T. Dimitrov, A. Moutran, S. Park, and K. H. Chon, “Analysis of Reproducibility of Noninvasive Measures of Sympathetic Autonomic Control Based on Electrodermal Activity and Heart Rate Variability.” *IEEE Access*, vol. 7, pp. 22523-22531, 2019, doi: 10.1109/access.2019.2899485.

[4] A. Terkelsen, H. Mølgaard, J. Hansen, N. Finnerup, K. Krøner, and T. Jensen, “Heart Rate Variability in Complex Regional Pain Syndrome during Rest and Mental and Orthostatic Stress.” *Anesthesiology*, vol. 116, no. 1, pp. 133-146, 2012, doi: 10.1097/aln.0b013e31823bbfb0.

[5] I. Šipinková, G. Hahn, M. Meyer, M. Tadlanek, and J. Hajek, "Effect of respiration and posture on heart rate variability." *Physiol. Res*, vol. 46, pp. 173-179, 1997.

[6] P. Sarang and S. Telles, “Effects of two yoga-based relaxation techniques on heart rate variability (HRV).” *International Journal of Stress Management*, vol. 13, no. 4, pp. 460-475, 2006, doi: 10.1037/1072-5245.13.4.460.

[7] G. G. Berntson, K. S. Quigley, G. J. Norman, and D. L. Lozano, "Cardiovascular Psychophysiology." *Handbook of Psychophysiology*, pp. 183-216, doi: 10.1017/9781107415782.009.

[8] J. L. Andreassi, "The Psychophysiology of cardiovascular reactivity." *International Journal of Psychophysiology*, vol. 25, no. 1, pp. 7-11, 1997, doi: 10.1016/s0167-8760(96)00732-5.

[9] G. G. BERNTSON, "Heart rate variability: Origins, methods, and interpretive caveats." *Psychophysiology*, vol. 34, no. 6, pp. 623-648, 1997, doi: 10.1111/j.1469-8986.1997.tb02140.x.

[10] B. N. Kyle and D. W. McNeil, "Autonomic Arousal and Experimentally Induced Pain: A Critical Review of the Literature." *Pain Research and Management*, vol. 19, no. 3, pp. 159-167, 2014, doi: 10.1155/2014/536859.

[11] F. R. Walker, A. Thomson, K. Pfingst, E. Vlemincx, E. Aidman, and E. Nalivaiko, "Habituation of the electrodermal response – A biological correlate of resilience?" *PLOS ONE*, vol. 14, no. 1, 2019, doi: 10.1371/journal.pone.0210078.

[12] H. Tsuji, "Reduced heart rate variability and mortality risk in an elderly cohort. The Framingham Heart Study." *Circulation*, vol. 90, no. 2, pp. 878-883, 1994, doi: 10.1161/01.cir.90.2.878.

[13] M. A. Nystoriak and A. Bhatnagar, "Cardiovascular Effects and Benefits of Exercise." *Frontiers in Cardiovascular Medicine*, vol. 5, 2018, doi: 10.3389/fcvm.2018.00135.

[14] G.D. Clifford, "Signal processing methods for heart rate variability analysis," Ph.D. dissertation, University of Oxford, 2002.

[15] C. H. Renu Madhavi, "Characterisation of Heart Rate Variability of Healthy, Cardiac and Non-cardiac Diseased Subjects using Nonlinear Techniques," Ph.D. dissertation, Avinashilingam University for Women, Coimbatore, 2012.

[16] M. Sylva, M. J. Van den Hoff, and A. F. Moorman, “Development of the human heart.” *American Journal of Medical Genetics Part A*, vol. 164, no. 6, pp. 1347-1371, 2013, doi: 10.1002/ajmg.a.35896.

[17] K. V. L. Siem, “Modelling fibre orientation of the left ventricular human heart wall,” master’s thesis, Institutt for datateknikk og informasjonsvitenskap, 2007.

[18] “Atrium (heart) - Wikipedia.” https://en.wikipedia.org/wiki/Atrium_(heart).

[19] B. S. Saini, “Signal Processing of Heart Rate Variability,” Ph. D. Thesis, Dr. B. R. Ambedkar National Institute of Technology, Jalandhar, 2009.

[20] E. Tze-Yeng Chang, “Towards understanding the electrogram: Theoretical & experimental multiscale modelling of factors affecting action potential propagation in cardiac tissue,” Ph. D. Thesis, Imperial College, London.

[21] https://ykhoa.org/d/image.htm?imageKey=CARD/63340

[22] Y. N. Singh, “ECG Delineation and its Application in Individual Identification,” M. Tech Thesis, Indian Institute of Technology, Kanpur, 2007.

[23] G. Q. Gao, “Computerised and Classification of five Cardiac Conditions,” M. E. Thesis, Auckland University of Technology, Auckland, Newzealand, 2003.

[24] S. Z. Fatemian, “A Wavelet-based Approach to Electrocardiogram (ECG) and Phonocardiogram (PCG) Subject Recognition,” Master of Applied REFERENCES Analysis of Heart Rate Variability in Menstrual Cycle of Women 237 Science Thesis, University of Toronto, Toronto, 2009.

[25] P. Madona, R. I. Basti, and M. M. Zain, “PQRST wave detection on ECG signals.” *Gaceta Sanitaria*, vol. 35, 2021, doi: 10.1016/j.gaceta.2021.10.052.

[26] D. J. Cornforth, M. P. Tarvainen, and H. F. Jelinek, “How to Calculate Renyi Entropy from Heart Rate Variability, and Why it Matters for Detecting Cardiac Autonomic Neuropathy.” *Frontiers in Bioengineering and Biotechnology*, vol. 2, 2014, doi: 10.3389/fbioe.2014.00034.

[27] C. Kappeler-Setz, F. Gravenhorst, J. Schumm, B. Arnrich, and G. Tröster, “Towards long term monitoring of electrodermal activity in daily life.” *Personal and Ubiquitous Computing*, vol. 17, no. 2, pp. 261-271, 2011, doi: 10.1007/s00779-011-0463-4.

[28] J. Shukla, M. Barreda-Angeles, J. Oliver, G. C. Nandi, and D. Puig, “Feature Extraction and Selection for Emotion Recognition from Electrodermal Activity.” *IEEE Transactions on Affective Computing*, vol. 12, no. 4, pp. 857-869, 2021, doi: 10.1109/taffc.2019.2901673.

[29] H. F. Posada-Quintero, “Time-varying analysis of electrodermal activity during exercise.” *PLOS ONE*, vol. 13, no. 6, 2018, doi: 10.1371/journal.pone.0198328.

[30] H. F. Posada-Quintero, J. P. Florian, Álvaro D. Orjuela-Cañón, and K. H. Chon, “Highly sensitive index of sympathetic activity based on time-frequency spectral analysis of electrodermal activity.” *American Journal of Physiology-Regulatory, Integrative and Comparative Physiology*, vol. 311, no. 3, 2016, doi: 10.1152/ajpregu.00180.2016.

[31] E. Syrjala, M. Jiang, T. Pahikkala, S. Salantera, and P. Liljeberg, “Skin Conductance Response to Gradual-Increasing Experimental Pain.” *2019 41st Annual International Conference of the IEEE Engineering in Medicine and Biology Society (EMBC),* 2019, doi: 10.1109/embc.2019.8857776.

[32] E. Babaei, B. Tag, T. Dingler, and E. Velloso, “A Critique of Electrodermal Activity Practices at CHI.” *Proceedings of the 2021 CHI Conference on Human Factors in Computing Systems*, 2021, doi: 10.1145/3411764.3445370.

[33] M. Kana, “Mathematical Models of Cardiovascular Control by the Autonomic Nervous System,” Ph. D. Thesis, Czech Technical University in Prague, Prague, 2010.

[34] J. Simmons, “Autonomic Nervous System Response to Repeated Cold Exposure”, M. S. Thesis, B.S., Louisiana State University, 2013.

[35] “Respiratory variations of the heart rate - I—The reflex mechanism of the respiratory arrhythmia.” *Proceedings of the Royal Society of London. Series B - Biological Sciences*, vol. 119, no. 813, pp. 191-217, 1936, doi: 10.1098/rspb.1936.0005.

[36] “Respiratory variations of the heart rate -The central mechanism of the respiratory arrhythmia and the inter-relations between the central and the reflex mechanisms.” *Proceedings of the Royal Society of London. Series B - Biological Sciences*, vol. 119, no. 813, pp. 218-230, 1936, doi: 10.1098/rspb.1936.0006.

[37] H. E. Hering, "A functional test of heart vagi in man." *Menschen Munchen Medizinische Wochenschrif,t* vol. 57, pp. 1931-1933, 1910.

[38] R. Hamlin, C. Smith, and D. Smetzer, “Sinus arrhythmia in the dog.” *American Journal of Physiology-Legacy Content*, vol. 210, no. 2, pp. 321-328, 1966, doi: 10.1152/ajplegacy.1966.210.2.321.

[39] B. W. HYNDMAN, R. I. KITNEY, and B. M. SAYERS, “Spontaneous Rhythms in Physiological Control Systems.” *Nature*, vol. 233, no. 5318, pp. 339-341, 1971, doi: 10.1038/233339a0.

[40] B. SAYKRS, “Analysis of Heart Rate Variability.” *Ergonomics*, vol. 16, no. 1, pp. 17-32, 1973, doi: 10.1080/00140137308924479.

[41] G. Chess, R. Tam, and F. Calaresu, “Influence of cardiac neural inputs on rhythmic variations of heart period in the cat.” *American Journal of Physiology-Legacy Content*, vol. 228, no. 3, pp. 775-780, 1975, doi: 10.1152/ajplegacy.1975.228.3.775.

[42] B. W. HYNDMAN and J. R. GREGORY, “Spectral Analysis of Sinus Arrhythmia during Mental Loading.” *Ergonomics*, vol. 18, no. 3, pp. 255-270, 1975, doi: 10.1080/00140137508931460.

[43] J. Penaz, N. Honzikova, and B. Fiser. "Spectral analysis of resting variability of some circulatory parameters in man." *Physiologia Bohemoslovaca,* vol. 27, no. 4, pp. 349-357, 1978.

[44] G. A. Myers, “Power Spectral Analysis of Heart Rate Varability in Sudden Cardiac Death: Comparison to Other Methods.” *IEEE Transactions on Biomedical Engineering*, no. 12, pp. 1149-1156, 1986, doi: 10.1109/tbme.1986.325694.

[45] M. Malik, T. Cripps, T. Farrell, and A. J. Camm, “Prognostic value of heart rate variability after myocardial infarction. A comparison of different data-processing methods.” *Medical & Biological Engineering & Computing*, vol. 27, no. 6, pp. 603-611, 1989, doi: 10.1007/bf02441642.

[46] K. Schreibman, C. Thomas, and M. Levy, “Spectral analysis of cardiac cycle length variations: resampling overcomes effects of nonuniform spacing.” *Images of the Twenty-First Century. Proceedings of the Annual International Engineering in Medicine and Biology Society*, Nov. 1989, doi: 10.1109/iembs.1989.95561.

[47] M. Merri, D. Farden, J. Mottley, and E. Titlebaum, “Sampling frequency of the electrocardiogram for spectral analysis of the heart rate variability.” *IEEE Transactions on Biomedical Engineering*, vol. 37, no. 1, pp. 99-106, 1990, doi: 10.1109/10.43621.

[48] R. Furlan, “Continuous 24-hour assessment of the neural regulation of systemic arterial pressure and RR variabilities in ambulant subjects.” *Circulation*, vol. 81, no. 2, pp. 537-547, 1990, doi: 10.1161/01.cir.81.2.537.

[49] M. Malik, and A. J. Camm, Eds., Heart Rate Variability, Armonk, NY: Futura, 1995.

[50] P. C. Ivanov, “Scaling behaviour of heartbeat intervals obtained by wavelet-based time-series analysis.” *Nature*, vol. 383, no. 6598, pp. 323-327, 1996, doi: 10.1038/383323a0.

[51] S. Jasson, “Instant Power Spectrum Analysis of Heart Rate Variability During Orthostatic Tilt Using a Time-/Frequency-Domain

Method.” *Circulation*, vol. 96, no. 10, pp. 3521-3526, 1997, doi: 10.1161/01.cir.96.10.3521.

[52] P. Laguna, G. Moody, and R. Mark, “Power spectral density of unevenly sampled data by least-square analysis: performance and application to heart rate signals.” *IEEE Transactions on Biomedical Engineering*, vol. 45, no. 6, pp. 698-715, 1998, doi: 10.1109/10.678605.

[53] H. V. Huikuri, T. Mäkikallio, K. Airaksinen, R. Mitrani, A. Castellanos, and R. J. Myerburg, “Measurement of heart rate variability: a clinical tool or a research toy?” *Journal of the American College of Cardiology*, vol. 34, no. 7, pp. 1878-1883, 1999, doi: 10.1016/s0735-1097(99)00468-4.

[54] F. Lombardi, "Heart rate variability: a contribution to a better understanding of the clinical role of heart rate." *European Heart Journal Supplements,* vol. 1, no. H, pp. 44-51, 1999.

[55] H. Chan, C. Lin, and Y. Ko, “Segmentation of heart rate variability in different physical activities.” *Computers in Cardiology* 2003, doi: 10.1109/cic.2003.1291099.

[56] Y. Yamamoto, K. Kiyono, and Z. R. Struzik, “Measurement analysis, interpretation of long-term heart rate variability,” *in Proceedings of SICE Annual Conference*, 2004, pp. 2598-2605.

[57] S. Osowski, L. Hoai, and T. Markiewicz, “Support Vector Machine-Based Expert System for Reliable Heartbeat Recognition.” *IEEE Transactions on Biomedical Engineering*, vol. 51, no. 4, pp. 582-589, 2004, doi: 10.1109/tbme.2004.824138.

[58] U. Rajendra Acharya, N. Kannathal, L. Mei Hua, and L. Mei Yi, “Study of heart rate variability signals at sitting and lying postures.” *Journal of Bodywork and Movement Therapies*, vol. 9, no. 2, pp. 134-141, 2005, doi: 10.1016/j.jbmt.2004.04.001.

[59] G. Kheder, A. Kachouri, M. Ben Messouad, and M. Samet, “Application of a Nonlinear Dynamic Method in the Analysis of the HRV (Heart Rate Variability) Towards Clinical Application: Tiresome Diagnosis.” *2006 2nd International Conference on Information & Communication Technologies*, vol. 1, pp. 177-182, 2004, doi: 10.1109/ictta.2006.1684366.

[60] Y. Zhang, Q. Zhang, and S. Wu, "Biomedical signal detection based on fractional fourier transform." *2008 International Conference on Technology and Applications in Biomedicine*, 2008, doi: 10.1109/itab.2008.4570600.

[61] R. Bailón, L. Mainardi, M. Orini, L. Sörnmo, and P. Laguna, "Analysis of heart rate variability during exercise stress testing using respiratory information." *Biomedical Signal Processing and Control*, vol. 5, no. 4, pp. 299-310, 2010, doi: 10.1016/j.bspc.2010.05.005.

[62] J. Rafiee, M. Rafiee, N. Prause, and M. Schoen, "Wavelet basis functions in biomedical signal processing." *Expert Systems with Applications*, vol. 38, no. 5, pp. 6190-6201, 2011, doi: 10.1016/j.eswa.2010.11.050.

[63] C. H. Renu Madhavi, and A. G. Ananth, "A Review of Heart Rate Variability and It's Association with Diseases," *International Journal of Soft Computing and Engineering (IJSCE)*, vol. 2, no. 3, 2012.

[64] K. Palanisamy, M. Murugappan, and S. Yaacob, "Multiple Physiological Signal-Based Human Stress Identification Using Non-Linear Classifiers." *Electronics and Electrical Engineering*, vol. 19, no. 7, 2013, doi: 10.5755/j01.eee.19.7.2232

[65] L. E. V. Silva, B. C. T. Cabella, U. P. da C. Neves, and L. O. Murta Junior, "Multiscale entropy-based methods for heart rate variability complexity analysis." *Physica A: Statistical Mechanics and its Applications*, vol. 422, pp. 143-152, 2015, doi: 10.1016/j.physa.2014.12.011.

[66] K. Rawal, B. S. Saini, and I. Saini, "Design of tree structured matched wavelet for HRV signals of menstrual cycle." *Journal of Medical Engineering & Technology*, vol. 40, no. 5, pp. 223-238, 2016, doi: 10.3109/03091902.2016.1162213

[67] A. Porta, V. Bari, G. Ranuzzi, B. De Maria, and G. Baselli, "Assessing multiscale complexity of short heart rate variability series through a model-based linear approach." *Chaos: An Interdisciplinary Journal of Nonlinear Science*, vol. 27, no. 9, 2017, doi: 10.1063/1.4999353.

[68] A. Porta, "On the Relevance of Computing a Local Version of Sample Entropy in Cardiovascular Control Analysis." *IEEE Transactions on*

Biomedical Engineering, vol. 66, no. 3, pp. 623-631, 2019, doi: 10.1109/tbme.2018.2852713.

[69] A. K. Verma, I. Saini, and B. S. Saini, "A new BAT optimization algorithm based feature selection method for electrocardiogram heartbeat classification using empirical wavelet transform and Fisher ratio." *International Journal of Machine Learning and Cybernetics*, vol. 11, no. 11, pp. 2439-2452, 2020, doi: 10.1007/s13042-020-01128-0.

[70] K. Rawal and G. Sethi, "Design of Matched Wavelet Using Improved Genetic Algorithm for Heart Rate Variability Analysis of the Menstrual Cycle." *International Journal of Image and Graphics*, p. 2150030, 2020, doi: 10.1142/s0219467821500303.

[71] W. Boucsein, "Electrodermal activity: Springer science & business media," *Broek, EL vd, Schut, MH, Westerink, JHDM, Herk, J. v., & Tuinenbreijer, K.* 2012 Feb.

[72] H. D. Critchley, "Review: Electrodermal Responses: What Happens in the Brain." *The Neuroscientist*, vol. 8, no. 2, pp. 132-142, 2002, doi: 10.1177/107385840200800209.

[73] M. E. Dawson, A. M. Schell, and D. L. Filion, "The Electrodermal System." *Handbook of Psychophysiology*, pp. 217-243, 2007, doi: 10.1017/9781107415782.010.

[74] J. L. Andreassi, "Psychophysiology." *Psychology Press.*, Jul. 2013, doi: 10.4324/9781410602817.

[75] J. T. Cacioppo, L. G. Tassinary, and G. G. Berntson, "Psychophysiological Science: Interdisciplinary Approaches to Classic Questions About the Mind." *Handbook of Psychophysiology*, vol. 3, pp. 1-16, 2007, doi: 10.1017/cbo9780511546396.001.

[76] J. A. Coan and J. J. Allen, "The Handbook of emotion elicitation and assessment." *Choice Reviews Online*, vol. 46, no. 3, 2007, doi: 10.5860/choice.46-1769.

[77] P. J. Lang and M. M. Bradley, "Emotion and the motivational brain." *Biological Psychology*, vol. 84, no. 3, pp. 437-450, 2010, doi: 10.1016/j.biopsycho.2009.10.007

[78] R. Metelka, “Heart rate variability - current diagnosis of the cardiac autonomic neuropathy. A review.” *Biomedical Papers*, vol. 158, no. 3, pp. 327-338, 2014, doi: 10.5507/bp.2014.025.

[79] A. Soni and K. Rawal, “A Review on Physiological Signals: Heart Rate Variability and Skin Conductance.” *Lecture Notes in Networks and Systems*, pp. 387-399, 2020, doi: 10.1007/978-981-15-3369-3_30.

[80] T. Chaspari, A. Tsiartas, L. I. Stein, S. A. Cermak, and S. S. Narayanan, “Sparse Representation of Electrodermal Activity with Knowledge-Driven Dictionaries.” *IEEE Transactions on Biomedical Engineering*, vol. 62, no. 3, pp. 960-971, 2015, doi: 10.1109/tbme.2014.2376960.

[81] T. Moretta, M. Kaess, and J. Koenig, “A comparative evaluation of resting state proxies of sympathetic and parasympathetic nervous system activity in adolescent major depression.” *Journal of Neural Transmission*, vol. 130, no. 2, pp. 135-144, 2023, doi: 10.1007/s00702-022-02577-3.

[82] H. F. Posada-Quintero, J. P. Florian, A. D. Orjuela-Cañón, T. Aljama-Corrales, S. Charleston-Villalobos, and K. H. Chon, “Power Spectral Density Analysis of Electrodermal Activity for Sympathetic Function Assessment.” *Annals of Biomedical Engineering*, vol. 44, no. 10, pp. 3124-3135, 2016, doi: 10.1007/s10439-016-1606-6.

[83] S. Yang, S. A. R. Hosseiny, S. Susindar, and T. K. Ferris, “Investigating Driver Sympathetic Arousal under Short-term Loads and Acute Stress Events.” *Proceedings of the Human Factors and Ergonomics Society Annual Meeting*, vol. 60, no. 1, pp. 1905-1905, 2016, doi: 10.1177/1541931213601434.

[84] T. Thong, L. Kehai, J. Mcnames, M. Aboy and B. Goldstein, ―Accuracy of ultra-short term HRV measures,” *in Proceedings of 25th Annual International Conference of IEEE EMBS, Cancun, Mexico*, pp. 17–21, 2003.

[85] S. Kay and S. Marple, “Spectrum analysis—A modern perspective.” *Proceedings of the IEEE*, vol. 69, no. 11, pp. 1380-1419, 1981, doi: 10.1109/proc.1981.12184.

[86] R. D. Berger, S. Akselrod, D. Gordon, and R. J. Cohen, “An Efficient Algorithm for Spectral Analysis of Heart Rate Variability.” *IEEE Transactions on Biomedical Engineering*, no. 9, pp. 900-904, 1986, doi: 10.1109/tbme.1986.325789.

[87] D. Singh, K. Vinod, S. C. Saxena, and K. K. Deepak, “Spectral evaluation of aging effects on blood pressure and heart rate variations in healthy subjects.” *Journal of Medical Engineering & Technology*, vol. 30, no. 3, pp. 145-150, 2006, doi: 10.1080/03091900500442855.

[88] A. Soni and K. Rawal, “EFFECT OF PHYSICAL ACTIVITIES ON HEART RATE VARIABILITY AND SKIN CONDUCTANCE.” *Biomedical Engineering: Applications, Basis and Communications*, vol. 33, no. 5, 2021, doi: 10.4015/s1016237221500381.

[89] T. H. Makikallio, J. M. Tapanainen, M. P. Tulppo, and H. V. Huikuri, “Clinical applicability of heart rate variability analysis by methods based on nonlinear dynamics,” *Cardiac Electrophysiology Review*, vol. 6, pp. 250–255, 2002.

[90] T. Hao, X. Zheng, H. Wang, K. Xu, and S. Chen, “Linear and nonlinear analyses of heart rate variability signals under mental load.” *Biomedical Signal Processing and Control*, vol. 77, p. 103758, 2022, doi: 10.1016/j.bspc.2022.103758.

[91] A. Soni and K. Rawal, “ANALYSIS OF HRV FOR POSTURAL CHANGE OF YOUNG ADULTS USING SIGNAL PROCESSING METHODS.” *Biomedical Engineering: Applications, Basis and Communications*, vol. 34, no. 5, 2022, doi: 10.4015/s1016237222500284.

[92] R. D. Berger, S. Akselrod, D. Gordon, and R. J. Cohen, “An Efficient Algorithm for Spectral Analysis of Heart Rate Variability.” *IEEE Transactions on Biomedical Engineering*, no. 9, pp. 900-904, 1986, doi: 10.1109/tbme.1986.325789.

[93] J. S. Richman and J. R. Moorman, “Physiological time-series analysis using approximate entropy and sample entropy.” *American Journal of Physiology-Heart and Circulatory Physiology*, vol. 278, no. 6, 2000, doi: 10.1152/ajpheart.2000.278.6.h2039.

[94] F. Yang and W. Liao, “Modeling and decomposition of HRV signals with wavelet transforms.” *IEEE Engineering in Medicine and Biology Magazine*, vol. 16, no. 4, pp. 17-22, 1997, doi: 10.1109/51.603643.

[95] H. L. Chan, S. C. Fang, Y. L. Ko, M. A. Lin, H. H. Huang, and C. H. Lin, “Heart Rate Variability Characterization in Daily Physical Activities Using Wavelet Analysis and Multilayer Fuzzy Activity Clustering.” *IEEE Transactions on Biomedical Engineering*, vol. 53, no. 1, pp. 133-139, 2006, doi: 10.1109/tbme.2005.859811.

[96] Y. Goren, L. Davrath, I. Pinhas, E. Toledo, and S. Akselrod, “Individual Time-Dependent Spectral Boundaries for Improved Accuracy in Time-Frequency Analysis of Heart Rate Variability.” *IEEE Transactions on Biomedical Engineering*, vol. 53, no. 1, pp. 35-42, 2006, doi: 10.1109/tbme.2005.859784.

[97] M. O. Mendez, “On arousal from sleep: time-frequency analysis.” *Medical & Biological Engineering & Computing*, vol. 46, no. 4, pp. 341-351, 2008, doi: 10.1007/s11517-008-0309-z.

[98] A. Tewfik, D. Sinha, and P. Jorgensen, “On the optimal choice of a wavelet for signal representation.” *IEEE Transactions on Information Theory*, vol. 38, no. 2, pp. 747-765, 1992, doi: 10.1109/18.119734.

[99] R. Rao and J. Chapa, “Algorithms for designing wavelets to match a specified signal.” *IEEE Transactions on Signal Processing*, vol. 48, no. 12, pp. 3395-3406, 2000, doi: 10.1109/78.887001.

[100] R. Gopinath, J. Odegard, and C. Burrus, “Optimal wavelet representation of signals and the wavelet sampling theorem.” *IEEE Transactions on Circuits and Systems II: Analog and Digital Signal Processing*, vol. 41, no. 4, pp. 262-277, 1994, doi: 10.1109/82.285705.

[101] K. Rawal, G. Sethi, B. S. Saini, and I. Saini, “HRV.” *Global Developments in Healthcare and Medical Tourism*, pp. 236-264, 2020, doi: 10.4018/978-1-5225-9787-2.ch013.

[102] K. Rawal, B. Saini, and I. Saini, “Effect of age and postural related changes on cardiac autonomic function in the pre-menopausal and post-menopausal

women." *International Journal of Medical Engineering and Informatics*, vol. 9, no. 4, p. 299, 2017, doi: 10.1504/ijmei.2017.086888.

[103] S. Vieluf, T. Hasija, R. Jakobsmeyer, P. J. Schreier, and C. Reinsberger, "Exercise-Induced Changes of Multimodal Interactions Within the Autonomic Nervous Network." *Frontiers in Physiology*, vol. 10, 2019, doi: 10.3389/fphys.2019.00240.

[104] G. E. Molina, C. J. G. Da Cruz, K. E. Fontana, E. M. K. V. K. Soares, L. G. G. Porto, and L. F. Junqueira, "Post-exercise heart rate recovery and its speed are associated with cardiac autonomic responsiveness following orthostatic stress test in men." *Scandinavian Cardiovascular Journal*, vol. 55, no. 4, pp. 220-226, 2021, doi:10.1080/14017431.2021.1879394.

[105] K. Hnatkova, "Sex differences in heart rate responses to postural provocations." *International Journal of Cardiology*, vol. 297, pp. 126-134, 2019, doi: 10.1016/j.ijcard.2019.09.044.

[106] R. Radhakrishna, D. Narayana Dutt, and V. K. Yeragani, "Nonlinear measures of heart rate time series: influence of posture and controlled breathing." *Autonomic Neuroscience*, vol. 83, no. 3, pp. 148-158, 2000, doi: 10.1016/s1566-0702(00)00173-9.

[107] G.B. Nepal, and B.H. Paudel, "Effect of posture on heart rate variability in school children," *Nepal Med Coll J*, *14*(4), pp.298-302, 2012.

[108] K. Rawal and G. Sethi, "HRV ANALYSIS OF DIFFERENT POSTURES OF YOUNG HEALTHY WOMEN USING SIGNAL PROCESSING METHODS." *Biomedical Engineering: Applications, Basis and Communications*, vol. 33, no. 1, p. 2150006, 2020, doi: 10.4015/s101623722150006x.

[109] A. D. Ryan, P. D. Larsen, and D. C. Galletly, "Comparison of heart rate variability in supine, and left and right lateral positions." *Anaesthesia*, vol. 58, no. 5, pp. 432-436, 2003, doi: 10.1046/j.1365-2044.2003.03145.x.

[110] C. J. G. Da Cruz, L. G. G. Porto, P. Da Silva Rolim, D. De Souza Pires, G. L. Garcia, and G. E. Molina, "Impact of heart rate on reproducibility of heart rate variability analysis in the supine and standing positions in healthy men." *Clinics*, vol. 74, 2019, doi: 10.6061/clinics/2019/e806.

[111] P. Kumar, A. K. Das, Prachita, and S. Halder, “Time-domain HRV Analysis of ECG Signal under Different Body Postures.” *Procedia Computer Science*, vol. 167, pp. 1705-1710, 2020, doi: 10.1016/j.procs.2020.03.435.

[112] S. Cecchi, A. Piersanti, A. Poli, and S. Spinsante, “Physical Stimuli and Emotions: EDA Features Analysis from a Wrist-Worn Measurement Sensor.” *2020 IEEE 25th International Workshop on Computer Aided Modeling and Design of Communication Links and Networks (CAMAD)*, 2020, doi: 10.1109/camad50429.2020.9209307.

[113] A. L. Callara, L. Sebastiani, N. Vanello, E. P. Scilingo, and A. Greco, “Parasympathetic-Sympathetic Causal Interactions Assessed by Time-Varying Multivariate Autoregressive Modeling of Electrodermal Activity and Heart-Rate-Variability.” *IEEE Transactions on Biomedical Engineering*, vol. 68, no. 10, pp. 3019-3028, 2021, doi: 10.1109/tbme.2021.3060867.

[114] U. Rajendra Acharya, K. Paul Joseph, N. Kannathal, C. M. Lim, and J. S. Suri, “Heart rate variability: a review.” *Medical & Biological Engineering & Computing*, vol. 44, no. 12, pp. 1031-1051, 2006, doi: 10.1007/s11517-006-0119-0.

[115] N. Ganapathy, Y. R. Veeranki, and R. Swaminathan, “Convolutional neural network based emotion classification using electrodermal activity signals and time-frequency features.” *Expert Systems with Applications*, vol. 159, p. 113571, 2020, doi: 10.1016/j.eswa.2020.113571.

[116] M. Javorka, I. Zila, T. Balhárek, and K. Javorka, “Heart rate recovery after exercise: relations to heart rate variability and complexity.” *Brazilian Journal of Medical and Biological Research*, vol. 35, no. 8, pp. 991-1000, 2002, doi: 10.1590/s0100-879x2002000800018.

[117] Z. Visnovcova, “Spectral and Nonlinear Analysis of Electrodermal Activity in Adolescent Anorexia Nervosa.” *Applied Sciences*, vol. 10, no. 13, p. 4514, 2020, doi: 10.3390/app10134514.

[118] T. Henriques, M. Ribeiro, A. Teixeira, L. Castro, L. Antunes, and C. Costa-Santos, “Nonlinear Methods Most Applied to Heart-Rate Time Series: A Review.” *Entropy*, vol. 22, no. 3, p. 309, 2020, doi: 10.3390/e22030309.

[119] D. Wejer, B. Graff, D. Makowiec, S. Budrejko, and Z. R. Struzik, “Complexity of cardiovascular rhythms during head-up tilt test by entropy of patterns.” *Physiological Measurement*, vol. 38, no. 5, pp. 819-832, 2017, doi: 10.1088/1361-6579/aa64a8.

[120] S. Pincus, “Approximate entropy: a complexity measure for biological time series data.” *Proceedings of the 1991 IEEE Seventeenth Annual Northeast Bioengineering Conference*, vol. 88, no. 6, pp. 2297-2301, 1991, doi: 10.1109/nebc.1991.154568.

[121] C. Bandt and B. Pompe, “Permutation Entropy: A Natural Complexity Measure for Time Series.” *Physical Review Letters*, vol. 88, no. 17, 2002, doi: 10.1103/physrevlett.88.174102.

[122] W. Chen, Z. Wang, H. Xie, and W. Yu, “Characterization of Surface EMG Signal Based on Fuzzy Entropy.” *IEEE Transactions on Neural Systems and Rehabilitation Engineering*, vol. 15, no. 2, pp. 266-272, 2007, doi: 10.1109/tnsre.2007.897025.

[123] W. Chen, J. Zhuang, W. Yu, and Z. Wang, “Measuring complexity using FuzzyEn, ApEn, and SampEn.” *Medical Engineering & Physics*, vol. 31, no. 1, pp. 61-68, 2009, doi: 10.1016/j.medengphy.2008.04.005.

[124] K. Huselius Gylling, “Quadratic sample entropy as a measure of burstiness: A study in how well Rényi entropy rate and quadratic sample entropy can capture the presence of spikes in time-series data,” 2017.

[125] D. Lake, “Renyi Entropy Measures of Heart Rate Gaussianity.” *IEEE Transactions on Biomedical Engineering*, vol. 53, no. 1, pp. 21-27, 2006, doi: 10.1109/tbme.2005.859782.

[126] A. Porta, B. De Maria, V. Bari, A. Marchi, and L. Faes, “Are Nonlinear Model-Free Conditional Entropy Approaches for the Assessment of Cardiac Control Complexity Superior to the Linear Model-Based One?” *IEEE Transactions on Biomedical Engineering*, vol. 64, no. 6, pp. 1287-1296, 2017, doi: 10.1109/tbme.2016.2600160.

[127] M. Costa, A. L. Goldberger, and C.-K. Peng, “Multiscale entropy analysis of biological signals.” *Physical Review E*, vol. 71, no. 2, 2005, doi: 10.1103/physreve.71.021906.

[128] N. Zhang, A. Lin, H. Ma, P. Shang, and P. Yang, “Weighted multivariate composite multiscale sample entropy analysis for the complexity of nonlinear times series.” *Physica A: Statistical Mechanics and its Applications*, vol. 508, pp. 595-607, 2018, doi: 10.1016/j.physa.2018.05.085.

[129] A. Porta, “On the Relevance of Computing a Local Version of Sample Entropy in Cardiovascular Control Analysis.” *IEEE Transactions on Biomedical Engineering*, vol. 66, no. 3, pp. 623-631, 2019, doi: 10.1109/tbme.2018.2852713.

[130] D. Shang, P. Shang, and Z. Zhang, “Efficient synchronization estimation for complex time series using refined cross-sample entropy measure.” *Communications in Nonlinear Science and Numerical Simulation*, vol. 94, p. 105556, 2021, doi: 10.1016/j.cnsns.2020.105556.

[131] S. Byun, “Entropy analysis of heart rate variability and its application to recognize major depressive disorder: A pilot study.” *Technology and Health Care*, vol. 27, pp. 407-424, 2019, doi: 10.3233/thc-199037.

[132] M. Baumert, B. Czippelova, A. Ganesan, M. Schmidt, S. Zaunseder, and M. Javorka, “Entropy Analysis of RR and QT Interval Variability during Orthostatic and Mental Stress in Healthy Subjects.” *Entropy*, vol. 16, no. 12, pp. 6384-6393, 2014, doi: 10.3390/e16126384.

[133] L. Faes, “Comparison of methods for the assessment of nonlinearity in short-term heart rate variability under different physiopathological states.” *Chaos: An Interdisciplinary Journal of Nonlinear Science*, vol. 29, no. 12, 2019, doi: 10.1063/1.5115506.

[134] M. Ribeiro, “Non-linear Methods Predominant in Fetal Heart Rate Analysis: A Systematic Review.” *Frontiers in Medicine*, vol. 8, 2021, doi: 10.3389/fmed.2021.661226.

[135] C. H. Renu Madhavi, &A. G. Ananth, “A review of heart rate variability and its association with diseases,” Int J Soft Comput Eng, vol. 2, pp.2231-2307, 2012.

[136] T. Pham, Z. J. Lau, S. H. A. Chen, and D. Makowski, “Heart Rate Variability in Psychology: A Review of HRV Indices and an Analysis Tutorial.” *Sensors*, vol. 21, no. 12, p. 3998, 2021, doi: 10.3390/s21123998.

[137] S. Chabchoub, S. Mansouri, and R. Ben Salah, “Signal processing techniques applied to impedance cardiography ICG signals – a review.” *Journal of Medical Engineering & Technology*, vol. 46, no. 3, pp. 243-260, 2022, doi: 10.1080/03091902.2022.2026508.

[138] A. Voss, S. Schulz, R. Schroeder, M. Baumert, and P. Caminal, “Methods derived from nonlinear dynamics for analysing heart rate variability.” *Philosophical Transactions of the Royal Society A: Mathematical, Physical and Engineering Sciences*, vol. 367, no. 1887, pp. 277-296, 2008, doi: 10.1098/rsta.2008.0232.

[139] L. Tóth and T. Tóth, “On Finding Better Wavelet Basis for Bearing Fault Detection.” *Acta Polytechnica Hungarica*, vol. 10, no. 3, pp. 17-35, 2013, doi: 10.12700/aph.10.03.2013.3.3.

[140] K. Deák, T. Mankovits, and I. Kocsis, “Optimal Wavelet Selection for the Size Estimation of Manufacturing Defects of Tapered Roller Bearings with Vibration Measurement using Shannon Entropy Criteria.” *Strojniški vestnik - Journal of Mechanical Engineering*, vol. 63, no. 1, pp. 3-14, 2017, doi: 10.5545/sv-jme.2016.3989.

[141] G. Quellec, M. Lamard, P. Josselin, G. Cazuguel, B. Cochener, and C. Roux, “Optimal Wavelet Transform for the Detection of Microaneurysms in Retina Photographs.” *IEEE Transactions on Medical Imaging*, vol. 27, no. 9, pp. 1230-1241, 2008, doi: 10.1109/tmi.2008.920619.

[142] D. D. M., “Adaptive Algorithms for Signature Wavelet recognition in the Musical Sounds.” *Journal of Soft Computing Paradigm*, vol. 2, no. 2, pp. 120-129, 2020, doi: 10.36548/jscp.2020.2.005.

[143] G. Quellec, M. Lamard, G. Cazuguel, B. Cochener, and C. Roux, “Wavelet optimization for content-based image retrieval in medical databases.” *Medical Image Analysis*, vol. 14, no. 2, pp. 227-241, 2010, doi: 10.1016/j.media.2009.11.004.

[144] V. Strela, P. Heller, G. Strang, P. Topiwala, and C. Heil, “The application of multiwavelet filterbanks to image processing.” *IEEE Transactions on Image Processing*, vol. 8, no. 4, pp. 548-563, 1999, doi: 10.1109/83.753742.

[145] L. K. Shark and C. Yu, “Design of matched wavelets based on generalized Mexican-hat function.” *Signal Processing*, vol. 86, no. 7, pp. 1451-1469, 2006, doi: 10.1016/j.sigpro.2005.08.004.

[146] C. Levkov, G. Michov, R. Ivanov, and I. K. Daskalov, “Subtraction of 50 Hz interference from the electrocardiogram.” *Medical & Biological Engineering & Computing*, vol. 22, no. 4, pp. 371-373, 1984, doi: 10.1007/bf02442109.

[147] M. Wachowiak, G. Rash, P. Quesada, and A. Desoky, “Wavelet-based noise removal for biomechanical signals: a comparative study.” *IEEE Transactions on Biomedical Engineering*, vol. 47, no. 3, pp. 360-368, 2000, doi: 10.1109/10.827298

[148] M. A. Salo, H. V. Huikuri, and T. Seppanen, “Ectopic Beats in Heart Rate Variability Analysis: Effects of Editing on Time and Frequency Domain Measures.” Annals of Noninvasive Electrocardiology, vol. 6, no. 1, pp. 5-17, 2001, doi: 10.1111/j.1542-474x.2001.tb00080.x.

[149] P. Tikkanen, “Characterization and applications of analysis methods for ECG and time interval variability data,” Ph. D Thesis, Oulu University, 1999.

[150] N. Lippman, K. M. Stein, and B. B. Lerman, “Comparison of methods for removal of ectopy in measurement of heart rate variability.” *American Journal of Physiology-Heart and Circulatory Physiology*, vol. 267, no. 1, 1994, doi: 10.1152/ajpheart.1994.267.1.h411.

[151] C. L. Birkett, M. G. Kienzle, and G. A. Myers, “Interpolation over ectopic beats increase low frequency power in heart rate variability spectra,” *Computers in Cardiology, IEEE Computer Society Press*, pp. 257-259, 1991.

[152] D. Singh, K. Vinod, S. C. Saxena, and K. K. Deepak, “Effects of RR segment duration on HRV spectrum estimation,” *Physiological Measurement,* vol. 25, pp. 721–735, 2004.

[153] D. Singh, K. Vinod and S. C. Saxena, “Sampling frequency of the RR-interval time series for spectral analysis of the heart rate variability,” *Journal of Medical Engineering and Technology*, vol. 28, pp. 263–272, 2004

[154] M. Pagani, F. Lombardi, S. Guzzetti, O. Rimoldi, R. Furlan, P. Pizzinelli, G. Sandrone, G. Malfatto, S. Dell’Orto, and E. Piccaluga, “Power spectral analysis of heart rate and arterial pressure variabilities as a marker of sympathovagal interaction in man and conscious dog,” *Circulation Research,* vol. 59, pp. 178-193, 1986

[155] B. W. Hyndman, and C. Zeelenberg, “Spectral analysis of HRV revisited: Comparison of the methods,” *in Proceedings of the IEEE International Conference on Computers in Cardiology, London, UK*, pp. 719-722, September 5-8, 1993.

[156] M. Di. Rienzo, P. Castiglloni, G. Parati, G. Mancia, and A. Pedotti, “Effects of sino-aortic denervation on spectral characteristics of blood pressure and pulse interval variability: a wide band approach,” *Medical and Biological Engineering and Computing,* vol. 34, pp.133-131, 1996.

[157] J. Vila, S. Barro, J. Presedo, R. Ruiz, and F. Palacios, “Analysis of heart rate variability with evenly spaced time values.” *Proceedings of the Annual International Conference of the IEEE Engineering in Medicine and Biology Society*, 1992, doi: 10.1109/iembs.1992.5761116.

[158] M. H. Vastenburg, T. Visser, M. Vermaas, and D. V. Keyson, “Designing Acceptable Assisted Living Services for Elderly Users.” *Lecture Notes in Computer Science*, pp. 1-12, 2008, doi: 10.1007/978-3-540-89617-3_1.

[159] M. E. Gomes, H. N. Guimarães, A. L. Ribeiro, and L. A. Aguirre, “Does preprocessing change nonlinear measures of heart rate variability?” *Computers in Biology and Medicine*, vol. 32, no. 6, pp. 481-494, 2002, doi: 10.1016/s0010-4825(02)00029-x.

[160] M. A. Peltola, “Role of editing of R–R intervals in the analysis of heart rate variability.” *Frontiers in Physiology*, vol. 3, no. 148, pp. 1-10, 2012, doi: 10.3389/fphys.2012.00148.

[161] http://en.wikipedia.org/wiki/Linear_interpolation

[162] http://en.wikipedia.org/wiki/Spline_interpolation

[163] http://en.wikipedia.org/wiki/Spline_%28mathematics%29

[164] http://www.paulinternet.nl/?page=bicubic

[165] O. Masek, “Heart Rate Variability Analysis,” Diploma Thesis, Czech Technical University in Prague, Prague, 2009.

[166] D. A. LITVACK, T. F. OBERLANDER, L. H. CARNEY, and J. P. SAUL, “Time and frequency domain methods for heart rate variability analysis: A methodological comparison.” *Psychophysiology*, vol. 32, no. 5, pp. 492-504, 1995, doi: 10.1111/j.1469-8986.1995.tb02101.x.

[167] S. Kay and S. Marple, “Spectrum analysis—A modern perspective.” *Proceedings of the IEEE*, vol. 69, no. 11, pp. 1380-1419, 1981, doi: 10.1109/proc.1981.12184.

[168] P. Castiglioni, G. Parati, A. Civijian, L. Quintin, and M. Di Rienzo, “Local Scale Exponents of Blood Pressure and Heart Rate Variability by Detrended Fluctuation Analysis: Effects of Posture, Exercise, and Aging.” *IEEE Transactions on Biomedical Engineering*, vol. 56, no. 3, pp. 675-684, 2009, doi: 10.1109/tbme.2008.2005949.

[169] Y. Saeki, F. Atogami, K. Takahashi, and T. Yoshizawa, “Reflex control of autonomic function induced by posture change during the menstrual cycle.” *Journal of the Autonomic Nervous System*, vol. 66, no. 1, pp. 69-74, 1997, doi: 10.1016/s0165-1838(97)00067-2.

[170] M. Van Dooren, J. (Gert-J. De Vries, and J. H. Janssen, “Emotional sweating across the body: Comparing 16 different skin conductance measurement locations.” *Physiology & Behavior*, vol. 106, no. 2, pp. 298-304, 2012, doi: 10.1016/j.physbeh.2012.01.020.

[171] N. Watanabe, J. Reece, and B. I. Polus, “Effects of body position on autonomic regulation of cardiovascular function in young, healthy

adults.” *Chiropractic & Osteopathy*, vol. 15, no. 1, pp. 1-8, 2007, doi: 10.1186/1746-1340-15-19.

[172] S. Pearson, A. P. Colbert, J. McNames, M. Baumgartner, and R. Hammerschlag, “Electrical Skin Impedance at Acupuncture Points.” *The Journal of Alternative and Complementary Medicine*, vol. 13, no. 4, pp. 409-418, 2007, doi: 10.1089/acm.2007.6258.

[173] A. Omidvarnia, M. Mesbah, M. Pedersen, and G. Jackson, “Range Entropy: A Bridge between Signal Complexity and Self-Similarity.” *Entropy*, vol. 20, no. 12, p. 962, 2018, doi: 10.3390/e20120962.

[174] V. S. Prasatha, H. A. A. Alfeilate, A. B. Hassanate, O. Lasassmehe, A. S. Tarawnehf, M. B. Alhasanatg, and H. S. E. Salmane. "Effects of distance measure choice on knn classifier performance-a review." *arXiv preprint arXiv:1708.04321*, pp. 56, 2017.

[175] P. Kumar, A. K. Das, S. Halder, “Statistical heart rate variability analysis for healthy person: Influence of gender and body posture.” *Journal of Electro cardiology*, vol. 79, pp. 81-88, 2023.

[176] K, Buszko, A. Piątkowska, E. Koźluk, T. Fabiszak, & G. Opolski, (2018). “Entropy Measures in Analysis of Head up Tilt Test Outcome for Diagnosing Vasovagal Syncope.” *Entropy*, vol. 20, no. 12, p. 976, 2018.

[177] A. D. Ryan, P. D. Larsen, and D. C. Galletly, “Comparison of heart rate variability in supine, and left and right lateral positions.” *Anaesthesia*, vol. 58, no. 5, pp. 432-436, 2003, doi: 10.1046/j.1365-2044.2003.03145.x.

[178] P. Le and W. S. Marras, “Evaluating the low back biomechanics of three different office workstations: Seated, standing, and perching.” *Applied Ergonomics*, vol. 56, pp. 170-178, 2016, doi: 10.1016/j.apergo.2016.04.001.

[179] A. Soni and K. Rawal, “Study the Effect of Body Postures on Skin Conductance Response and Heart Rate.” *Proceedings of International Conference on Women Researchers in Electronics and Computing*, pp. 30-37, 2021, doi: 10.21467/proceedings.114.5.

[180] F. Shaffer and J. P. Ginsberg, “An Overview of Heart Rate Variability Metrics and Norms.” *Frontiers in Public Health*, vol. 5, pp. 258, 2017, doi: 10.3389/fpubh.2017.00258.

[181] Čukić Milena, “Linear and Non-Linear Heart Rate Variability Indexes from Heart-Induced Mechanical Signals Recorded with a Skin-Interfaced IMU.” *Sensors*, vol. 23, no. 3, p. 1615, 2023, doi: 10.3390/s23031615.

[182] S. Mallat, “A theory for multiresolution signal decomposition: the wavelet representation.” *IEEE Transactions on Pattern Analysis and Machine Intelligence*, vol. 11, no. 7, pp. 674-693, 1989, doi: 10.1109/34.192463.

[183] R. M. Rao, “Wavelet Transforms: Introduction to Theory and Applications.” *Journal of Electronic Imaging*, vol. 8, no. 4, p. 478, 1999, doi: 10.1117/1.482718.

[184] O. Rioul and M. Vetterli, “Wavelets and signal processing.” *IEEE Signal Processing Magazine*, vol. 8, no. 4, pp. 14-38, 1991, doi: 10.1109/79.91217.

[185] M. Unser and A. Aldroubi, “A review of wavelets in biomedical applications.” *Proceedings of the IEEE*, vol. 84, no. 4, pp. 626-638, 1996, doi: 10.1109/5.488704.

[186] U. Wiklund, M. Akay, S. Morrison, and U. Niklasson, “Wavelet decomposition of cardiovascular signals for baroreceptor function tests in pigs.” *IEEE Transactions on Biomedical Engineering*, vol. 49, no. 7, pp. 651-661, 2002, doi: 10.1109/tbme.2002.1010848.

[187] J. Karel, R. Peeters, R. Westra, K. Moermans, S. Haddad, and W. Serdijn, “Optimal discrete wavelet design for cardiac signal processing.” *2005 IEEE Engineering in Medicine and Biology 27th Annual Conference*, pp. 2769-2772, 2005, doi: 10.1109/iembs.2005.1617046.

[188] R. S. S. Kumari, S. Bharathi, and V. Sadasivam, “Design of Optimal Discrete Wavelet for ECG Signal Using Orthogonal Filter Bank.” *International Conference on Computational Intelligence and Multimedia Applications (ICCIMA 2007)*, vol. 1, pp. 96-100, 2007, doi: 10.1109/iccima.2007.273.

[189] G. Shi, Ai. Ding, and N. Zhang, “Design of wavelet based on waveform matching and its application to signal compression.” *48th Midwest*

Symposium on Circuits and Systems, 2005., vol. 2, pp. 1696-1699, 2005, doi: 10.1109/mwscas.2005.1594446.

[190] H. Salimi, "Stochastic Fractal Search: A powerful metaheuristic algorithm." *Knowledge-Based Systems*, vol. 75, pp. 1-18, 2015, doi: 10.1016/j.knosys.2014.07.025.

[191] T. Tyagi, H. M. Dubey, and M. Pandit, "Multi-Objective Optimal Dispatch Solution of Solar-Wind-Thermal System Using Improved Stochastic Fractal Search Algorithm." *International Journal of Information Technology and Computer Science*, vol. 8, no. 11, pp. 61-73, 2016, doi: 10.5815/ijitcs.2016.11.08.

[192] H. M. Dubey, M. Pandit, B. K. Panigrahi, and T. Tyagi, "Multi-objective Power Dispatch Using Stochastic Fractal Search Algorithm and TOPSIS." *Swarm, Evolutionary, and Memetic Computing*, pp. 154-166, 2016, doi: 10.1007/978-3-31

APPENDIX

INTERNET SOURCES

- http://en.wikipedia.org/wiki/Elecrocardiography
- http://en.wikipedia.org/wiki/Linear_interpolation
- http://en.wikipedia.org/wiki/Spline_interpolation
- http://en.wikipedia.org/wiki/Spline_%28mathematics%29
- http://www.paulinternet.nl/?page=bicubic
- https://archive.physionet.org/tutorials/hrv-toolkit/
- https://users.rowan.edu/~polikar/WTpart1.html
- https://in.mathworks.com/matlabcentral/fileexchange/69381-sample-entropy
- http://hrventerprise.com/seminar.html
- https://en.wikipedia.org/wiki/Electrodermal_activity
- http://www.sciencedirect.com/science/article/pii/S0950705114002822
- https://in.mathworks.com/matlabcentral/fileexchange/47565-stochastic-fractal-search-sfs

Authors Research Contribution

LIST OF PUBLICATIONS

1. **A. Soni** and K. Rawal, "Effect of Physical Activities on Heart Rate Variability and Skin Conductance." *Biomedical Engineering: Applications, Basis and Communications*, vol. 33, no. 5, p. 2150038, 2021, doi: 10.4015/s1016237221500381.

2. **A. Soni** and K. Rawal, "Analysis of HRV for Postural Change of Young Adults using Signal Processing Methods." *Biomedical Engineering: Applications, Basis and Communications*, vol. 34, no. 5, p. 2250028, 2022, doi: 10.4015/s1016237222500284.

3. **A. Soni** and K. Rawal, "Analyzing the effect of postural change on heart rate variability using multi-distance sample entropy (MDSE)." *Biomedical Signal Processing and Control*, vol. 87, no. Part B, p. 105476, 2024, doi: 10.1016/j.bspc.2023.105476.

4. **A. Soni**, K. Rawal, and T. Tyagi, "The study of the response of postural stimuli in relation to Heart rate and Skin conductance in the nonlinear domain," *International Journal of Biomedical Engineering and Technology*, vol. 45, no. 2, p. 164-182, 29 May 2024. https://doi.org/10.1504/IJBET.2024.138713

5. **A. Soni**, and K. Rawal, T. Tyagi, "A Novel Composite Distance Sample Entropy Method (CDSE) to investigate the effect of Different Body Postures on Heart Rate Variability and Skin Conductance," in *Frontiers.* (**Communicated**)

6. **A. Soni**, K. Rawal, and T. Tyagi, "Unveiling the Dynamics of Postural Changes: Optimized Filter Bank Analysis of HRV for Sympathetic and Parasympathetic Nervous System Activity Using Stochastic Fractal Search Algorithm," *Biomedical Signal Processing and Control*. (**Communicated**).

LIST OF CONFERENCES

1. **A. Soni** and K. Rawal, "A Review on Physiological Signals: Heart Rate Variability and Skin Conductance." *Lecture Notes in Networks and Systems*, pp. 387-399, 2020, doi: 10.1007/978-981-15-3369-3_30.

2. **A. Soni** and K. Rawal, "Study the Effect of Body Postures on Skin Conductance Response and Heart Rate." *Proceedings of International Conference on Women Researchers in Electronics and Computing*, pp. 30-37, Sep. 2021, doi: 10.21467/proceedings.114.5.
3. **A. Soni** and K. Rawal, "Nonlinear analysis of postural provocations in the response of Heart rate and Skin Conductance," In *the 4th International e-Conference on Intelligent Circuits and Systems (ICICS-2022),* held on April 8-9th, 2022.